A STUDY OF THE PIEZOELECTRIC BEHAVIOUR OF QUARTZ AND QUARTZITES

by JACOBUS ANDRIES RETIEF

DISSERTATION

submitted as fulfilment of the requirements for

the degree

MASTER OF SCIENCE

in

GEOLOGY

in the

FACULTY OF SCIENCE

at the

RAND AFRIKAANS UNIVERSITY

SUPERVISOR: PROF. W.J. VAN BILJON

CO-SUPERVISOR: PROF. A.G.K. LUTSCH

ABSTRACT

Certain crystals, of which quartz is an example, produce an electric charge when subjected to mechanical stress. This phenomenon is known as the piezoelectric effect.

Due to certain shortcomings in the existing methods of measuring stress underground in a mine, it had been decided to investigate the piezoelectric effect in quartzites with the possibility of applying this effect underground to determine stresses.

For callibration purposes tests have been carried out on 58 quartz cylinders by applying load with the static method. An average value for a d modulus for quartz has been determined as $1,43 \times 10^{-12}$ C/N which is one-third lower than the general accepted value of $2,3 \times 10^{-12}$ C/N.

Tests were carried out on quartzites taken from various zones on Loraine Gold Mines, Limited. Certain problems were encountered, such as the phenomenon of drift observed in the piezoelectric charge, even without loading the cylinder.

In the results on some of the quartzites piezoelectric polarization values as high as $12,5 \times 10^{-6}$ C/m^2 have been measured while others yielded very little or no readings at all.

These piezoelectric readings could have either been the consequence of stress on a few large quartz grains in the specimen, or as a result of a preferential orientation of the quartz grains.

Before a conclusion can be reached regarding the usefulness of this method in the mines, further investigation should be carried out in the laboratory on the drift in quartzites, as well as the orientation of quartzite specimens in order to obtain the highest readings. In addition, the feasability of the dynamic rather than the static method should also be investigated.

UITTREKSEL

Sekere kristalle, waaronder kwarts, besit die eienskap om 'n elektriese lading vry te stel onder meganiese belading. Hierdie verskynsel word die piezoelektriese effek genoem.

Aangesien daar sekere tekortkominge bestaan in die huidige metodes om spanninge ondergrond te meet, is besluit om hierdie verskynsel van die piezoelektriese-effek by kwartsiete te ondersoek met die moontlikheid om dit te gebruik om spannings ondergrond in 'n myn te meet.

Vir kalibrasie doeleindes is toetse op 58 kwartssilinders uitgevoer deur gebruik te maak van statiese-belading. 'n Gemiddelde waarde vir 'n d module van kwarts is op 1,43 X 10^{12} C/N bepaal wat een derde laer is as die erkende waarde van 2,3 X 10^{-12} C/N.

Toetse op die kwartsiete, geneem uit die verskillende sones op Loraine Goudmyn Beperk, het heelwat moeilikhede opgelewer. Die verskynsel van dryf in die piezoelektriese-lading, selfs sonder enige meganiese-lading toegepas op die kwartsietsilinder, het heelwat probleme veroorsaak.

In die resultate op sommige kwartsiete is piezoelektriese polarisasie-waardes tot so hoog as 12,5 X 10^{-6} C/m^2 gemeet, terwyl ander baie lae of feitlik geen waardes gegee het nie.

Daar is twee moontlike alternatiewe vir die ontstaan van hierdie waardes nl : óf deur belading van 'n paar uitsonderlike groot kwatskorrels in die monster, óf as gevolg van 'n voorkeuroriëntasie van die kwartskorrels.

Alvorens enige gevolgtrekking aangaande die bruikbaarheid van hierdie metode in myne gemaak kan word, sal verdere laboratoriumondersoeke ten opsigte van die dryf-verskynsel by kwartsiete, asook die oriëntasie van kwartsietmonsters ter verkryging van die hoogste lesings, uitgevoer moet word. Verder behoort die moontlikheid van die dinamiese metode in plaas van die statiese metode ook ondersoek te word.

CONTENTS.

LIST OF TABLES

FIGURES

FIGURES

Page

Page

LIST OF PLATES

1. PURPOSE OF THE STUDY.

1.1. Stresses in Rock Leading to Rock Failure.

The total stress field must be determined in order to define the stability of the rock adjacent to workings and in the macro-aspect of mining situations. Mathematical calculations, based on the elastic properties of the rock, are used to predict the stress redistribution which takes place with mining, so that induced and total stress can be determined, and stability predictions made.

The primitive stress, (Virgin state of stress), existing before any mining proceeds, is assumed to be equal to the weight of the overburden and does not allow for any geological stress due to the structural history of the particular mining field. It is also crucial to know the actual primitive stress, as obviously it is often the major factor in determining the total stress after induced stress has been calculated. Furthermore, non-elastic characteristics, such as geological discontinuities, dykes and plasticity in the rock, could have a determining influence on the stress distribution, both in size and direction.

As stability is largely determined by the difference between principal maximum and minimum stress as well as their orientations, a reliable method of stress measurement would be extremely valuable to the mining industry.

By observing the condition of the hangingwall, sidewall or footwall of an excavation underground, it is possible to assess immediate stress problems which are reflected in their result, e.g. hangingwall fractures or sidewall

scaling, but any hidden stress a few metres ahead of the face can only be located with more advanced techniques. Some of the techniques will be discussed briefly.

1.2. Techniques Used to Locate High Stress Fields Underground.

As science and technology have advanced over the years, various methods have been developed in the laboratory and applied underground to measure or predict high stress levels in rocks which might lead to rock failure.

1.2.1. Hydraulic Jack Method.

In this method the absolute stress is determined by a stress relieving technique using hydraulic jacks. Leeman (1964, p64 - 68).

A 30 centimetre slot is cut in the sidewall of a tunnel or on the face of a stope. A flat hydraulic jack, consisting of two flat thin metal plates with an area of 30 centimetres square welded around their perimeter and connected to a tube to allow oil to be pumped in between the plates, is grouted in the slot. Prior to cutting the slot, a row of pins is installed on either side, parallel to the centre line of the slot. This is used to measure displacement across the slot. By increasing the pressure in the jack, the displacement brought about by cutting the slot, can be restored. This pressure should be equal to the stresses perpendicular to the plane of the slot prior to cutting. One disadvantage of this method is that it only measures stress concentration near the surface of the rock due to excavation shape and not field stress. For stresses deeper in the rock, curved jacks are installed in boreholes.

1.2.2. Borehole Deformation Strain Cells.

The majority of rock stress measuring instruments have been

based upon the measuring of strain in the rock i.e. the actual deformation of the rock. Such an instrument is the borehole deformation strain cell which measures changes in the dimensions of one or more diameters of a borehole which is discussed in a paper by Leeman (1964, p51 - 54).

These changes in borehole diameter are employed to calculate the stress in the surrounding rock. The main disadvantage here is that it has got to be calibrated beforehand. This method cannot be used in deep mines and also requires pre-calibration.

1.2.3. Borehole Inclusion Stressmeter.

Changes in stress in the rock causes changes in strain in the measuring components of the stressmeter. These changes in strain in the measuring components are measured and expressed in terms of changes in stress in the surrounding rock.

When the effective modulus of elasticity of the stressmeter is greater than five times the modulus of the rock in which it is to be used, it is not necessary to know the modulus of elasticity of the rock with great accuracy. Calibration need not take place in situ, but in the laboratory in a material having a modulus of elasticity close to that of the rock to be measured. This method is quite suitable for measuring increases in compressive stress but requires prestressing for measuring decreases in compressive stress or changes in tensile stress.

1.2.4. Borehole Strain Gauge Devices.

This technique makes use of a rosette of resistant wire strain gauges mounted on a circular piece of shim, 35 millimetres in

diameter.

In the latest model strain cell, a rosette consisting of three gauges to measure strains in the vertical, horizontal and 45 degree directions is glued to the shim. This strain cell is then glued to the flat end of a BX diamond drill borehole. The three strain measurements are used to calculate the principal stresses σ_1' , and σ_2' on the flat end of the borehole. In order to calculate the principal stresses in the surrounding rock, it is necessary to obtain the relationship between σ_1' and σ_1 as well as σ_2' and σ_2. This is done in the laboratory by applying the same experimental procedure as used underground to cubes of steel, granite and araldite. It was found that the principal stresses in the rock surrounding the flattened end of the borehole are 2/3 of the principal stresses on the end of the borehole.

By extending the length of the hole with a coring crown, the stress in the rock to which the strain gauge is cemented, is relieved. This method, developed by Mohr (1956, p178 - 189), enables the core to be removed from the hole, whereafter it can be loaded in the laboratory in order to deduce the stress in the underground rock from where it was taken.

The main problem with this method is that the stress concentration at the end of the borehole is not clear.

1.2.5. Photostress Method.

This method is based on the photo-elastic principle, and is applied to determine changes in stress on the surface of the rock. The flat surface of the rock is sprayed with reflective paint, whereafter it is coated with transparent photo-elastic plastic. Any change in stress in the rock will result in a change in strain on the rock surface. This change will be transmitted

to the plastic coating which becomes birefringent. When the rock surface is illuminated with polarized light, a photo-elastic fringe pattern can be observed in the plastic coating. According to Emery (1960, p54 - 59), this pattern will be related to the change in stress on the rock surface.

1.2.6. The Sonic Method.

This method is based on the fact that when a rock surface is struck with a hammer or when a high frequency energy passes through it, a longitudinal or compressional wave and a shear wave are propagated through the medium in the direction of the energy wave.

By using a cathode ray oscilloscope, the travelling time for the compressional wave between a transducer near the source of impact and a second transducer near the end of the line of travel, can be measured.

In the application of this method it is assumed that the modulus of elasticity, Poissons's ratio and the density of the rock changes with variation in stress.

Calibration tests are carried out in the laboratory on cylindrical or cubic rock specimens from the area where stress measurements are to be taken. These rock cylinders or cubes are placed under various compressive stresses, and for each stress level, the travelling time of a sonic or ultrasonic wave propagated in the direction of the applied stress, is measured. These tests enables the observer to deduce the stress levels in rocks underground from velocity measurements. Various investigators (Leeman, 1964, p69 - 71) used this method to obtain stresses in rock pillars by measuring the sonic wave created by a hammer blow on the surface of the rock.

Due to the very minute changes in the velocity of the wave with

changes in stress, this method could not be applied to measure stress in rocks of the Witwatersrand.

1.2.7. Resistivity Method.

According to Isaacson (1958, p185 - 186) the electrical resistivity in rock decreases with increasing pressure. This assumption is based on compressive tests conducted on blocks of hornblende schists from the Kolar Gold Fields, India. In his experiment, the stress versus resistance curve flattens at high stress values. It is quite obvious that this flattening of the curve at high stress values, such as those that would be encountered at great depths, eliminates the use of this method for South African deep mines.

Tests carried out on quartzites from a gold mine on the Witwatersrand, failed to produce an observable electrical resistance change with change in stress.

1.2.8. Computer Models Based on the Elastic Theory of Rocks.

Although not a direct method to measure stress underground, it has become a very useful method to predict stresses underground. It has been proved by experimental evidence, as also mentioned earlier on, that the rock mass surrounding an excavation in a gold mine responds in an elastic manner. This theory has been applied to develop digital and analogue computer models which make it possible to calculate changes in stress and displacement in the rock around any excavation underground. It is also possible to evaluate the rate of energy release per unit area mined out, which in turn is very important for stope support design.

With the computer technique it is possible to predict beforehand what will happen underground to an excavation long before mining has actually started. The only information necessary is the

shape of the excavation, the depth below surface and the positions at which the information is required.

1.2.9. Estimation of Rock Stresses from Borehole Sidewall Fractures.

The existence of a high stress field deep in the sidewall of an excavation is reflected in the side of a horizontal or near horizontal borehole, when drilled into the sidewall of the excavation. In the case of compressive stress the borehole tends to take an elliptical shape with the long axis orientated at right angles to stress direction. This deformation is due to fracturing or scaling of the side of the borehole, but the latter may also be due to geological factors e.g. thin shale partings.

1.2.10. Estimation of Rock Stress from Diamond Core Fractures.

Fractures in diamond drill core are a qualitative method to assess stress in rock. Core obtained from a diamond drill hole drilled into a highly stressed rock always tends to be in the form of a series of thin discs. Jaeger et. al. (1963, p1759 - 1765) has confirmed with laboratory tests, that the ratio of the diameter to the thickness of the discs decreases as the rock stress increases.

1.3. Studies carried out by Hoenig.

Since 1975 Hoenig (1976, p4 - 5) has been carrying out tests in the laboratory closely related to these to be discussed in this dissertation.

By applying the slab-in-bending system on a rock specimen, one side is placed under tension and the opposite under compression. This is a simulation of conditions underground where both compression and tension are some of the controlling factors in rock-falls. The electric currents dissipated from both the upper (tensions) and lower (compression) surfaces were measured

on a picro-ammeter whilst the slab was being loaded. It was observed that with each increment of load a current in the form of a 'spike' was generated. This 'spike' receded back to zero in the beginning when the load applied was still fairly low, but as the load was increased these 'spikes' no longer receded to zero.

These experiments were also carried out on 75 centimetre long drill core specimens under load in a press.

These 'spikes' observed at low load levels are interpreted by Hoenig as piezoelectric effects.

1.4. Definition of Piezoelectricity.

In certain crystaline materials e.g. quartz, a potential difference between two faces is observed when subjected to mechanical stress. This relationship between electrical charge and mechanical stress is termed direct piezoelectric effect, and was discovered by P and J Curie in 1880.

1.4.1. Piezoelectric Charge Measurements as Possible Method to Determine Stresses Underground.

It is obvious from the discussion on the various techniques of stress measurement that most of the methods are poor due to certain limitations, such as the inability to measure field stress in deep mines where measurements are affected by spalling and fracturing of rock. The purpose of this study is therefore to determine whether a piezoelectric charge is generated in quartzite due to the application of stress, if possible up to breaking point. If present, it will be investigated whether this property can be used as a quantitative measurement of the stress in the rock by merely measuring the electric charge on the rock surface.

In order to simulate stress conditions underground, the static

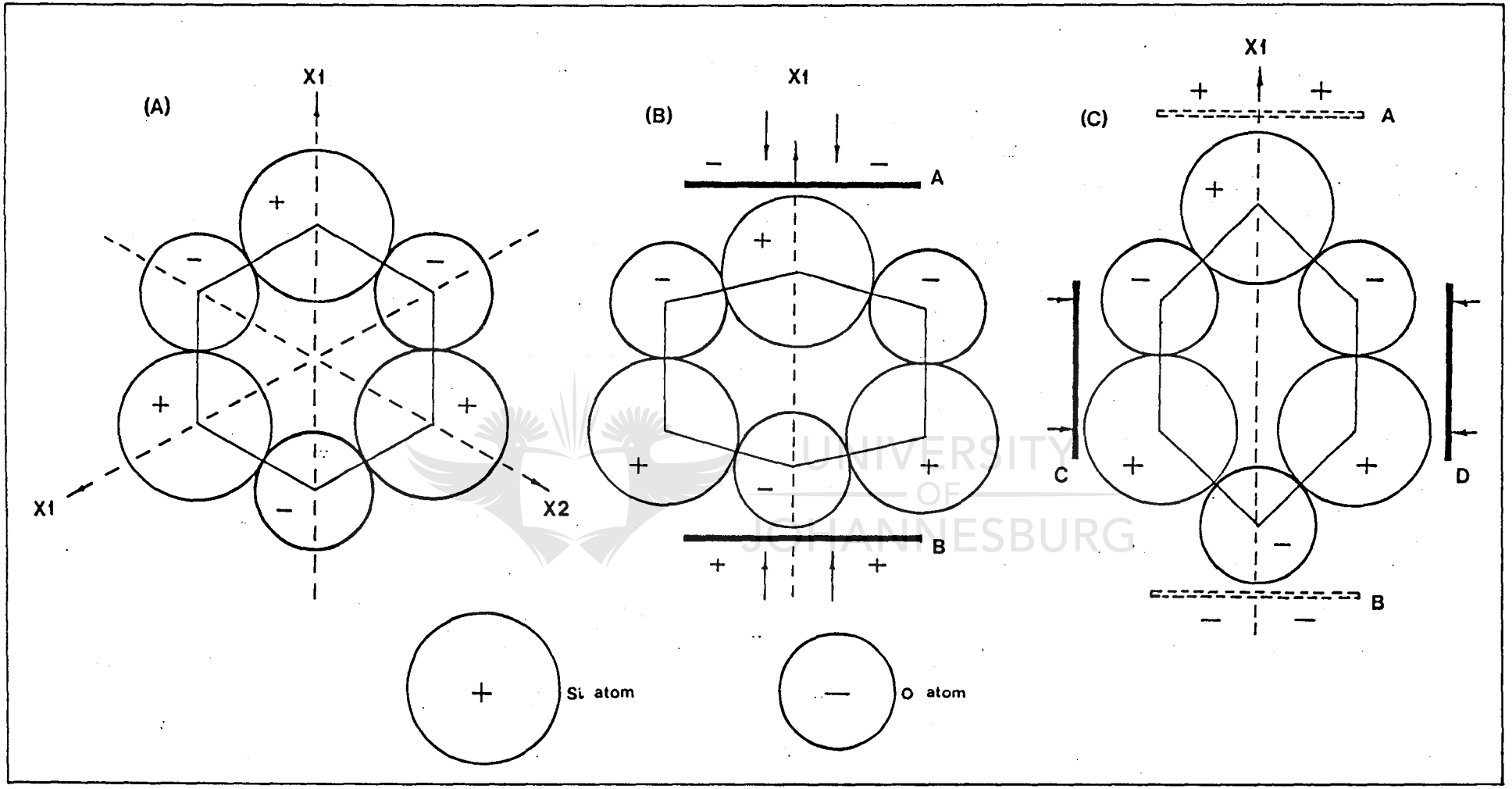

Figure 1 : Mechanical excitation of electric charge in development of the Piezoelectric effect in quartz. (Parkhomenko, 1971, figure 10).

method of applying load was utilised in the laboratory.

To test the validity of the exercise, the first part of the study was carried out on quartz because of its known piezoelectric property.

This study should thus be seen as a preliminary investigation into the behaviour of different quartzites at various stress levels.

2. NATURE AND ORIGIN OF PIEZOELECTRICITY.

Although the brothers P and J Curie discovered the piezoelectric phenomena in 1880, it was Lord Kelvin (1893, p331 - 341) at the end of the nineteenth century who presented a rough mechanical illustration of the theory of electric atoms to account for the piezoelectric properties of crystals.

His experiment consisted of a stack of 24 double plate units. Each unit consisted of a copper plate and a zinc plate soldered together. The double plates were then simply placed on top of one another. He showed that when a weight of a few kilogrammes was dropped from a height of a few millimetres above the top plate, an electric charge was liberated.

In the following paragraphs a possible explanation for the mechanical excitation of a piezoelectric charge in quartz as postulated by Meissner and given by Parkhomenko (1971, p38 - 39) will be discussed. Meissner's theory for the excitation of a piezoelectric effect is illustrated in Figure 1.

Assume that the silicon and oxygen atoms in silica are arranged in a six-sided configuration with each silicon atom having four positive unit charges, and each of the two oxygen atoms two negative unit charges. Due to structural arrangement of the silicon and oxygen atoms in the molecule, the latter is in a state of electrical neutrality.

In Figure 1 the two oxygen atoms surrounding the silicon atom are represented by a negative sign within a small circle. A disturbance in the relative positions of the atoms of each molecule, as will be the case when the crystal is stressed or strained, will lead to instability of the neutral electric charge. When stress is applied along the X_1 axis (electric axis) in Figure 1B, the silicon atom is forced between the oxygen pairs, resulting in a negative charge appearing on surface A, and a positive charge on surface B (a longitudinal piezoelectric effect). With stress applied perpendicular to the X_1 axis as in Figure 1C, the silicon atom moves outwards from the oxygen pairs thus causing a positive charge on surface A and a negative charge on surface B (transverse piezoelectric effect). This charge is measured in coulomb which is, by definition, the quantity of electricity passing any section of a circuit in one second when the current is one international ampere.

The polarization charge per unit area is given by $P = d\sigma$ where d is a constant called the piezoelectric modulus, and σ the tensile, compressive or shear stress. It is found that when a general stress σ_{ij} acts on a piezoelectric crystal e.g. quartz, each component of polarization P_i is linearly related to all the components of σ_{ij}. In general the relationship between P_i and σ_{ij} is written as $P_i = d_{ijk}\,\sigma_{jk}$ For quartz the (d_{ij}) matrix is expressed in the following form:

$$\begin{array}{c} \\ P_1 \\ P_2 \\ P_3 \end{array} \begin{array}{c} \begin{array}{cccccc} \sigma_1 & \sigma_2 & \sigma_3 & \sigma_4 & \sigma_5 & \sigma_6 \end{array} \\ \begin{bmatrix} d_{11} & d_{11} & 0 & d_{14} & 0 & 0 \\ 0 & 0 & 0 & 0 & -d_{14} & -2d_{11} \\ 0 & 0 & 0 & 0 & 0 & 0 \end{bmatrix} \end{array}$$

where P_1, and P_3 are polarizations along the various crystal axes. As can be seen from the third line of the matrix no condition of

stressing can produce polarization along the X_3 axis (optical axis).

If P and σ in the relationship $P = d\sigma$ are expressed in terms of charge Q and force F, then it can be seen from the equation below that for a thin long plate or rod cut parallel to the X_2 axis (transverse piezoelectric effect), the magnitude of the charge depends on the dimensions of the specimen

$$Q = d \times \frac{\text{area over which charge appears}}{\text{area over which pressure is applied}} \times F$$

From the above equation it follows that the charge which is measured, increases as the area on which it appears increases, or as the area on which the pressure is applied, decreases. According to Nye (1972, p126 - 129), when a quartz plate has been cut perpendicular to any arbitrary direction and subjected to a normal tensile stress, polarization will be set up with components in the direction of all the axes.

By making use of Polar-co-ordinates, Nye has shown mathematically that, as the direction of applied tensile stress moves around anti-clockwise, the longitudinal component of polarization gradually decreases until it becomes zero. This position is reached when the angle θ between the radius vector and the direction of the X_1 axis becomes zero. By further rotation of the tensile stress to θ' equal to 60° a diad axis is reached again, and the polarization becomes a maximum in that direction. From the above discussion it is obvious that maximum polarization can only occur if a rod or plate is cut parallel to the X_1 or X_2 axes of a quartz crystal.

3. INSTRUMENTATION.

3.1. Hydraulic Press.

Numerous problems have been experienced to obtain a press rigid

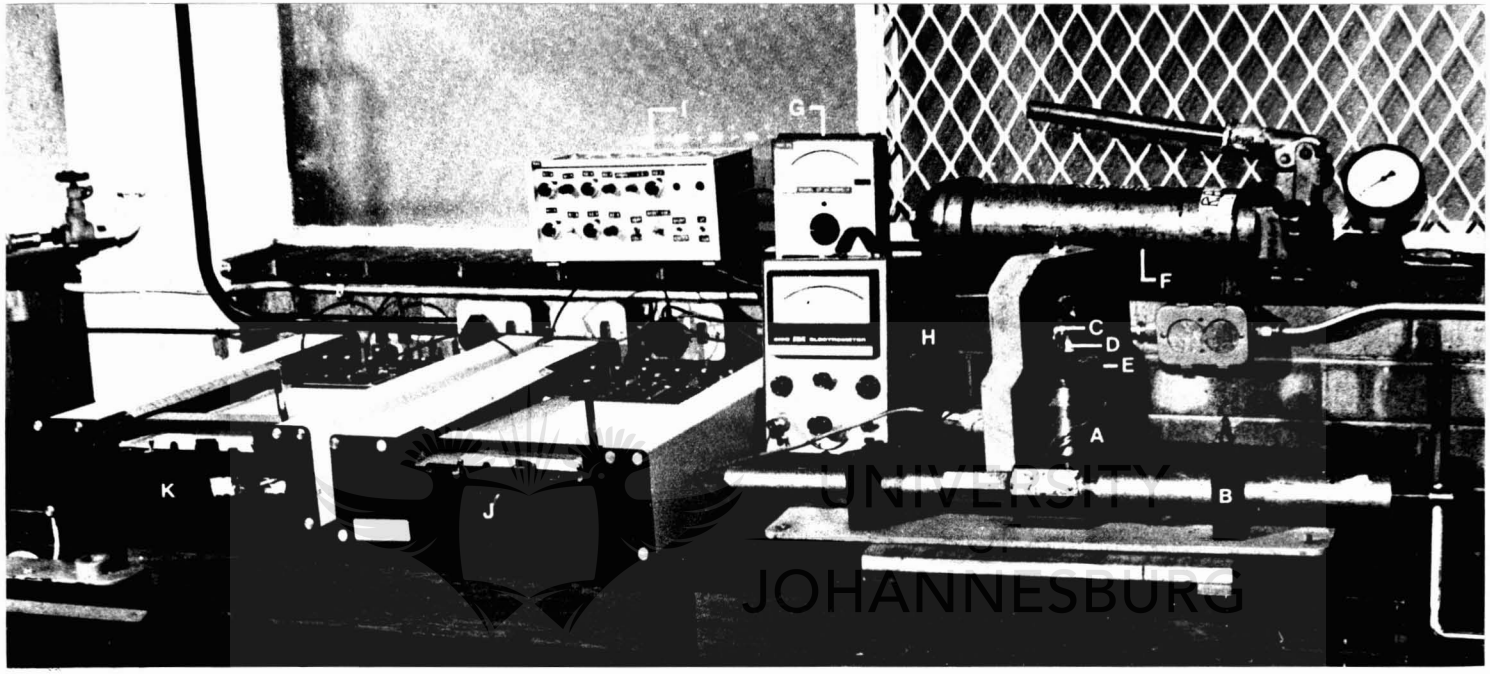

PLATE I Complete set-up for tests carried out in small hydraulic press.

A small hydraulic press
B intensifier
C cylindrical specimen between platens
D micrometers
E strain gauge and load cell unit
F hydraulic hand pump
G Philips electronic voltmeter
H Keithley model 610C electrometer
I power supply and amplifier for load cell and strain gauge
J X-Y plotter for load vs. electric charge
K X-Y plotter for load vs. displacement

and solid enough, where the load could be applied at a fairly constant and slow rate. The solution was found in a little hydraulic press that was specially built for this purpose by the Chamber of Mines Research Laboratories, Johannesburg, and can be seen in Plate 1. The frame, approximately 290 millimetres high, was cut from 50 millimetres mild steel in the shape of a bell. The cylinder of the hydraulic system is made of EN8 steel, with an outside diameter of 132 millimetres, an inside diameter of 89 millimetres and stands 94 millimetres high. The entrance of the oil is at the bottom of the cylinder. The 70 millimetre long piston is made of EN9 steel and has an area of 6207 square millimetres. The piston and the cylinder are highly polished with a clearance of between 0,0025 and 0,015 millimetres. The system is filled and bled with a hydraulic hand pump, whereafter the system is closed off with a tap. Load is applied by turning the handle of the intensifier. The intensifier which is being used for fine manipulations of load, consists of an outside cylindrical steel casing approximately 750 millimetres long with a threaded crank 12,7 millimetres in diameter . The piston attached to the crank has an area of 126,7 square millimetres. One turn on the intensifier crank represents 1,4 millimetres movement on the piston of the intensifier. The ratio of the piston of the intensifier to the piston of the hydraulic cylinder being 49:1 allows for very accurate application of load on the specimen in the press.

3.2. Top and Bottom Platens.

The top and bottom platens are made of EN30B steel hardened and machined down to the size of the specimens to be tested i.e. 10 millimetres diameter.

The bottom platen acts as the load-cell and fits in a ring-shaped

PLATE II Strain gauges and load cell unit used in small hydraulic press.

A bottom platen forming load cell
B strain gauges mounted on cantilevers
C pressure points for micrometers
D sourier plug for strain gauge amplifier
E sourier plug for load cell amplifier
F ring shaped base plate
G adjusting screws for cantilevers

base plate with the cantilevers attached to it. The strain gauges used in constructing the load-cell, has a k factor of 120 ohm, whereas those used for the strain or deformation measurements has a k factor of 600 ohm. Plate II illustrates the load-cell and cantilevers clearly. Strain was recorded by means of two steel rods pressing down on the cantilevers, each steel rod having a micrometer-head in order to calibrate the instrument.

3.3. Strain Gauge Amplifier.

3.3.1. Power Supply.

The power supply unit supplies voltages of + and - 15 volts D C for linear integrated circuits, as well as +5 volts D C for digital integrated circuits.

3.3.2. Signal Generator.

The signal generator has an adjustable frequency of 600, 1200 and 2400 Hz providing a symmetrical square wave swinging about zero potential (adjustable with a 10 ohm trimpot), and potential adjustment with a 10 turn potentiometer from 0 to ca.6.2. volts.

3.3.3. Strain Gauge Supply.

The signal from the signal generator is worked into two outputs 180° out of phase and amplified such, that the potential difference between the two outputs is equal to the digital reading in volts on the dial of the 10 turn potentiometer.

The output of the strain gauge supply is such, that any strain gauge bridge between 100 and 1000 ohm can be used without any noticeable change in the output voltage.

3.3.4. Differential Amplifier.

Differential amplifier with a constant gain of 10 is followed by an adjustable gain amplifier with a gain factor of 0-100 i.e. the adjustment of the amplifier is done with a 10 turn potentiometer

which indicates directly on the dial, the total gain of the amplifier.

3.3.5. Balancing the Bridge.

Tolerances of up to 1 per cent of the strain gauge resistance value can be balanced with the aid of two potentiometers (fine and coarse). Balancing is carried out with zero load (mechanical load on load cell) and adjusted for minimum output.

3.3.6. Rectifier and Recorder Output.

The rectifier is a full wave rectifier with ideal diodes, to filter the output to the peak value, and followed by a voltage follower which supplies the correct signal to drive the recorders.

3.3.7. X-Y Plotter type PL 100.

Two X-Y plotters type PL 100 were used to record all the measurements. It is a single pen recorder manufactured by J J Instruments, England. The one plotter was used to record load versus electric charge and the other for load versus displacement. This type of plotter has been designed for frequencies up to 1 Hz, but with the plug-in pre-amplifier type PL 120, it became more flexible because it provided variable gain, controlled by stepped attenuator and gain control.

The time base plug-in pre-amplifier type PL 121 was used for recording drift in electric charge.

The maximum writing speed for the above plotter is claimed to be 200 mm/sec with a repeatability of $\pm$ 0,5 per cent and linearity of $\pm$ 0,1 per cent.

The plug-in pre-amplifier type PL 120 for the strain gauge bridge on the load cell was operated at a scale setting of 100 mv/cm.

PLATE III Stiff testing machine of the Chamber of Mines Research Laboratories, Johannesburg.

A stiff testing machine

B micrometer (X 2)

C Philips electronic voltmeter

D load vs. electric charge and strain plotter

E time vs. electric charge plotter for drift

PLATE IV Cylindrical specimen in stiff testing machine.

A loading piston

B cylindrical specimen showing electrode coupling

C micrometer in position (X 2)

D lead from electrodes to electrometer

E machine frame

F bottom platen support

With the vernier adjustment the sensitivity of the recorder was turned to 100 mv/cm for quartz and quartzite respectively. Coulomb readings were recorded at 66,6 mv/cm and displacement at 10 mv/cm.

3.3.8. Calibration Procedure of Load Cell.

In order to make use of the load cell, it is necessary to calibrate it against a known load. For this purpose the rigid stiff testing machine at the Chamber of Mines Research Laboratories in Johannesburg, has been used.

The supply voltage of V_b to the load cell bridge was fixed at 2,5 V although it was also calibrated at supply voltages of 5 V and 10 V.

(a) Calibrate the X-Y plotter

(b) set V_b at the required voltage for the load cell e.g. 2,5 V, 5 V and 10 V

(c) balance load cell bridge with maximum gain and zero load on load cell

(d) turn gain down to zero and place a known load on the load cell e.g. 10 kN

(e) turn gain up until output voltage of load cell bridge is e.g. 0,2 V and record gain factor.

Table 1. Calibration of Load Cell Amplifier.

V	G	V/10 kN	X-Y Plotter Setting			
			100 mV/cm	200 mV/cm	500 mV/cm	1 V/cm
2,5	218	0,2	5 kN/cm	10 kN/cm	25 kN/cm	50 kN/cm
5,0	218	0,4	2,5 kN/cm	5 kN/cm	12,5 kN/cm	25 kN/cm
10	218	0,8	1,25 kN/cm	2,5 kN/cm	6,25 kN/cm	12,5 kN/cm
2,5	436	0,4	2,5 kN/cm	5 kN/cm	12,5 kN/cm	25 kN/cm
5,0	436	0,8	1,25 kN/cm	2,5 kN/cm	6,25 kN/cm	12,5 kN/cm
10	436	1,6	0,625 kN/cm	1,25 kN/cm	3,125 kN/cm	6,25 kN/cm

3.3.9. Calibration Procedure for Strain Measurement.

Calibration of strain gauges takes place at zero load.

(a) Calibrate X-Y plotter

(b) set V_b at 10 V for strain gauges and turn gain to zero

(c) increase each micrometer by 0,6 mm and adjust gain to record 200 mm on recorder

(d) turn micrometers back to a position where they are just touching the cantilevers, and then increase the reading on each micrometer individually to give 20 mm on recorder.

(e) move X-Y plotter to the starting point whereafter each micrometer reading is increased by 0,6 mm.

(f) do final adjustment for gain in order to reach 200 mm deviation on X axis of the X-Y plotter.

A deviation of 200 mm on the graph is representative of 0,6 mm displacement on the specimen.

3.3.10. Coulombmeter.

The electric charge set free by the specimen under stress is measured with a Keithley electrometer model 610C with an input impedance of greater than 10^{14} ohm. This electrometer has seventeen 1 X and 3 X ranges from 10^{-13} coulomb full scale to 10^{-5} coulomb with an accuracy of + 5 per cent of full scale on all ranges. It is claimed by the manufacturers that drift due to an offset current does not exceed 5×10^{-15} coulomb/second. All coulomb measurements were taken with feedback switch on fast. The output from the elctrometer was recorded on one of the X-Y plotters.

Block diagram in figure 3 clearly illustrates the electronics part of the experiment, whereas block diagram in figure 2 and plate 1 displays the arrangement as used in the laboratory.

3.4. Problems Encountered At The Beginning Of The Tests.

3.4.1. Specimen Shape and Size.

In the initial stages of the experiment, tests were carried out

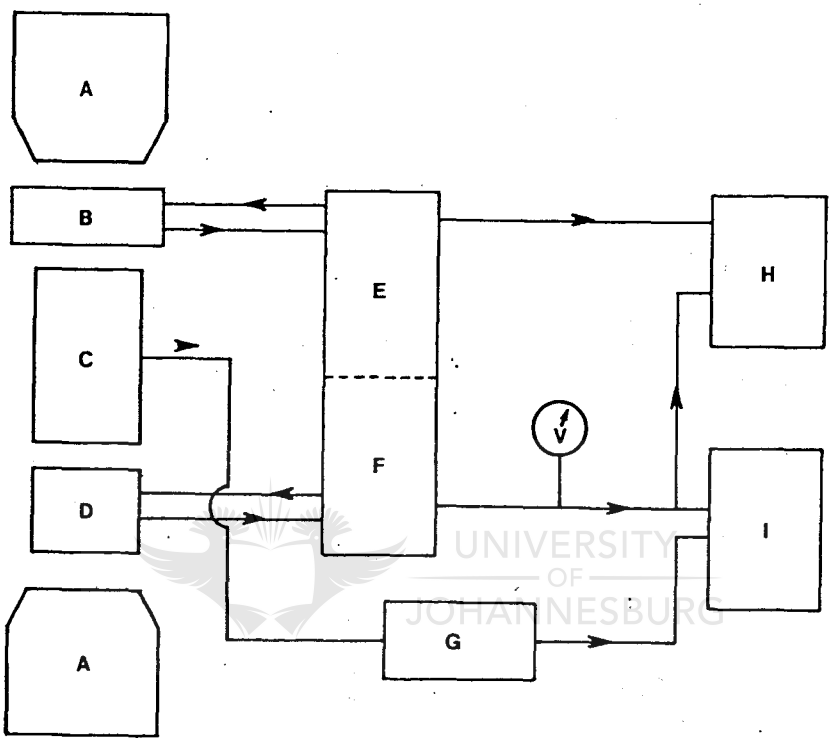

Figure 2 : Schematic arrangement for tests carried out in the small hydraulic press.

- A top and bottom platens
- B strain gauges for measuring deformation of cylinder
- C load cell
- D specimen
- E strain gauge power supply and amplifier
- F load cell power supply and amplifier
- G electrometer
- H X-Y plotter for load vs strain
- I X-Y plotter for load vs electric charge
- V Philips electronic voltmeter.

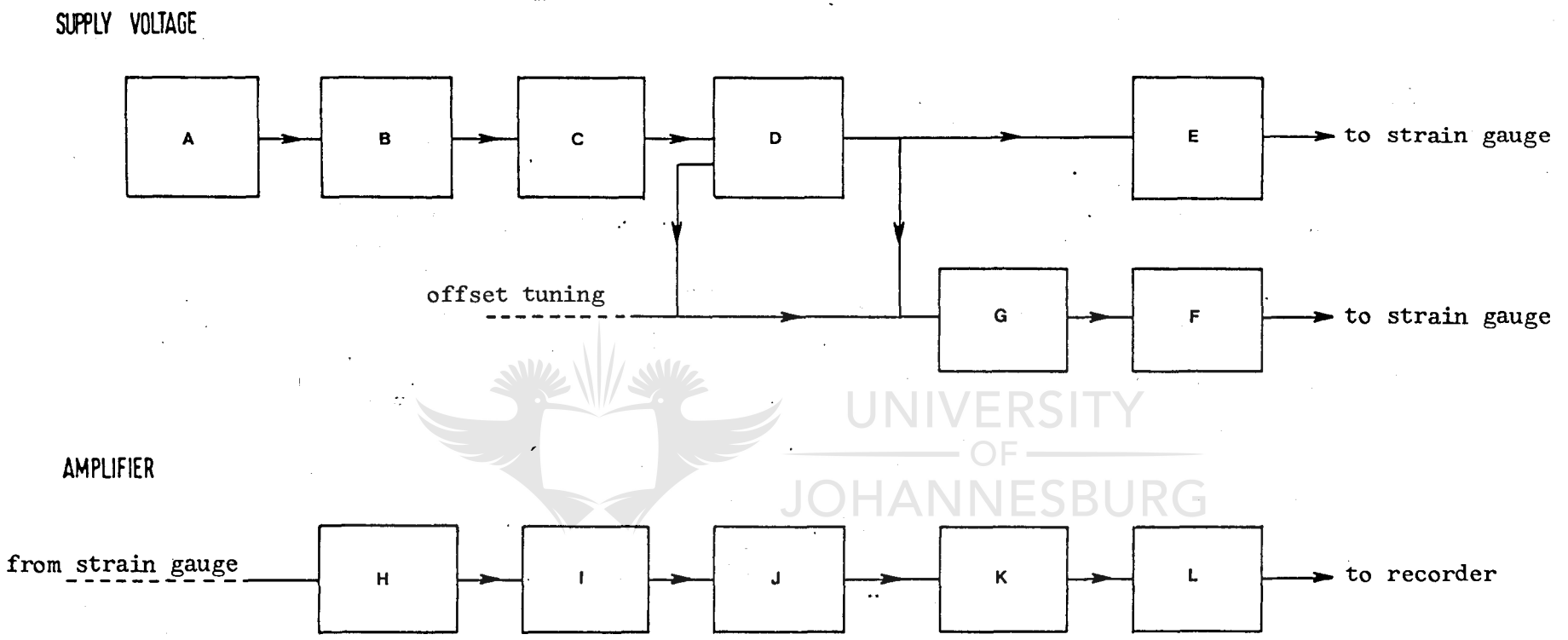

Figure 3 : Schematic diagram for supply voltage and amplifier system for load cell and strain gauges. (x 2)

A Signal generator
B limitter
C voltage devider
D constant gain amplifier
E driver
F driver
G polarity inverter
H differential amplifier and balance system
I tuning amplifier
J ideal amplifier
K filter
L driver

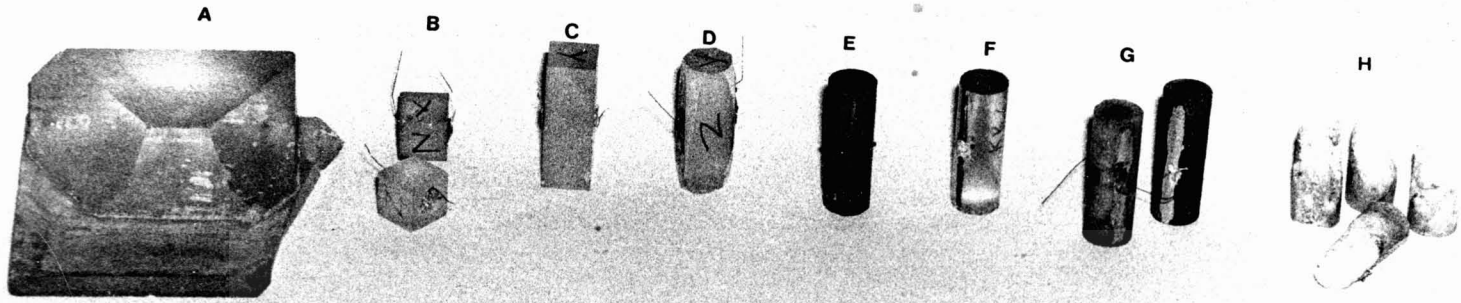

PLATE V Various specimen shapes and sizes.

A A natural quartz crystal from which quartz specimens were cut

B 1 cm cubes with the X and Z axes marked on sides and gold plated electrode wires

C 1 cm x 1 cm x 3 cm specimen with Y axis marked on top

D 1 cm x 1 cm x 3 cm specimen with spalling diagonally across corners

E gold coated 1 cm x 3 cm cylinder

F cylinder with pencil carbon and silver epoxy resin lines parallel to sides

G quartzite cylinders with electrodes and silver epoxy resin lines parallel to sides

H conical fracturing in quartzite cylinders.

on one centimetre quartz cubes which were cut and polished by Standard Telephone and Cables South Africa, Limited, Germiston. This shape and size proved very soon to be unsuitable for various reasons :-

(a) difficulty in handling the small cubes between the two platens

(b) difficulty in coupling electrodes for piezoelectric readings

(c) with a length to diameter ratio of 1:1 specimen failure under stress was very inconsistent which can be attributed to the rigidity of the platens restricting the lateral expansion of the ends of the specimen.

These problems were soon solved by using specimens one centimetre square and 3 centimetres long. This led to another problem of spalling diagonally across the corners of the specimen, that was not so prominent in the small cubes.

Finally it was decided to go to cylindrical specimens with a length to diameter ratio of 3:1 as laid down by the International Society for Rock Mechanics (1972, p6). This required changes in the shape of the top and bottom platens of the press, but certainly helped to eliminate diagonal spalling and in most cases conical fracturing. Jaeger et at (1969, p137 - 139) is of the opinion that with the two platens the same section as that of the specimen, any effects due to bending of the interface are eliminated, and those due to lateral restraint diminished because the platens also expand radially.

In the case of the quartz cylinders, the lateral expansion between the platens and quartz is for all practical purposes the same because the ratio ν/E in both cases is very close. In some quartzite cylinders, conical fracturing due to end effects was still experienced.

3.4.2. Electrode Coupling.

Three methods of electrode coupling were tried out :-

3.4.2.1. Two electrodes made out of alco-foil were placed between the cylinder and the top and bottom platens of the press. The lead from the electrometer was coupled to the electrodes by means of crocodile clips. With alco-foil as electrodes, it was very difficult to centre the cylinder on the bottom platen which not only led to early fracturing or uneven spalling of the cylinder, but also complicated strain measurements.

3.4.2.2. The second method was to take readings on the press. For this purpose a big mica washer was placed between the top platen and the frame of the press. A bolt screwed into the top platen and protruding through a hole in the frame served as the one electrode, whereas the base of the press served as the second electrode. To avoid contact between the platen and the frame, the bolt was encased in a nylon sleeve.

3.4.2.3. Eventually the electrodes were placed directly on the sides of the quartz or quartzite cylinder. Here again trial and error method was used to obtain the best contact between electrometer lead and cylinder.

(a) Quartz cylinders were gold coated except for two clean strips approximately 2 millimetres wide on either side to coincide with the axis which was marked beforehand on one of the flat ends of the crystal by the suppliers. Thin gold plated wires were then fused onto these gold coated sides half-way down the middle of the cylinder in order to connect the lead from the electrometer. Unfortunately readings were very irregular for some unknown reason.

(b) Electrodes made of thin wire and glued onto the cylinder with silver epoxy resin were finally accepted. The lead of the coulombmeter was soldered directly to the electrodes which proved to be the most effective method to record electric charge readings, especially in the case of quartzites.

An attempt to improve the contact area by two silver epoxy resin or graphite lines on the sides of the cylinder did not bring about any noticeable improvement in the readings.

When piezoelectric measurements were taken on quartzite specimens, very much lower readings were registered which required a low scale setting on the electrometer. It was found that at scale settings of 1×10^{-8} coulomb full range or lower, the electrometer became very sensitive to electrical disturbances, in particular static electricity.

On one occasion a bat was flying up against the ceiling of the room whilst drift readings were being taken with zero load on the cylinder. This caused the needle of the electrometer to move backwards and forwards so fast over the full scale range, that the instrument had to be switched off.

To overcome this instability, a short co-axial cable was constructed to replace the original lead supplied with the instrument, and to fight stray electricity, a Faraday cage made of copper-gauze and a cardboard box was placed over the press. The latter did not really improve the condition and was soon abandoned.

4. RESULTS OBTAINED ON QUARTZ CYLINDERS.

4.1. Origin of Quartz Cylinders.

The quartz cylinders used during the first part of this project

TABLE 2 PIEZOELECTRIC POLARIZATION VALUES AT DIFFERENT MECHANICAL STRESS LEVELS FOR STC QUARTZ CYLINDERS TESTED IN SMALL HYDRAULIC PRESS

STC QUARTZ NUMBER	LOAD kN	UNIAXIAL COMPRESSIVE STRESS MPa	PIEZOELECTRIC POLARIZATION $C/m^2 \times 10^{-4}$	PIEZOELECTRIC MODULUS d $C/N \times 10^{-12}$	AVERAGE d $C/N \times 10^{-12}$
STC 1	10	127,3	2,00	1,57	
	20	254,6	4,00	1,57	1,56
	30	381,9	5,93	1,55	
	35	445,6	6,67	1,55	
STC 2	10	127,3	2,00	1,57	
	20	254,6	4,11	1,61	1,60
	30	381,9	6,22	1,63	
	31,5	401,0	6,22	1,62	
STC 3	10	127,3	2,22	1,74	
	20	254,6	4,30	1,69	1,70
	30	381,9	6,38	1,67	
STC 4	10	127,3	2,22	1,74	
	20	254,6	4,44	1,74	1,74
	30	381,9	6,67	1,74	
STC 5	10	127,3	1,78	1,40	
	20	254,6	3,56	1,40	1,40
	29	369,2	5,11	1,40	
STC 6	10	127,3	2,00	1,57	
	20	254,6	4,22	1,66	1,64
	30	381,9	6,44	1,69	
STC 7	10	127,3	1,56	1,23	
	20	254,6	3,00	1,18	1,17
	30	381,9	4,44	1,16	
	40	509,2	5,67	1,11	
STC 8	10	127,3	1,78	1,40	
	20	254,6	3,78	1,48	1,45
	30	381,9	5,56	1,46	
STC 9	10	127,3	1,72	1,35	
	20	254,6	3,22	1,26	1,33
	30	381,9	5,22	1,37	
	37,5	477,4	6,11	1,35	
STC 10	10	127,3	1,50	1,18	
	20	254,6	3,06	1,20	1,18
	30	381,9	4,56	1,19	
	31	394,7	4,67	1,19	
STC 11	10	127,3	1,44	1,13	
	20	254,6	2,89	1,14	1,14
	30	381,9	4,44	1,16	

TABLE 2 (CONTINUED) PIEZOELECTRIC POLARIZATION VALUES AT DIFFERENT MECHANICAL STRESS LEVELS FOR STC QUARTZ CYLINDERS TESTED IN SMALL HYDRAULIC PRESS

STC QUARTZ NUMBER	LOAD kN	UNIAXIAL COMPRESSIVE STRESS MPa	PIEZOELECTRIC POLARIZATION $C/m^2 \times 10^{-4}$	PIEZOELECTRIC MODULUS d $C/N \times 10^{-12}$	AVERAGE d $C/N \times 10^{-12}$
STC 12	10	127,3	1,73	1,36	1,34
	20	254,6	3,37	1,32	
STC 13	10	127,3	1,33	1,04	1,03
	20	254,6	2,56	1,00	
STC 14	10	127,3	1,11	0,87	
	20	254,6	2,22	0,87	
	30	381,9	3,11	0,81	
	40	509,2	4,22	0,83	0,84
	50	636,5	5,33	0,84	
	60	763,8	6,22	0,82	
	70	891,2	7,33	0,82	
	80	1018,5	8,44	0,83	
	86	1095,5	9,11	0,81	
STC 15	10	127,3	2,37	1,86	
	20	254,6	4,44	1,74	
	30	381,9	6,67	1,75	
	40	509,2	8,89	1,76	1,75
	50	636,2	11,11	1,75	
	60	763,8	13,33	1,75	
	70	891,2	15,57	1,75	
STC 16	10	127,3	1,67	1,31	
	20	254,6	3,33	1,31	
	30	381,9	4,89	1,28	
	40	509,2	6,44	1,26	
	50	636,5	8,22	1,29	1,28
	60	763,8	9,78	1,28	
	70	891,2	11,33	1,27	
	80	1018,5	12,89	1,27	
	83,5	1063,0	13,33	1,26	
STC 17	10	127,3	2,00	1,57	
	20	254,6	3,89	1,53	
	30	381,9	5,67	1,49	
	40	509,2	7,33	1,44	
	50	636,5	9,11	1,43	1,45
	60	763,8	10,89	1,31	
	70	891,2	12,78	1,43	
	80	1018,5	14,44	1,92	
	88	1120,0	15,78	1,41	
STC 18	10	127,3	1,78	1,40	
	20	254,6	3,44	1,35	
	30	381,9	5,20	1,36	
	40	509,2	6,92	1,36	1,38
	50	636,5	8,88	1,40	
	60	763,8	10,67	1,40	
	70	891,2	12,44	1,40	
	80	1018,5	14,24	1,40	
	90	1145,8	15,89	1,38	

TABLE 2 (CONTINUED) PIEZOELECTRIC POLARIZATION VALUES AT DIFFERENT MECHANICAL STRESS LEVELS FOR STC QUARTZ CYLINDERS TESTED IN SMALL HYDRAULIC PRESS

STC QUARTZ NUMBER	LOAD kN	UNIAXIAL COMPRESSIVE STRESS MPa	PIEZOELECTRIC POLARIZATION $C/m^2 \times 10^{-4}$	PIEZOELECTRIC MODULUS d $C/N \times 10^{-12}$	AVERAGE d $C/N \times 10^{-12}$
STC 19	10	127,3	1,83	1,44	
	20	254,6	3,72	1,46	
	30	381,9	5,47	1,43	
	40	509,2	7,17	1,41	1,43
	50	636,5	9,06	1,42	
	60	763,8	11,00	1,44	
	70	891,2	12,44	1,40	
STC 20	10	127,3	1,33	1,04	
	20	254,6	2,64	1,04	
	30	381,9	4,27	1,12	1,12
	40	509,2	5,70	1,12	
	50	636,5	7,44	1,17	
	56	712,9	8,44	1,10	
STC 21	10	127,3	1,78	1,40	
	20	254,6	3,50	1,37	
	30	381,9	5,28	1,38	1,38
	40	509,2	7,00	1,37	
	40,5	515,6	7,22	1,36	
STC 22	10	127,3	1,68	1,40	
	20	254,6	3,35	1,32	
	30	381,9	5,13	1,34	
	40	509,2	6,72	1,32	1,32
	50	636,5	8,28	1,30	
	60	763,8	9,78	1,28	
	70	891,2	11,11	1,25	
STC 23	10	127,3	2,00	1,57	
	20	254,6	4,00	1,52	
	30	381,9	5,87	1,54	
	40	509,2	7,81	1,53	
	50	636,5	9,72	1,53	1,51
	60	763,8	11,49	1,50	
	70	891,2	13,56	1,52	
	80	1018,5	15,33	1,51	
	90	1145,8	17,33	1,51	
STC 24	10	127,3	1,87	1,47	
	20	254,6	3,71	1,46	1,46
	30	381,9	5,49	1,44	
	40	509,2	7,50	1,47	
STC 25	10	127,3	2,04	1,60	
	20	254,6	4,44	1,74	
	30	381,9	6,67	1,75	1,71
	40	509,2	8,78	1,72	
	50	636,5	11,00	1,73	

TABLE 2 (CONTINUED) PIEZOELECTRIC POLARIZATION VALUES AT DIFFERENT MECHANICAL STRESS LEVELS FOR STC QUARTZ CYLINDERS TESTED IN SMALL HYDRAULIC PRESS

STC QUARTZ NUMBER	LOAD kN	UNIAXIAL COMPRESSIVE STRESS MPa	PIEZOELECTRIC POLARIZATION $C/m^2 \times 10^{-4}$	PIEZOELECTRIC MODULUS d $C/N \times 10^{-12}$	AVERAGE d $C/N \times 10^{-12}$
STC 26	10	127,3	1,94	1,52	
	20	254,6	3,94	1,55	
	30	381,9	5,94	1,56	1,55
	40	509,2	7,76	1,52	
	50	636,5	9,64	1,51	
	58,5	744,7	11,56	1,52	
STC 27	10	127,3	1,89	1,48	
	20	254,6	3,78	1,48	
	30	381,9	5,61	1,47	
	40	509,2	7,46	1,47	
	50	636,5	9,25	1,45	1,44
	60	763,8	10,85	1,42	
	70	891,2	12,29	1,38	
	80	1018,5	14,11	1,39	
	89	1133,0	15,56	1,37	
STC 28	10	127,3	1,44	1,13	
	20	254,6	3,11	1,22	
	30	381,9	4,56	1,19	1,20
	40	509,2	6,22	1,22	
	50	636,5	7,78	1,22	
STC 29	10	127,3	2,00	1,57	
	20	254,6	3,86	1,52	
	30	381,9	5,68	1,49	
	40	509,2	7,63	1,50	1,50
	50	636,5	9,52	1,50	
	60	763,8	11,40	1,49	
	70	891,2	13,04	1,46	
	80	1018,5	14,78	1,45	
	85	1082,0	15,00	1,39	
STC 30	10	127,3	2,11	1,66	
	20	254,6	4,16	1,63	
	30	381,9	6,33	1,66	
	40	509,2	8,40	1,65	
	50	636,5	10,60	1,66	1,66
	60	763,8	12,75	1,67	
	70	891,2	14,75	1,66	
	80	1018,5	16,89	1,66	
STC 31	10	127,3	2,22	1,74	
	20	254,6	4,50	1,77	
	30	381,9	6,74	1,76	
	40	509,2	8,98	1,76	1,74
	50	636,5	11,16	1,75	
	60	763,8	13,19	1,73	
	70	891,2	15,22	1,71	
	80	1018,5	17,44	1,71	

TABLE 2 (CONTINUED) PIEZOELECTRIC POLARIZATION VALUES AT DIFFERENT MECHANICAL STRESS LEVELS FOR STC QUARTZ CYLINDERS TESTED IN SMALL HYDRAULIC PRESS

STC QUARTZ NUMBER	LOAD kN	UNIAXIAL COMPRESSIVE STRESS MPa	PIEZOELECTRIC POLARIZATION $C/m^2 \times 10^{-4}$	PIEZOELECTRIC MODULUS $C/N \times 10^{-12}$	AVERAGE d $C/N \times 10^{-12}$
STC 32	10	127,3	2,00	1,57	
	20	254,6	4,05	1,59	
	30	381,9	6,06	1,59	
	40	509,2	8,17	1,60	
	50	636,5	10,28	1,62	
	60	763,8	12,27	1,61	
	70	891,2	14,25	1,60	1,60
	80	1018,5	16,26	1,60	
	90	1145,8	18,28	1,60	
	100	1273,0	20,22	1,59	
STC 33	10	127,3	2,00	1,51	
	20	254,6	3,92	1,54	
	30	381,9	5,87	1,54	
	40	509,2	7,78	1,53	
	50	636,5	9,67	1,52	1,54
	60	763,8	11,67	1,53	
	70	891,2	13,83	1,55	
	80	1018,5	15,67	1,54	
STC 34	10	127,3	1,78	1,40	
	20	254,6	3,69	1,45	
	30	381,9	5,62	1,47	
	40	509,2	7,07	1,39	
	50	636,5	8,78	1,38	1,41
	60	763,8	10,59	1,39	
	70	891,2	12,41	1,39	
	80	1018,5	14,44	1,42	
	86	1094,8	15,22	1,40	
STC 35	10	127,3	2,00	1,57	
	20	254,6	4,11	1,61	
	30	381,9	6,22	1,63	
	40	509,2	8,33	1,64	
	50	636,5	10,33	1,62	
	60	763,8	12,44	1,63	1,61
	70	891,2	14,55	1,63	
	80	1018,5	16,56	1,63	
	90	1145,8	18,56	1,62	
	100	1273,0	20,44	1,61	
	110	1400,4	22,44	1,60	
	120	1527,7	24,33	1,59	
STC 36	10	127,3	1,89	1,48	
	20	254,6	3,78	1,48	
	30	381,9	5,56	1,46	
	40	509,2	7,43	1,46	1,47
	50	636,5	9,33	1,47	
	60	763,8	11,22	1,47	
	70	891,2	13,11	1,47	
	73,5	935,7	13,22	1,41	

TABLE 2 (CONTINUED) PIEZOELECTRIC POLARIZATION VALUES AT DIFFERENT MECHANICAL STRESS LEVELS FOR STC QUARTZ CYLINDERS TESTED IN SMALL HYDRAULIC PRESS

STC QUARTZ NUMBER	LOAD kN	UNIAXIAL COMPRESSIVE STRESS MPa	PIEZOELECTRIC POLARIZATION $C/m^2 \times 10^{-4}$	PIEZOELECTRIC MODULUS d $C/N \times 10^{-12}$	AVERAGE d $C/N \times 10^{-12}$
STC 37	10	127,3	1,11	0,87	
	20	254,6	2,33	0,92	
	30	381,9	3,33	0,87	0,86
	40	509,2	4,29	0,84	
	50	636,5	5,22	0,82	
	60	763,8	6,28	0,82	
STC 38	10	127,3	1,96	1,54	
	20	254,6	4,11	1,61	
	30	381,9	6,19	1,62	
	40	509,2	8,40	1,65	
	50	636,5	10,58	1,66	1,58
	60	763,8	12,48	1,63	
	70	891,2	14,21	1,59	
	80	1018,5	15,11	1,47	
	90	1145,8	17,00	1,46	
	95	1209,0	17,89	1,48	
STC 39	10	127,3	1,69	1,33	
	20	254,6	3,54	1,39	
	30	381,9	5,61	1,47	
	40	509,2	7,55	1,48	
	50	636,5	9,39	1,47	
	60	763,8	11,30	1,48	1,46
	70	891,2	13,28	1,49	
	80	1018,5	14,94	1,47	
	90	1145,8	17,17	1,50	
	100	1273,0	18,83	1,53	
	102,5	1305,0	19,39	1,49	
STC 40	10	127,3	1,89	1,48	
	20	254,6	3,89	1,53	
	30	381,9	5,78	1,51	
	40	509,2	7,67	1,51	1,51
	50	636,5	9,67	1,52	
	60	763,8	11,56	1,51	
	70	891,2	13,44	1,51	
STC 41	10	127,3	2,09	1,64	
	20	254,6	4,49	1,76	
	30	381,9	6,74	1,76	
	40	509,2	9,09	1,77	
	50	636,5	11,37	1,79	1,77
	60	763,8	13,60	1,78	
	70	891,2	15,78	1,77	
	80	1018,5	18,28	1,79	
	90	1145,8	20,61	1,80	
	100	1273,0	22,78	1,85	
	101	1286,0	23,22	1,80	

TABLE 2 (CONTINUED) PIEZOELECTRIC POLARIZATION VALUES AT DIFFERENT MECHANICAL STRESS LEVELS - FOR STC QUARTZ CYLINDERS TESTED IN SMALL HYDRAULIC PRESS.

STC QUARTZ NUMBER	LOAD kN	UNIAXIAL COMPRESSIVE STRESS MPa	PIEZOELECTRIC POLARIZATION $C/m^2 \times 10^{-4}$	PIEZOELECTRIC MODULUS d $C/N \times 10^{-12}$	AVERAGE d $C/N \times 10^{-12}$
STC 42	10	127,3	2,10	1,65	
	20	254,6	4,30	1,69	
	30	381,9	6,33	1,66	1,74
	40	509,2	8,67	1,96	
	50	636,5	11,00	1,73	
STC 43	10	127,3	1,22	0,95	
	20	254,6	2,50	0,98	
	30	381,9	3,94	1,03	
	40	509,2	5,28	1,04	
	50	636,5	6,61	1,04	1,03
	60	763,8	8,00	1,05	
	70	891,2	9,44	1,06	
	80	1018,5	10,66	1,05	
	83,5	1063,0	11,11	1,05	

TABLE 3 AVERAGE PIEZOELECTRIC POLARIZATION VALUES AT DIFFERENT MECHANICAL STRESS LEVELS FOR QUARTZ CYLINDERS TESTED IN SMALL HYDRAULIC PRESS.

LOAD kN	UNIAXIAL COMPRESSIVE STRESS MPa	PIEZOELECTRIC POLARIZATION $C/m^2 \times 10^{-4}$	PIEZOELECTRIC MODULUS d $C/N \times 10^{-12}$	NUMBER OF CYLINDERS TESTED
10	127,3	1,78	1,40	43
20	254,6	3,57	1,40	43
30	381,9	5,37	1,41	40
40	509,2	7,28	1,43	31
50	636,5	9,20	1,45	28
60	763,8	10,98	1,49	23
70	891,2	12,95	1,45	22
80	1018,5	14,66	1,44	17
90	1145,8	18,12	1,58	6
100	1273,0	20,57	1,62	4
110	1400,4	22,44	1,60	1
120	1527,7	24,33	1,59	1

TABLE 4 PIEZOELECTRIC POLARIZATION VALUES AT DIFFERENT MECHANICAL STRESS LEVELS FOR STC QUARTZ CYLINDERS TESTED IN STIFF TESTING MACHINE

STC QUARTZ NUMBER	LOAD kN	UNIAXIAL COMPRESSIVE STIRESS MPa	PIEZOELECTRIC POLARIZATION $C/m^2 \times 10^{-4}$	PIEZOELECTRIC MODULUS $C/N \times 10^{-12}$	AVERAGE d $C/N \times 10^{-12}$
STC 44	10	127,3	0,50	0,39	
	20	254,6	1,00	0,39	
	30	381,9	1,60	0,42	0,40
	40	509,2	2,00	0,39	
	50	636,5	2,60	0,41	
	60	763,8	3,10	0,41	

TABLE 4 (CONTINUED) PIEZOELECTRIC POLARIZATION VALUES AT DIFFERENT MECHANICAL STRESS LEVELS FOR STC QUARTZ CYLINDERS TESTED IN STIFF TESTING MACHINE.

STC QUARTZ NUMBER	LOAD kN	UNIAXIAL COMPRESSIVE STRESS MPa	PIEZOELECTRIC POLARIZATION $C/m^2 \times 10^{-4}$	PIEZOELECTRIC MODULUS d $C/N \times 10^{-12}$	AVERAGE d $C/N \times 10^{-12}$
STC 45	10	127,3	0,60	0,47	
	20	254,6	1,10	0,43	
	30	381,9	1,70	0,45	
	40	509,2	2,20	0,43	0,44
	50	636,5	2,80	0,44	
	60	763,8	3,40	0,45	
	61,3	780,3	3,50	0,45	
STC 46	10	127,3	0,70	0,55	
	20	254,6	1,30	0,51	
	30	381,9	1,95	0,51	
	40	509,2	2,55	0,50	
	50	636,5	3,20	0,50	0,51
	60	763,8	3,90	0,51	
	70	891,2	4,55	0,51	
	80	1018,5	5,20	0,51	
	85,1	1083,3	5,53	0,51	
STC 47	10	127,3	0,65	0,51	
	20	254,6	1,30	0,51	
	30	381,9	2,00	0,51	0,51
	40	509,2	2,60	0,51	
	50	636,5	3,20	0,50	
	60	763,8	4,00	0,52	
	70	891,2	4,60	0,52	
	80	1018,5	5,20	0,51	
	85	1083,2	5,53	0,51	

TABLE 5 PIEZOELECTRIC POLARIZATION VALUES AT DIFFERENT MECHANICAL STRESS LEVELS FOR 2 cm LONG QUARTZ CYLINDERS TESTED IN STIFF TESTING MACHINE

STC QUARTZ NUMBER	LOAD kN	UNIAXIAL COMPRESSIVE STRESS MPa	PIEZOELECTRIC POLARIZATION $C/m^2 \times 10^{-4}$	PIEZOELECTRIC MODULUS d $C/N \times 10^{-12}$	AVERAGE d $C/N \times 10^{-12}$
STC 48	10	127,3	0,40	0,31	
	20	254,6	0,90	0,35	
	30	381,9	1,30	0,34	
	40	509,2	1,70	0,33	
	50	636,5	2,10	0,33	0,33
	60	763,8	2,60	0,34	
	70	891,2	3,00	0,34	
	80	1018,5	3,40	0,33	
	90	1145,8	3,80	0,33	
	100	1273,0	4,30	0,34	
	110	1400,4	4,70	0,34	
	118	1508,5	5,03	0,33	

TABLE 5 (CONTINUED) PIEZOELECTRIC POLARIZATION VALUES AT DIFFERENT MECHANICAL STRESS LEVELS FOR 2 cm LONG QUARTZ CYLINDERS TESTED IN AVERY TESTING MACHINE

STC QUARTZ NUMBER	LOAD kN	UNIAXIAL COMPRESSIVE STRESS MPa	PIEZOELECTRIC POLARIZATION $C/m^2 \times 10^{-4}$	PIEZOELECTRIC MODULUS d $C/N \times 10^{-12}$	AVERAGE d $C/N \times 10^{-12}$
STC 49	10	127,3	0,50	0,39	
	20	254,6	0,95	0,37	
	30	381,9	1,40	0,37	
	40	509,2	1,80	0,35	0,35
	50	636,5	2,25	0,35	
	60	763,8	2,70	0,35	
	70	891,2	3,15	0,35	
	80	1018,5	3,60	0,35	
	90	1145,8	4,00	0,35	
	100	1273,0	4,45	0,35	
	110	1400,4	4,85	0,35	
	111,6	1420,8	4,90	0,34	
STC 50	10	127,3	0,60	0,47	
	20	254,6	1,15	0,45	
	30	381,9	1,80	0,46	
	40	509,2	2,30	0,45	
	50	636,5	3,00	0,47	
	60	763,8	3,60	0,47	0,46
	70	891,2	4,15	0,47	
	80	1018,2	4,75	0,46	
	90	1145,8	5,30	0,46	
	100	1273,0	5,90	0,46	
	110	1400,4	6,50	0,46	
	120	1530,0	7,10	0,47	

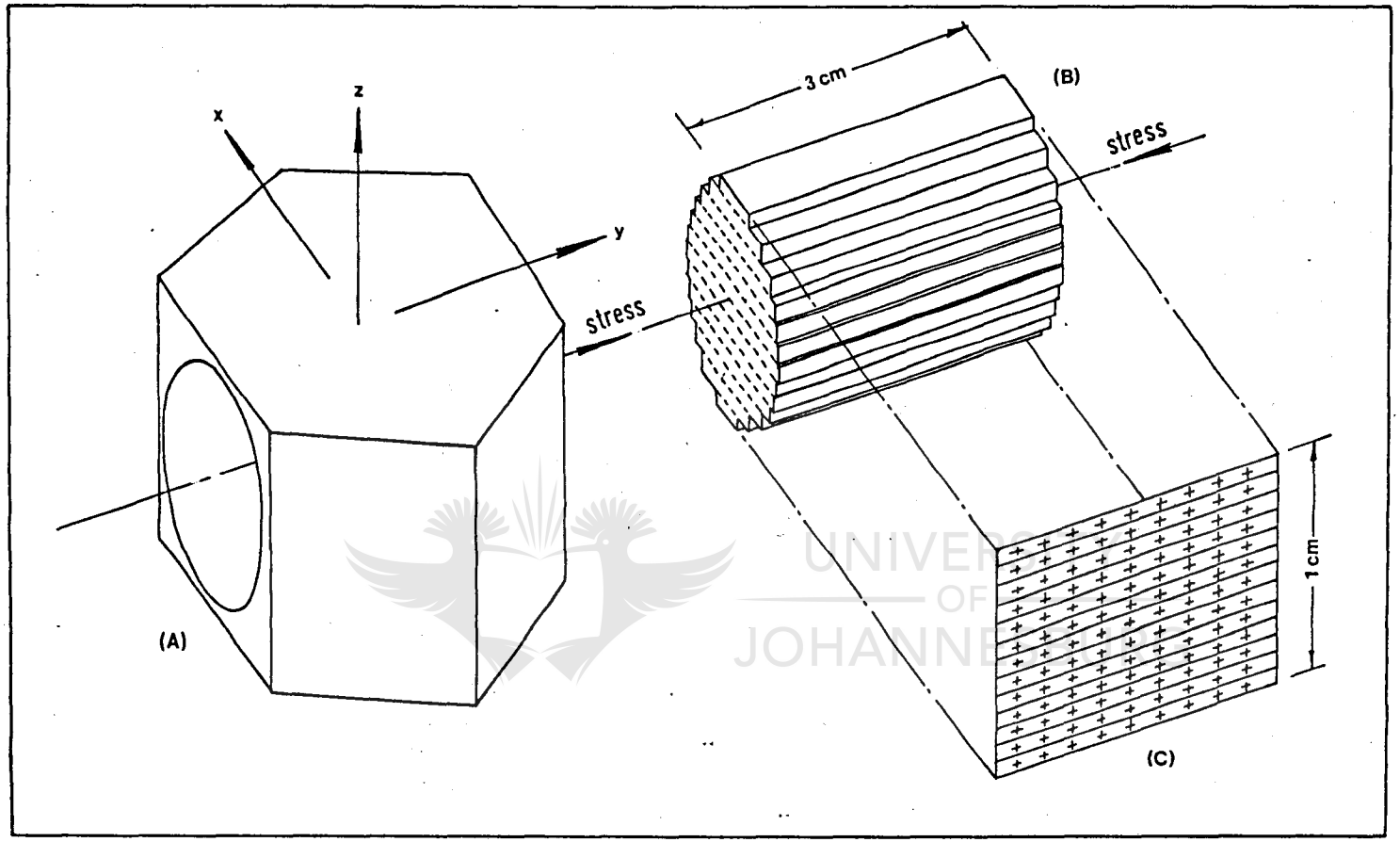

Figure 4 : Area of piezoelectric polarization in quartz cylinder.

(a) quartz crystal with directions of X, Y and Z axes.

(b) cylindrical specimen theoretically divided up into numerous very thin rectangular plates parallel to X and Y axes.

(c) piezoelectric charge appearing on projected flat surface, 3 cm x 1 cm with application of compressive stress parallel to Y axis.

were cut by Standard Telephones and Cables of South Africa, Limited, from natural quartz crystals with a very low impurity content.

All cylinders were cut with the long axis parallel to the Y axis of the mother crystal, whereafter the direction of the X axis was marked on both flat ends of each individual cylinder.

4.2. Effective Area of Polarization.

During laboratory tests quartz cylinders were subjected to various compressive stresses parallel to the Y axis, and the electric charge thus generated measured on the surface perpendicular to the X axis. This notation differs from that of Parkhomenko (1971, p40, figure 11) where X_1, X_2 and X_3 are replaced by X, Y and Z respectively.

In using this method the piezoelectric effect is transverse, in which case, according to Parkhomenko (1971, p40), the magnitude of the electric charge depends on the dimensions of the specimen.

In order to calculate the piezoelectric charge or polarization per unit area, it is necessary to define the area on which the charge appears. This is done by dividing the quartz cylinder for all practical purposes up into numerous very thin rectangular plates parallel to the Y and X axes as shown in figure 4.

When stress is applied along the Y axis of the cylinder, a minute electric charge will appear on the surface perpendicular to the X axis of each individual thin plate. The total area over which polarization takes place will be the sum total of the areas of all the little rectangular plates which in the above case is 3 cm^2.

4.3. Nature of Piezoelectricity on Quartz.

From a total of 66 quartz cylinders subjected to uniaxial compressive

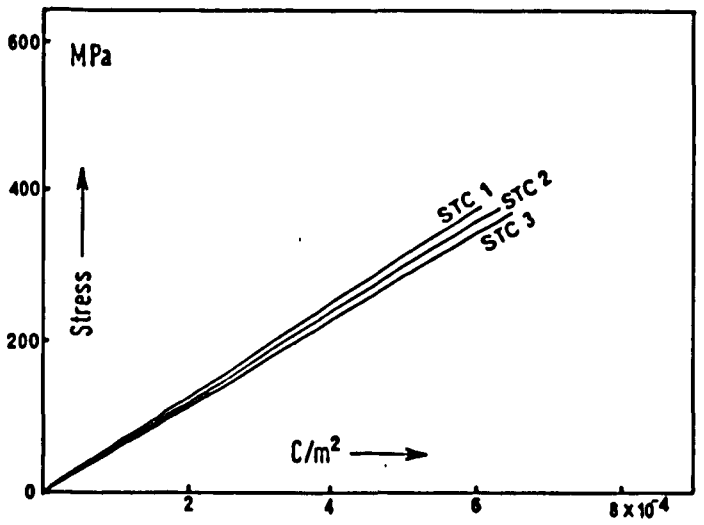

Figure 5 : Relationship between mechanical stress and piezoelectric polarization for STC 1, STC 2 and STC 3 tested in small hydraulic press.

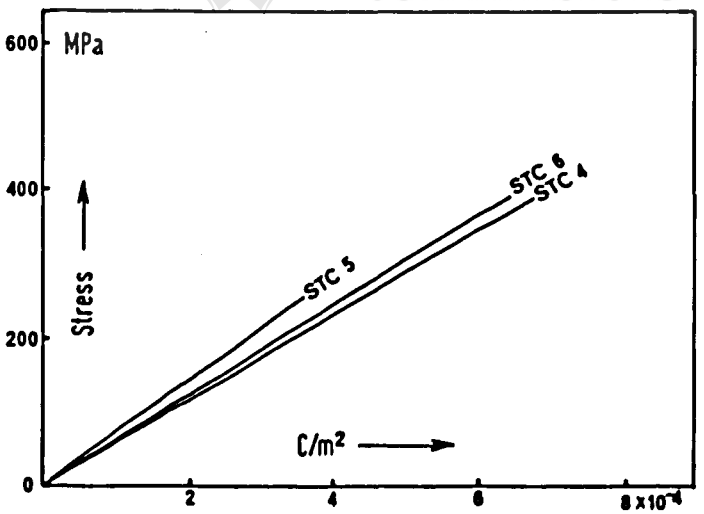

Figure 6 : Relationship between mechanical stress and piezoelectric polarization for STC 4, STC 5 and STC 6 tested in small hydraulic press.

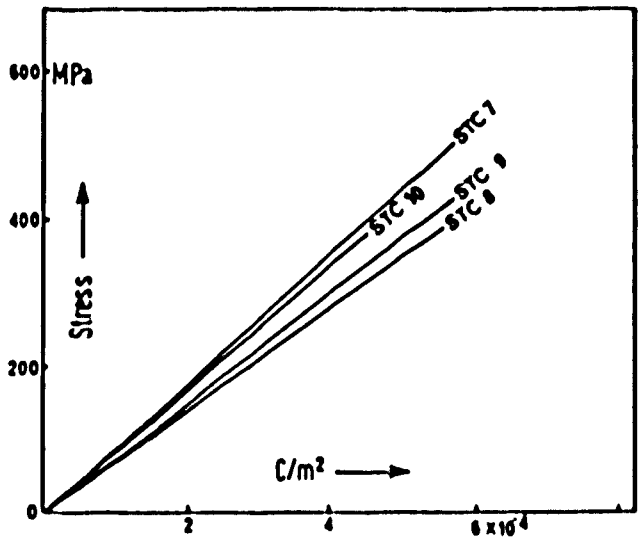

Figure 7 : Relationship between mechanical stress and piezo-electric polarization for STC 7, STC 8, STC 9 and STC 10 tested in small hydraulic press.

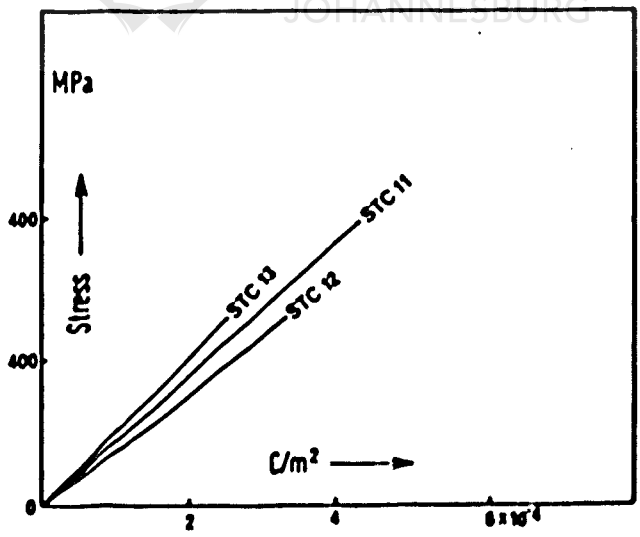

Figure 8 : Relationship between mechanical stress and piezo-electric polarization for STC 11, STC 12 and STC 13 tested in small hydraulic press.

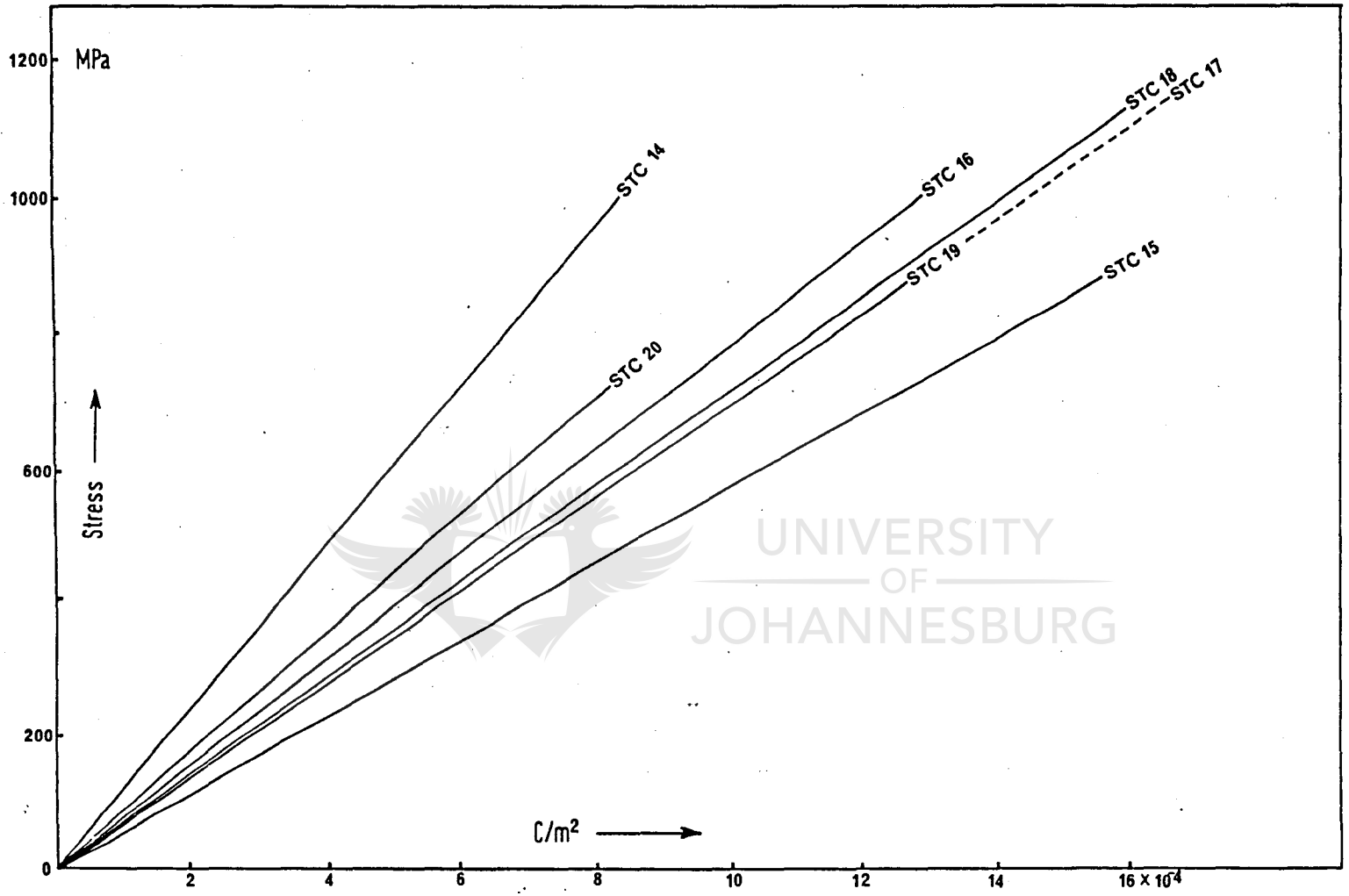

Figure 9 : Relationship between mechanical stress and piezoelectric polarization for STC 14, STC 15, STC 16, STC 17, STC 18, STC 19 and STC 20 tested in small hydraulic press.

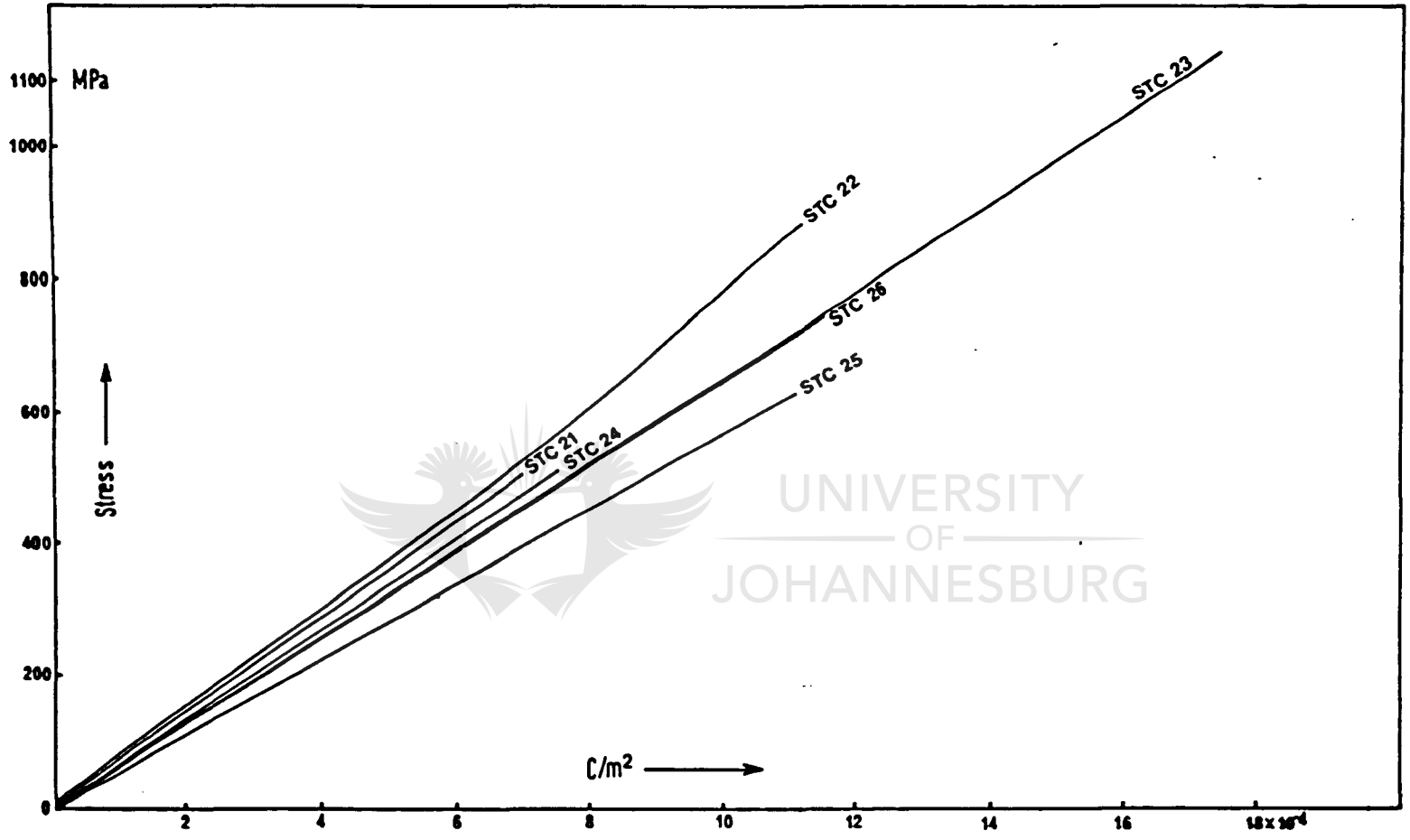

Figure 10 : Relationship between mechanical stress and piezoelectric polarization for STC 21, STC 22, STC 23, STC 24, STC 25 and STC 26 tested in small hydraulic press.

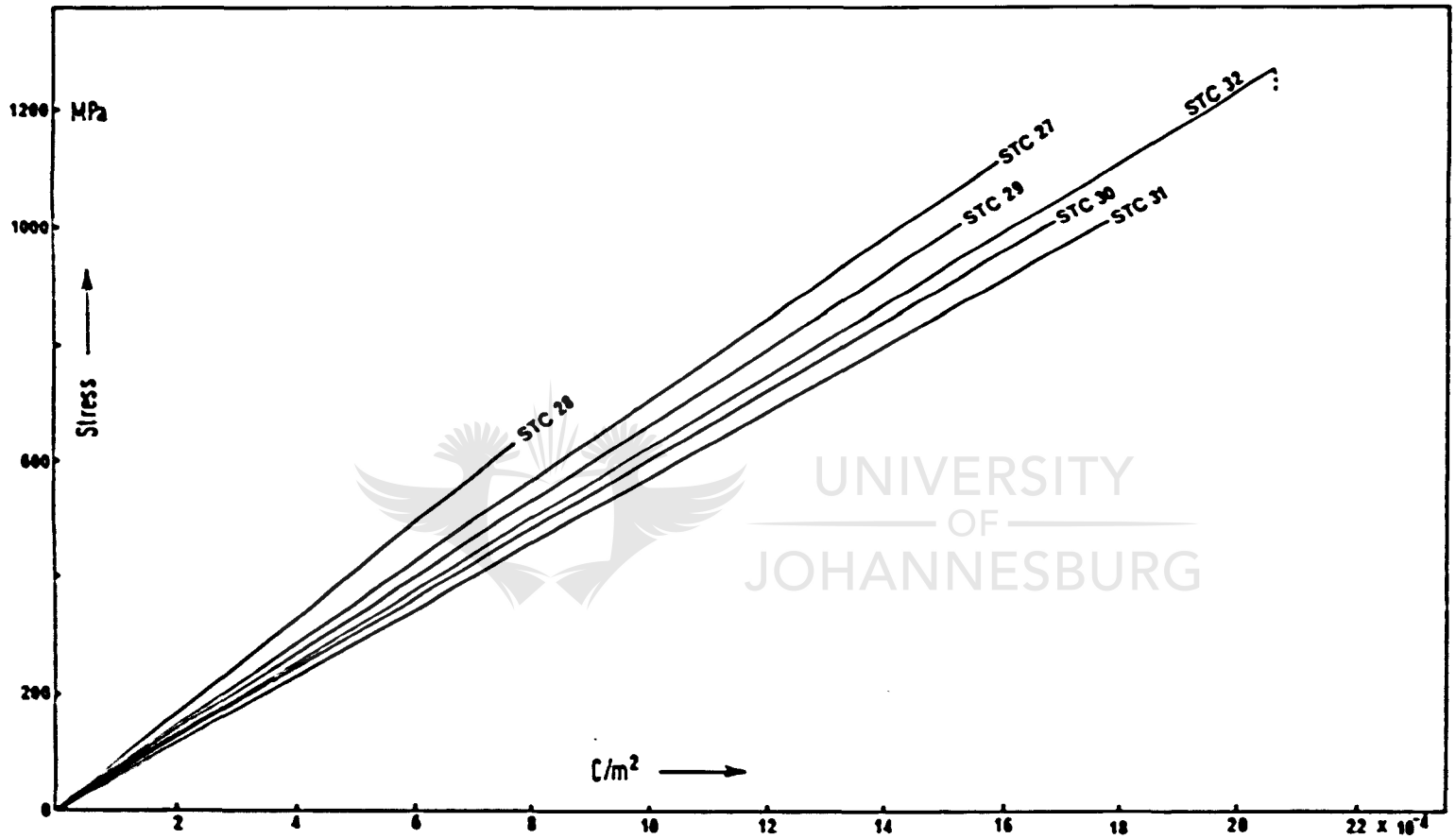

Figure 11 : Relationship between mechanical stress and piezoelectric polarization for STC 27, STC 28, STC 29, STC 30, STC 31 and STC 32 tested in small hydraulic press.

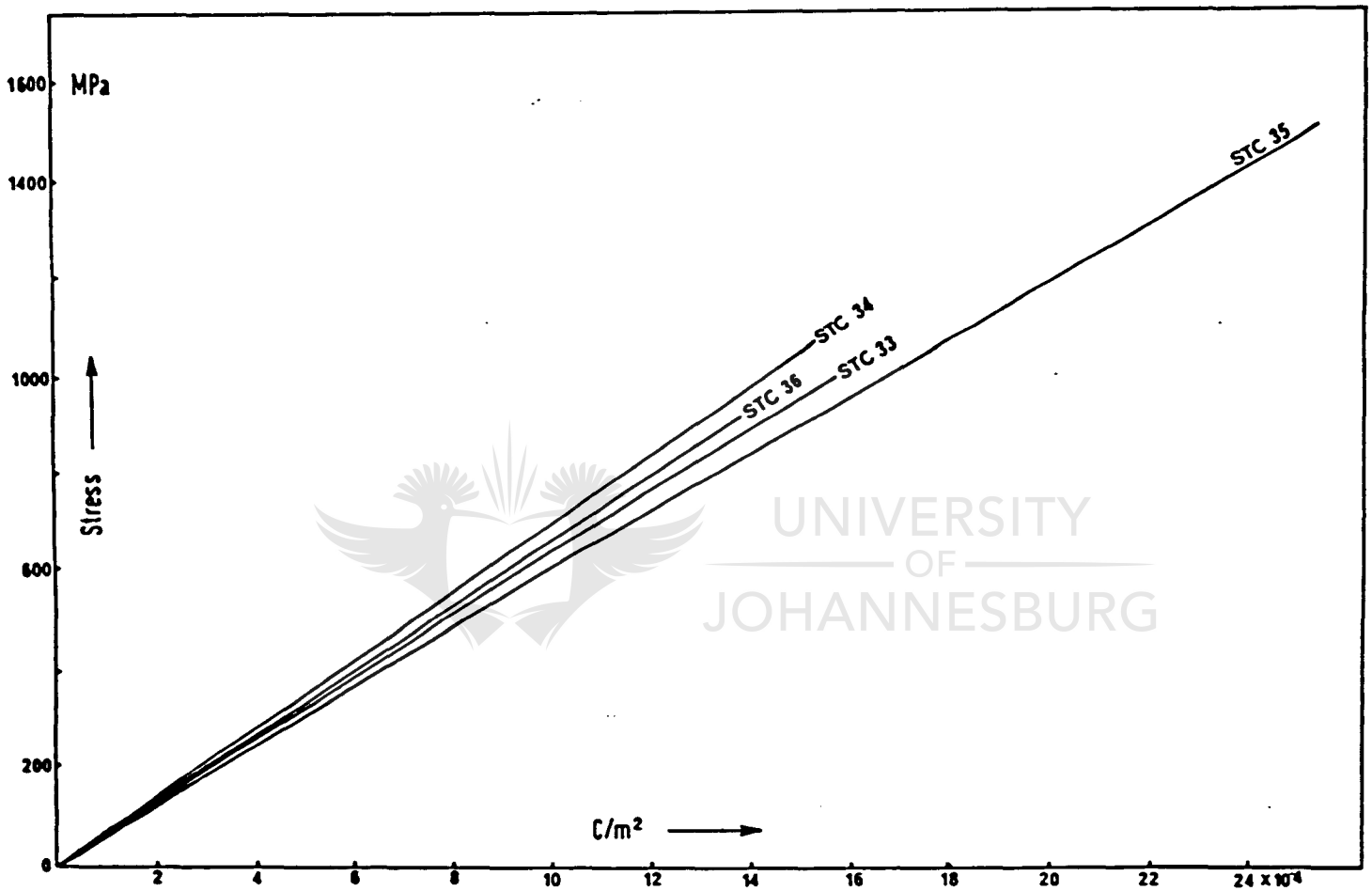

Figure 12 : Relationship between mechanical stress and polarization for STC 33, STC 34, STC 35 and STC 36 tested in small hydraulic press.

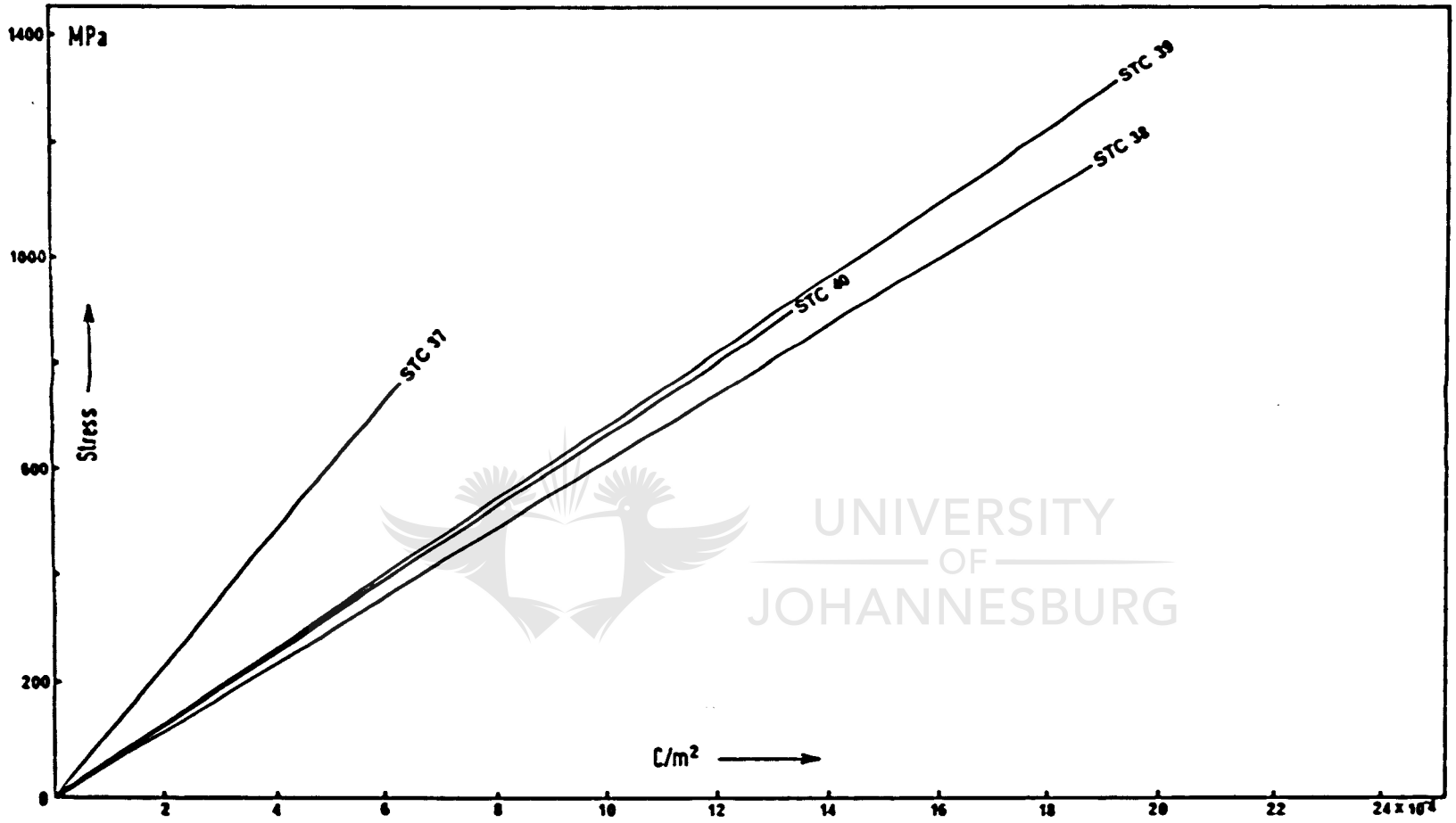

Figure 13 : Relationship between mechanical stress and piezoelectric polarization for STC 37, STC 38, STC 39 and STC 40 tested in small hydraulic press.

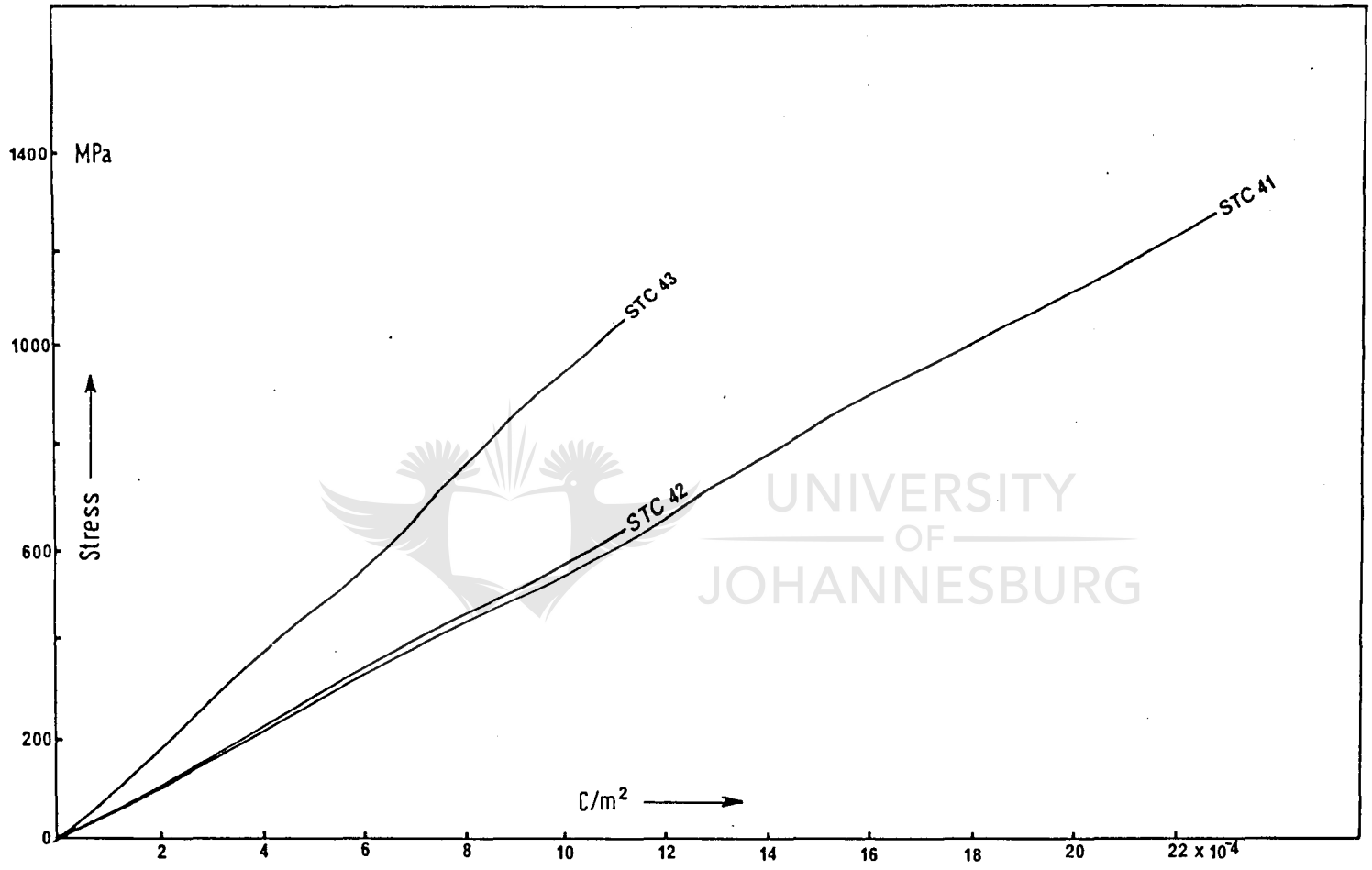

Figure 14 : Relationship between mechanical stress and piezoelectric polarization for STC 41, STC 42 and STC 43 tested in small hydraulic press.

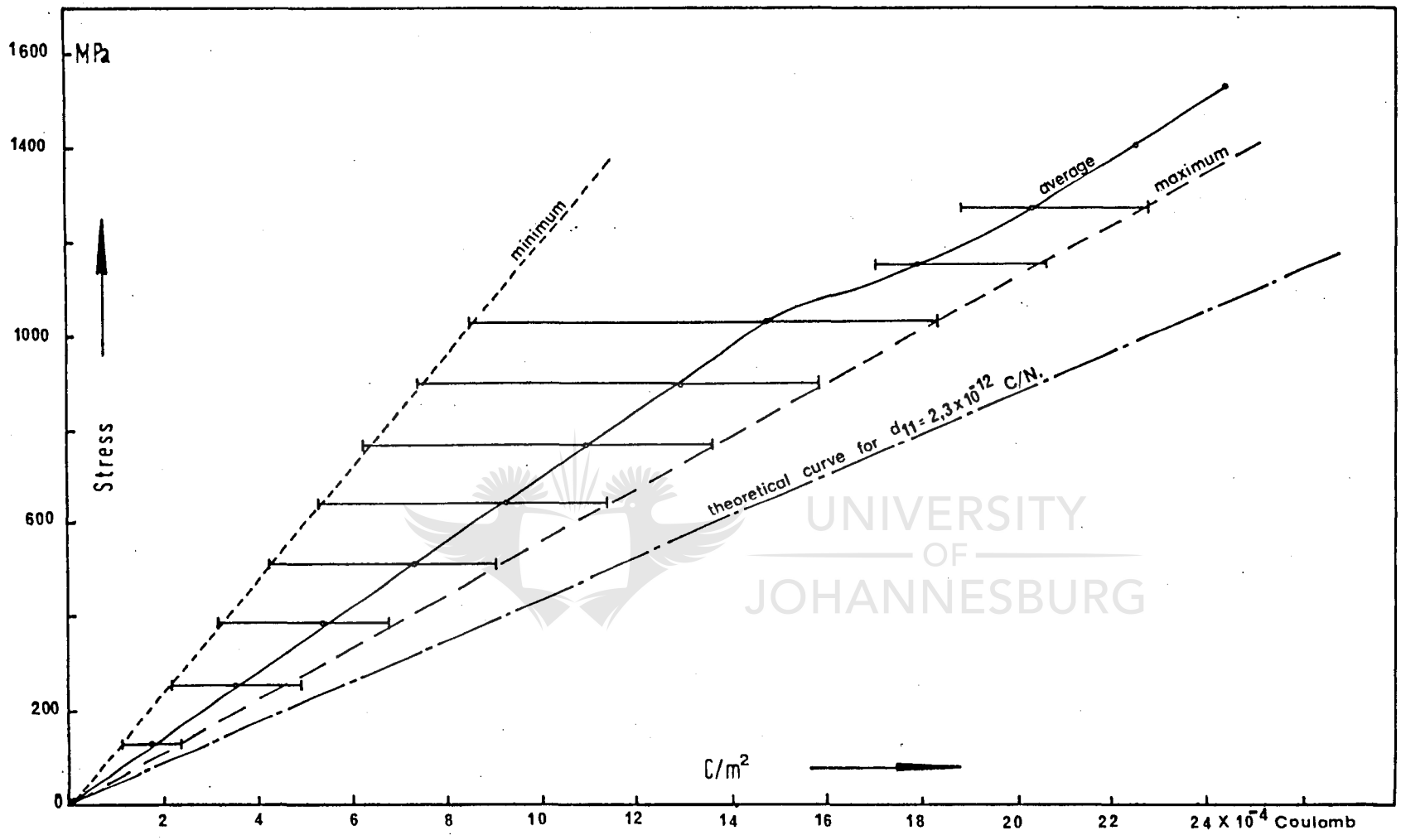

Figure 15 The minimum, maximum and average polarization curves for all STC quartz tested are compared with the theoretical curve for $d_{11} = 2,3 \times 10^{-12}$ C/N. The horizontal bars represent the maximum and minimum deviation from the average plot.

stress, 58 were tested in the small hydraulic press and the remaining eight were placed under stress in the stiff testing machine of the Chamber of Mines Research Laboratories in Johannesburg. See plates 3 and 4. Throughout this dissertation all quartz cylinders will be referred to as STC quartz.

In tables 2 and 5, charge per unit area or piezoelectric polarization is given as coulomb per square metre, whereas stress is given as mega newton per square metre which is by definition a mega pascal.

The number of quartz cylinders involved in calculating the average stress-polarization relationship at various stress levels, is given in column five, table 3.

Each individual curve in itself is an average plot of a number of curves arrived at by a series of stressing and destressing the quartz cylinder, each consecutive time to a higher stress level. The most striking feature displayed by all the curves plotted in Figures 5 to 15 is the linear relationship that exists between mechanical stress and piezoelectric polarization even up to stresses of 1000 MPa. The results utilized to construct these curves were obtained from more than 70 per cent of the STC quartz cylinders used during the tests.

In figure 15 the minimum, maximum and average polarization curves are compared with the theoretical curve for $d_{11} = 2,3 \times 10^{-12}$ C/N. The reason for all the values being less than that of the theoretical curve is most probably due to incorrect orientation of the electrodes on the quartz cylinders. This is also the most probable reason for the scatter in the experimentally measured curves as indicated by the horizontal bars.

The kink in the mean curve beyond 1000 MPa does not reflect a sudden increase in polarization value at stress levels exceeding 1000 MPa, but is merely due to the small number of curves involved in calculating the mean value. Results obtained in the stiff testing machine have not been included when calculating the mean curve. On the grounds of the linear relationship between mechanical stress and piezoelectric polarization, which fulfills the requirements for the piezoelectric effect, a value of $1,43 \times 10^{-12}$ C/N for a d modulus for STC quartz has been computed. This figure is the average value derived from the first eight piezoelectric moduli given in column 4, table 3. The first eight rows have been chosen because it was taken over a larger number of cylinders tested.

Using the above value for a d modulus for STC quartz, and applying a compressive stress of 1018,5 MPa parallel to the Y axis of the cylinder, the polarization thus calculated is given by

$$P = (1,43 \times 10^{-12}) \times (1018,5 \times 10^{6}) = 14,56 \times 10^{-4} \text{ C/m}^2$$

with a d_{11} modulus value of $2,3 \times 10^{-12}$ C/N for quartz as given by Nye (1972, p126) and the same stress, the polarization value becomes $23,42 \times 10^{-4}$ C/m^2.

It is obvious that the polarization value thus obtained for STC quartz is 38 per cent lower than the figure obtained by using a d_{11} modulus as quoted in the literature for quartz. The reason for this will be discussed in chapter 6.2.

4.4. The Relationship Between the Rate at which Load is Applied and Piezoelectric Effect.

The rate of load applied has a known relationship to the rate

of strain development. It is easier to measure strain rate than load rate, therefore the rate of strain development has been used to determine the effect that various loading rates have on the piezoelectric charge. Although the rate of strain development does not enter in the expression for piezoelectric effect, the time taken to collect the electric charge has a definite influence on the final reading. Tests carried out by Parkhomenko (1971, p116), on a single sample of granite have shown that for a strain rate of 10 mm/min, the end result was smaller by a factor 1,4 or 28 per cent when compared to a strain rate of 20 mm/min.

During tests carried out on STC quartz in the small hydraulic press, all electric charge readings were recorded at a strain rate of 1 mm/min except for three quartz cylinders where strain was developed at a rate of 4 mm/min.

In one specific case, three different strain rates were applied consecutively to STC 26. At a strain rate of 1 mm/min the electric charge was four per cent smaller than at a rate of 1,5 mm/min. When the rate was increased to 4 mm/min, there was an increase of 24,6 per cent in the electric charge generated, as can be seen in figure 17. The same affect was observed in STC 25, figure 16 where an increase from 0,17 mm/min to 1 mm/min brought about an increase of 15,7 per cent in the reading. After increasing the rate to 4 mm/min, the electric charge went up by 21,3 per cent.

On the contrary, results plotted in figure 18 for STC 47 in the stiff testing machine, have produced no increase in

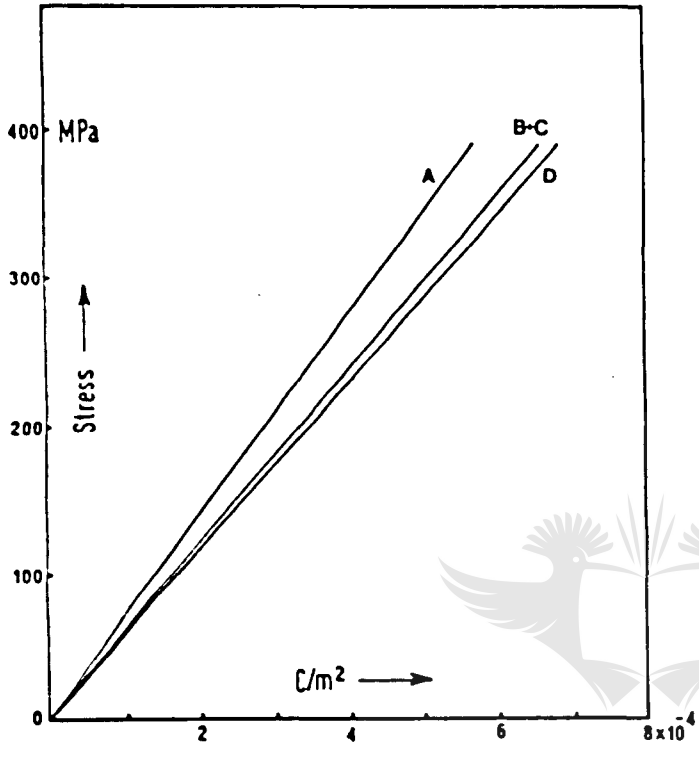

Figure 16 : Relationship between mechanical stress and piezoelectric polarization for STC 25 at different loading rates : A 0,17 mm/min; B and C 1 mm/min; D 4 mm/min, tests carried out in small hydraulic press.

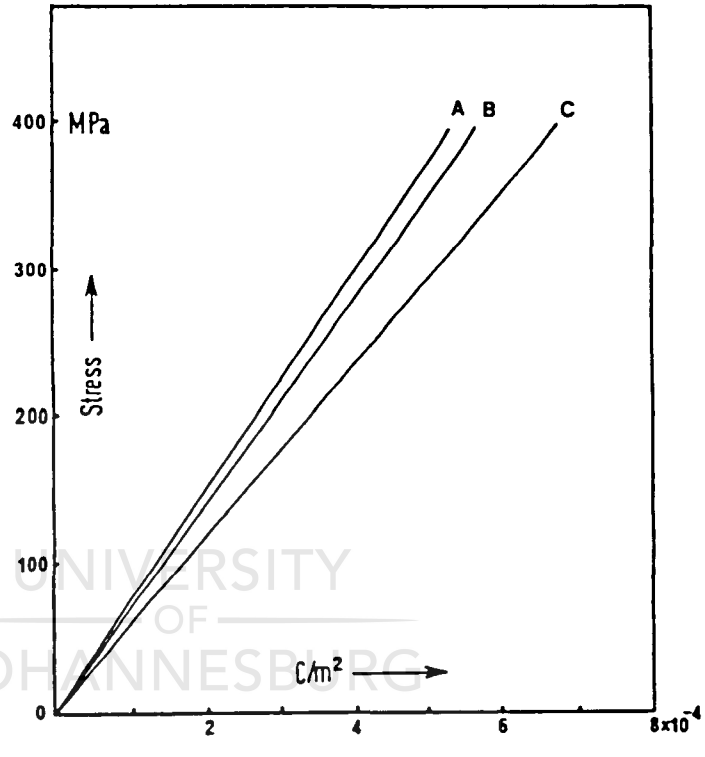

Figure 17 : Relationship between mechanical stress and piezoelectric polarization for STC 26 at different loading rates : A 1,0 mm/min; B 1,5 mm/min; C 4 mm/min, tests carried out in small hydraulic press.

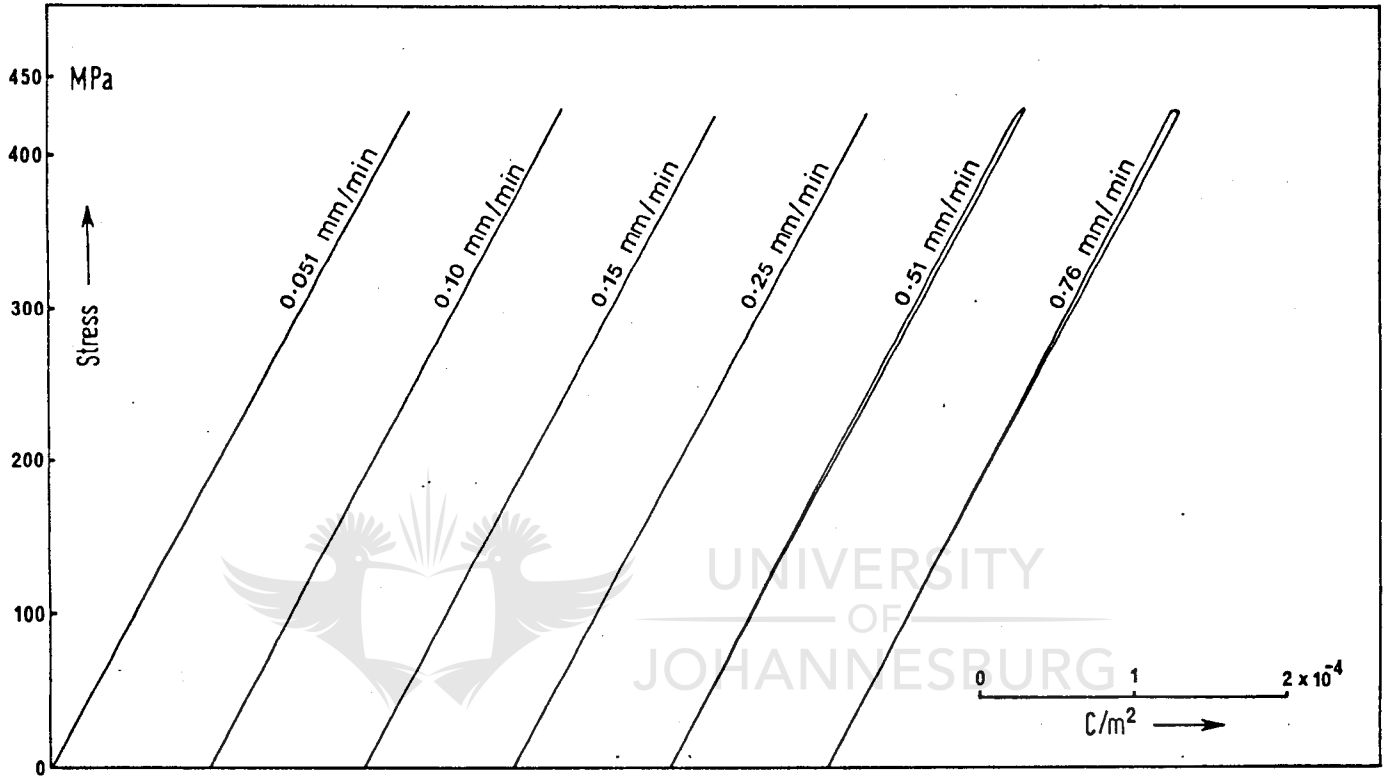

Figure 18 : Relationship between mechanical stress and piezoelectric polarization for STC 47 at different loading rates, tests carried out in stiff testing machine.

charge for a series of strain rates ranging from 0,05 mm/min. The amount of charge leakage from the polarization system is determined by the resistivity of the specimen to be tested, as well as the time taken to collect this charge. With quartz having a resistivity in the vicinity of 10^{14} ohms/cm leakage can only take place along contact dirt.

In the experiments carried out by Parkhomenko (1971, p25), the duration of loading was restricted to 2 or 3 seconds, whereas the duration time for loading STC quartz to e.g. 90 kN could be as high as 90 seconds. During this time, leakage to the press can take place along contact dirt on the surface of the cylinder, thus resulting in a loss in the charge drained by the electrometer.

4.5. The Effect of Repetitive Application of Load on Piezoelectric Polarization.

The uniformity in electric charge with repetitive application of load or stress is clearly illustrated in the stress vs polarization curves for two individual STC quartz cylinders in figures 19 and 20. These curves are representative of all the stress-polarization curves for approximately forty different cylinders.

The following examples clearly illustrate this statement :-

For STC 19 the electric charge generated at a stress level of 200 MPa (dotted line in figure 19) is the same in all four curves i.e. $3,0 \times 10^{-4}$ C/m^2.

At a stress level of 500 MPa chosen for STC 41 in figure 20 the electric charge recorded on the coulombmeter was the same in all eight consecutive tests.

The complete linearity observed in all electric charge curves recorded throughout the study, even up to high loads, has proved

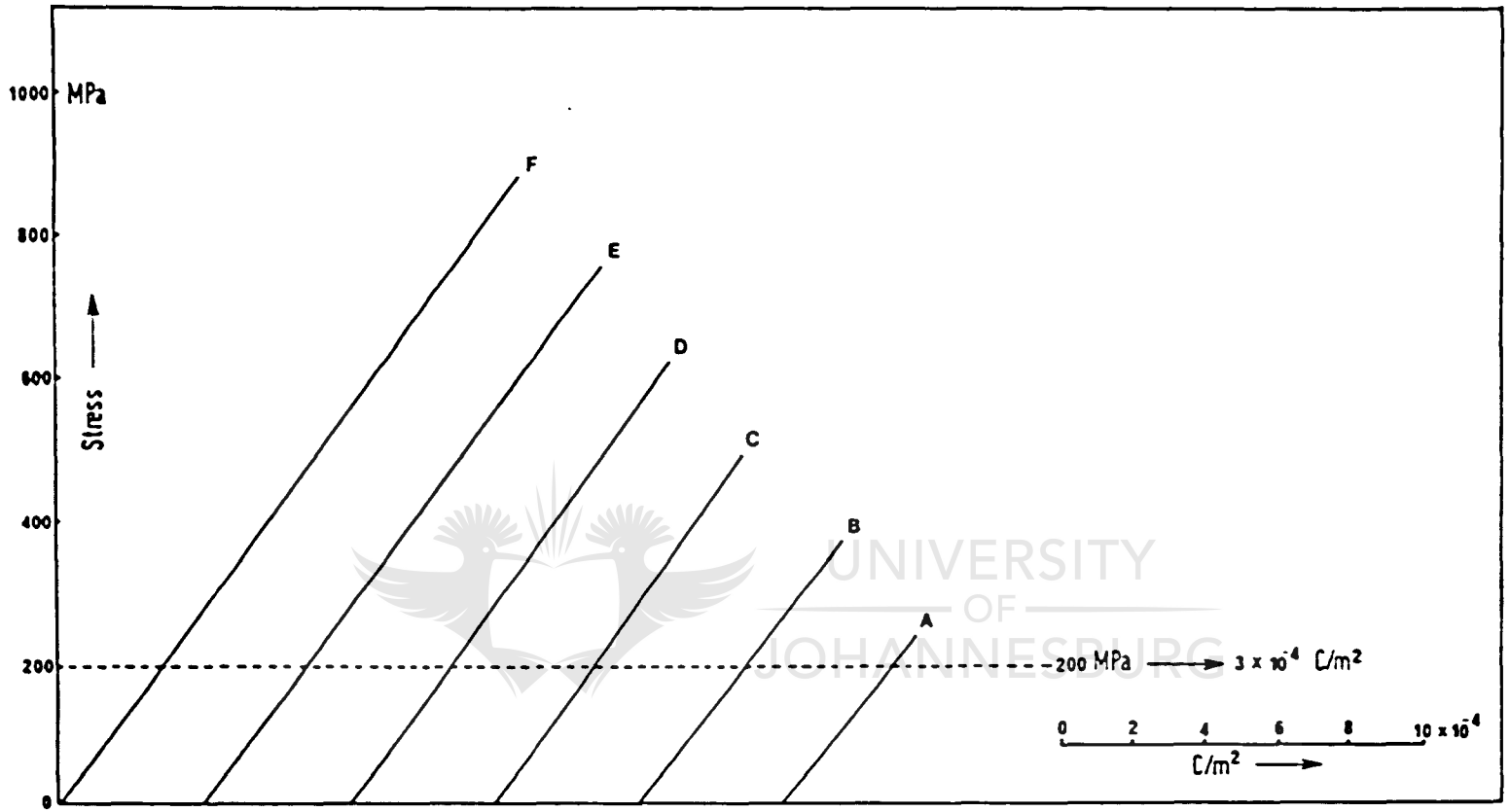

Figure 10 : Set of stress-polarization curves for STC 19 to illustrate consistency in piezoelectric values with repetitive stressing in small hydraulic press. At 200 MPa a constant value of 3×10^{-4} C/m^2 was recorded.

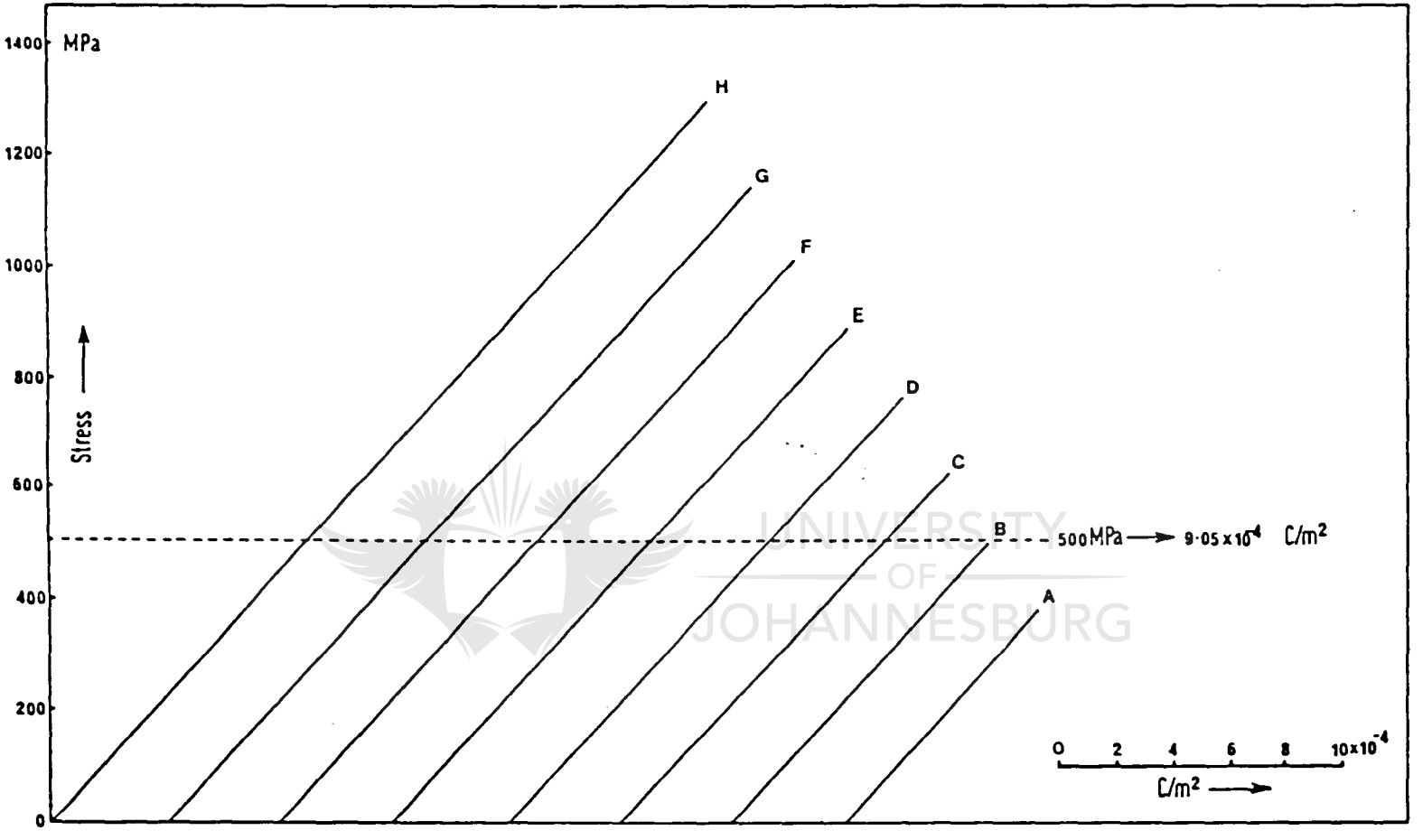

Figure 20 : Set of stress-polarization curves for STC 41 to illustrate consistency in piezoelectric values with repetitive stressing in small hydraulic press. At 500 MPa a constant value of $9,05 \times 10^{-4}$ C/m^2 was recorded.

that there is no decrease in piezoelectric constant with increase in stress. According to Parkhomenko (1971, p76), this has been a point of dispute between many authors in the past.

4.6. Electric Charge at Breaking Point.

For various reasons it was impossible to record the piezoelectric effect at breaking point.

4.6.1. In some cases when the cylinder exploded, the lead to the electrometer touched the frame of the press thus giving an exceptionally high positive or negative reading.

4.6.2. For more than 90 per cent of the cases, where spalling did occur during the test, there was a small increase in charge registered by the meter. In one instance the increase was as high as 8×10^{-8} coulomb. Especially at high stress levels very close to, or at breaking point, where severe spalling and cracking took place before total disintegration of the cylinder, the large electric charges set free were too fast for the X-Y plotter type PL 100 to record, due to its limited writing speed of 200 mm/sec. For the reasons given above it had been decided to use, for polarization calculation purposes, only the section of the recorded load-charge curve to a point immediately before severe spalling and cracking took place.

5. RESULTS OBTAINED ON VARIOUS QUARTZITES FROM THE ORANGE FREE STATE GOLD FIELDS.

For the second part of the study, rock samples from various zones in the Central Rand Group of the Witwatersrand Supergroup have been used. The different localities of the samples are marked on the generalised geological column for Loraine Gold Mines, Limited, in Figure 21, and the names of the different zones as applicable to Loraine have been used.

The rocks from the selected zones are, in general, very rich in quartz. The composition of the rock specimens, as determined by point count analysis, is given below in Table 6. All these specimens fall within the areas where active mining is taking place.

TABLE 6.

Specimen Number	Quartz Per Cent	* Muscovite Per Cent	** Other Minerals Per Cent
L 1	84,4	15,3	0,3
L 2	83,5	12,0	4,5
L 3	95,4	4,3	0,3
L 4	100	0	0
L 5	96,5	3,3	0,2
L 6	58,5	40,5	1,0
L 7	80,8	18,2	1,0
L 8	89,9	8,6	1,5
L 9	64,4	35,3	0,3
L 10	87,3	7,1	5,6
L 11	87,8	10,2	2,0
L 12	92,9	7,1	0
L 13	88,1	8,2	3,7

* Muscovite, sericite and pyrophyllite not differentiated.

** Chlorite, chert and opaque minerals.

Rock specimens from six different zones have been selected, either from boreholes or from working places underground.

From each rock specimen, between four and six cylinders similar to the quartz cylinders have been cut.

Cylinders L 5, L 6, L 12 and L 13 were cut in three different directions for each individual rock specimen. All cylinders marked A after the number, have been cut parallel to dip, cylinders marked B, parallel to strike and all those marked C, perpendicular to both strike and dip.

The sequence of numbering the cylinders are best illustrated in

LORAINE GOLD MINES LIMITED

GENERALISED GEOLOGICAL COLUMN

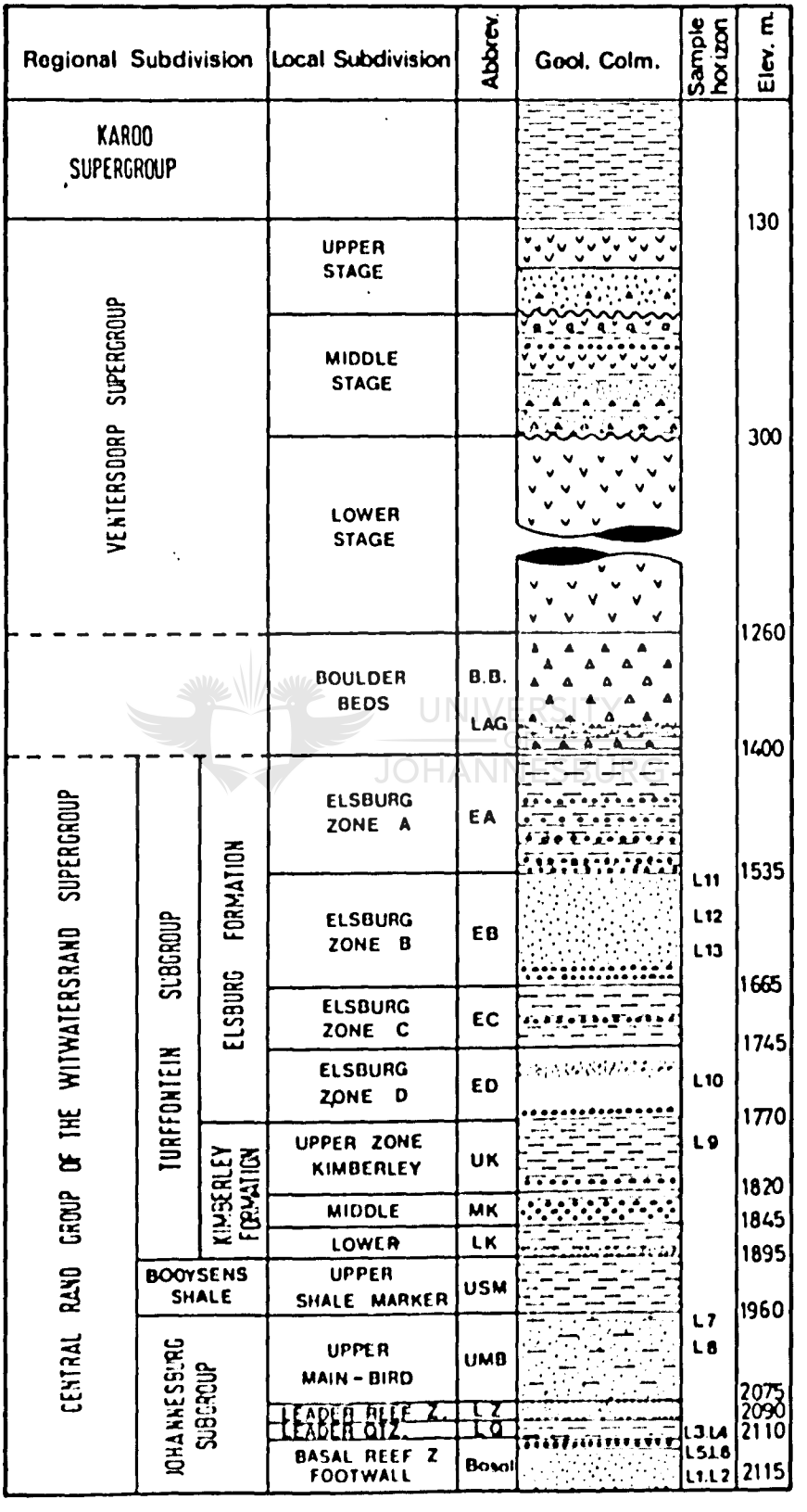

Figure 21.

the following example. In the case of cylinder L 12A (2) the L 12 denotes locality and specimen number, A, the direction in which the cylinder was cut as explained before and (2) the number of the consecutive cylinder cut from the same specimen. If a further letter follows it simply indicates that more than one curve has been plotted for the same cylinder.

Preferential orientations on the c axes of the quartz grains in all the specimens have been determined in thin section under the microscope with the aid of the Federov stage.

Two rock specimens of Brixton quartzite from the Hospital Hill Subgroup, as well as three silcrete samples from Botswana, have also been included in the study for reasons to be discussed later.

5.1. Locality, Composition and Texture of Quartzites.

Each individual rock specimen will now be discussed briefly with respect to locality, composition and texture:

5.1.1. Johannesburg Subgroup.

5.1.1.1. Basal Reef Zone.

Rock specimens L 1 and L 2 come from a borehole that has been drilled in the footwall of the Basal Reef in the above Subgroup. The footwall quartzite is light in colour with a greenish tinge and faint yellow specks. It is a coarse-grained quartzite with subrounded grains. Although the average grain size is 0,8 mm, occasional grains up to 2 mm in diameter have been observed in thin section under the microscope. Macroscopically pyrite stringers are visible in hand specimens. The matrix consists mainly of phyllosilicates which are very difficult to identify under the microscope. According to the classification of Pettijohn

et al (1972, p158), this rock can be classified as quartzwacke. Both L 1 and L 2 show a definite optic orientation of the quartz grains which can be seen in figures 22 and 23. A photomicrograph of specimen L 2 is given in plate VI.

Rock specimens L 3, L 4, L 5 and L 6 belong to the Middling quartzite immediately above the Basal Reef. This quartzite ranges in thickness from 15 cm in the North to 120 cm in the South on Loraine Gold Mines. It is a very clean light grey glassy quartzite with thin stringers of pyrite marking the bedding and cross-bedding. The glassy appearance is due to a very high quartz content which ranges from 95 to 100 per cent. The texture of the rock can be described as coarse - to medium - grained with subangular to sub-rounded grains. Using the classification of the configuration of contacts by Griffiths (1967, p173), the contact between the individual grains in this rock can be classified as complete. This complete contact is shown in a photomicrograph of specimen L 4 in plate VII. Specimen L 6 was included because of its very high muscovite-sericite content in the matrix, which explains the dirty appearance of the rock in a hand specimen.

In figure 26 it can be seen that the Middling quartzite displays a preferential orientation of the optic axes of the quartz grains when studied under the microscope.

5.1.1.2. Upper Main Bird Zone.

Rock specimens L 7 and L 8, typical of this zone, consist of a light grey quartzite with occasional small grits, the odd scattered pebble or fragment of chert and quartz, as

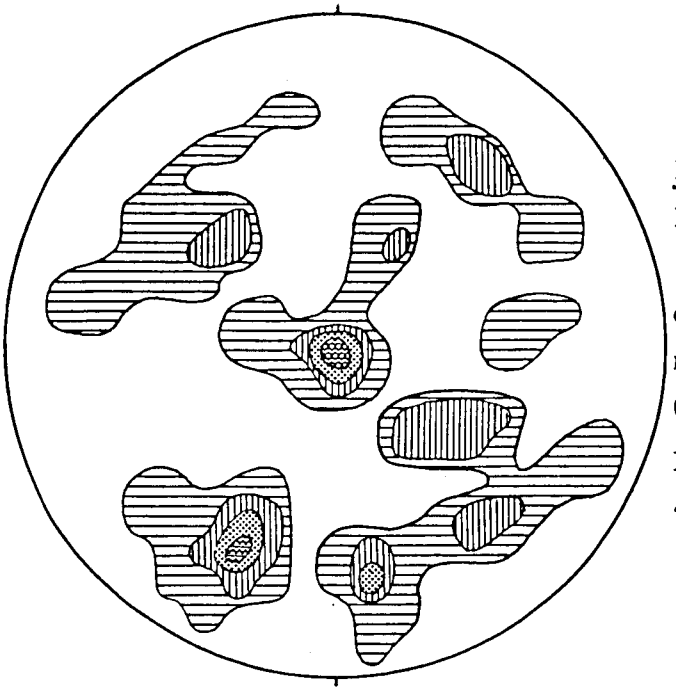

Figure 22 :
Fabric diagram prepared from specimen L 1. The c axes of 64 quartz grains were measured in thin section. Contours : 1-2-3-4 per cent per 1 per cent area, maximum 4 per cent.

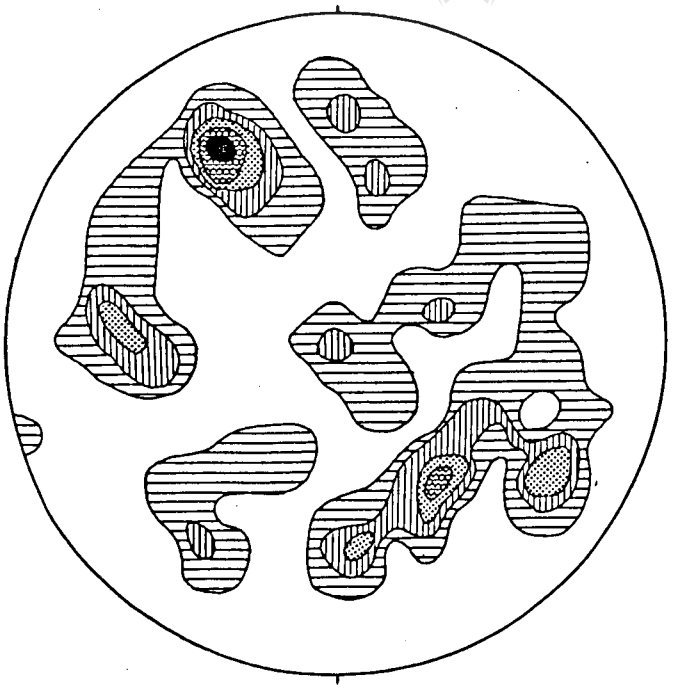

Figure 23 :
Fabric diagram prepared from specimen L 2. The c axes of 66 quartz grains were measured in thin section. Contours : 1-2-3-4-5 per cent per 1 per cent area, maximum 5 per cent.

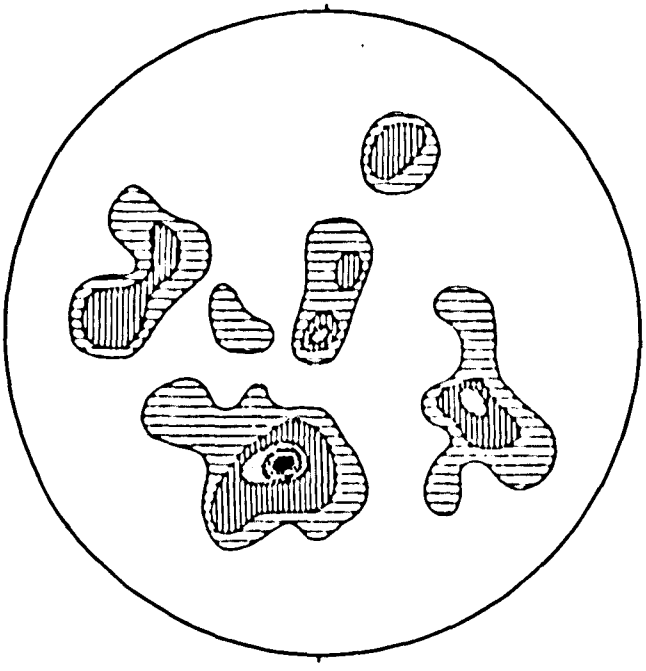

Figure 24 :
Fabric diagram prepared from specimen L 3. The c axes of 52 quartz grains were measured in thin section. Contours : 1-2-3-4-5 per cent per 1 per cent area, maximum 5 per cent.

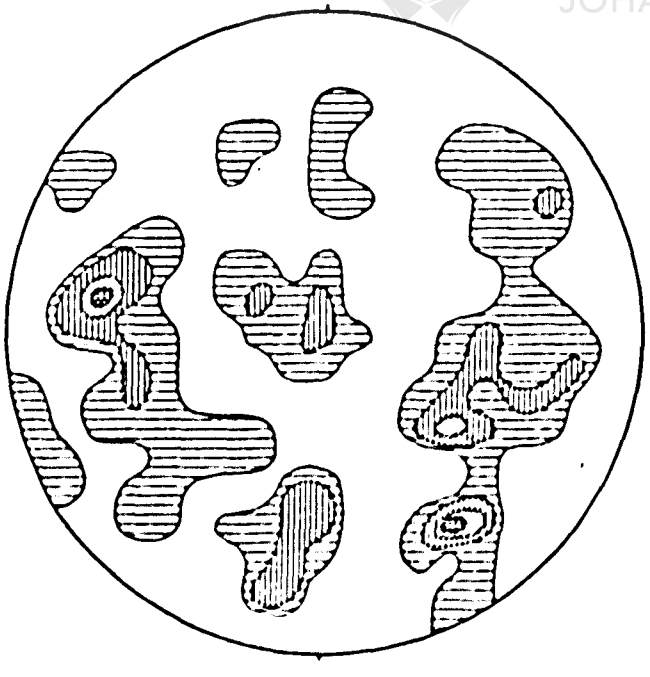

Figure 25 :
Fabric diagram prepared from specimen L 4. The c axes of 60 quartz grains were measured in thin section. Contours : 1-2-3-4 per cent per 1 per cent area, maximum 4 per cent.

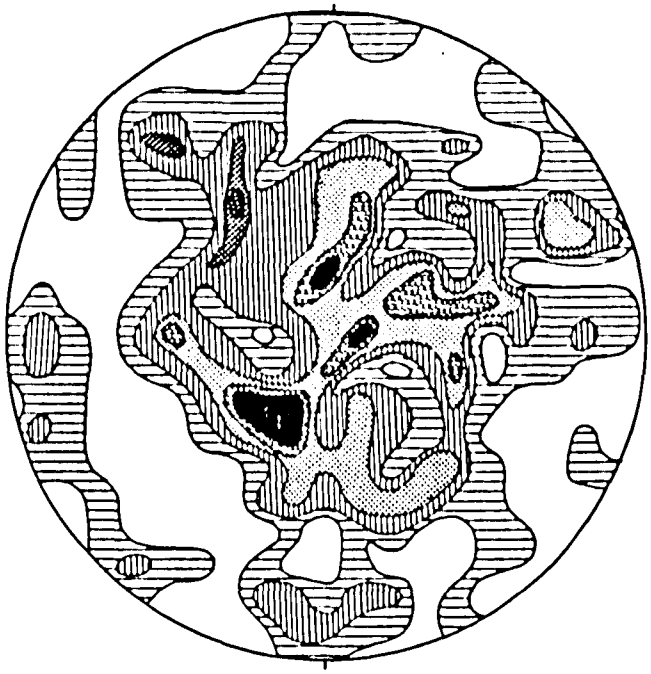

Figure 26 :
Fabric diagram prepared from specimen L 5. The c axes of 124 quartz grains were measured in thin section. Contours : 1-2-3-4-5 per cent per 1 per cent area, maximum 5 per cent. (Measurements by J.J. Bensch).

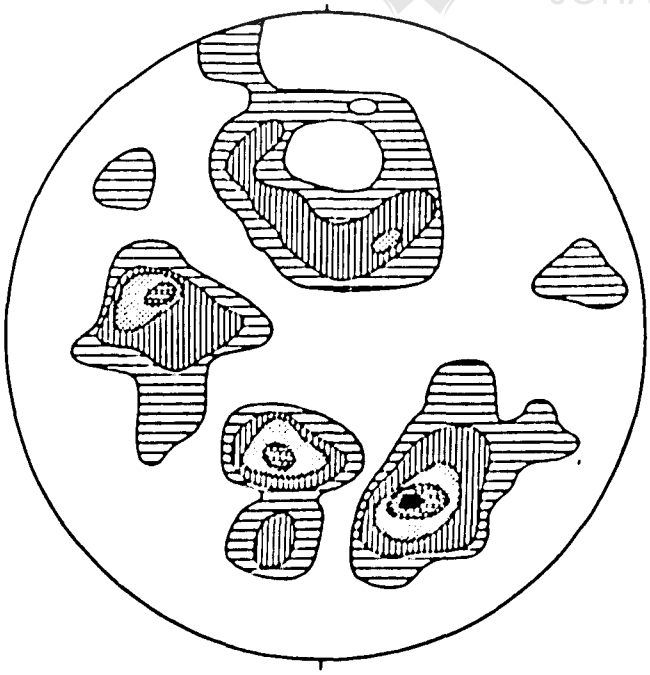

Figure 27 :
Fabric diagram prepared from specimen L 6. The c axes of 58 quartz grains were measured in thin section. Contours : 1-2-3-4-5 per cent per 1 per cent area, maximum 5 per cent.

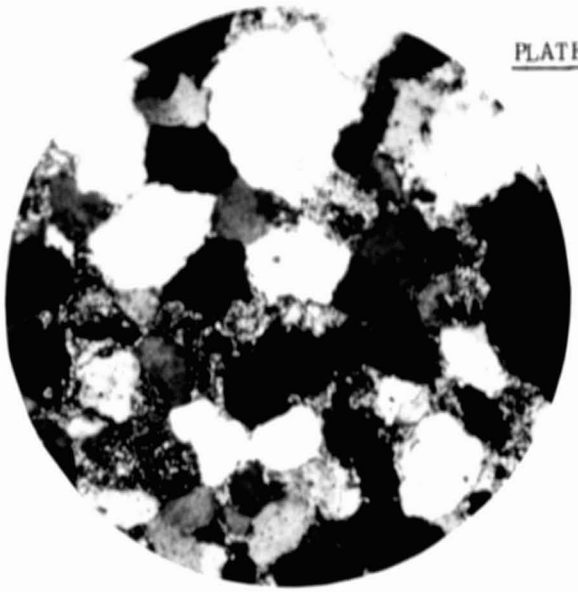

PLATE VI Photomicrograph of Specimen L 2 from the footwall of the Basal Reef Loraine Gold Mines, Limited. Crossed Nicols x 65 Diameters.

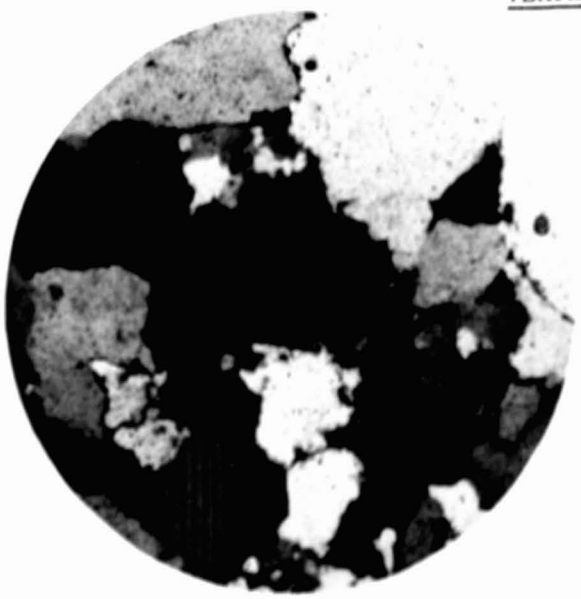

PLATE VII Photomicrograph of Specimen L 4 from the Middling Quartzite above the Basal Reef, Loraine Gold Mines, Limited. Crossed Nicols x 65 Diameters.

well as some well dispersed colourful specks of mudstone and chert. The quartzwacke is composed of more than 80 per cent quartz with a matrix of phyllosilicates as high as 18 per cent. The shape of the grains vary from angular to subrounded with a long contact between quartz grains. Although this rock is classified as coarse-grained, very few individual grains exceed 0,8 mm in diameter. The optic orientation of the quartz grains was measured and is shown in fabric diagram figures 28 and 29. A photomicrograph of specimen L 7 is given in plate VIII.

5.1.2. Turffontein Subgroup.

5.1.2.1. Upper Kimberley Zone.

This zone forms part of the Kimberley Formation of the Turffontein Subgroup. The coarse-grained argillaceous quartzite is yellowish-brown in colour with a sugary appearance. Scattered throughout the quartzite are well dispersed pebbles of chert and quartz which become concentrated higher up in this zone to form loosely packed conglomerate bands.

The matrix of this rock constitutes 35 per cent of the rock and is composed of pyrophyllite which was determined by X-ray diffraction. Chert fragments up to 3 mm long are quite a common occurrence in thin section under the microscope. A photomicrograph of specimen L 9, which was sampled from this zone can be seen in plate IX.

5.1.2.2. Elsburg Zone.

This zone on Loraine Gold Mines, is better known as the ED zone. Rock specimen L 10 was taken from the core of a diamond drill hole drilled in the hangingwall of an ED Reef stope. This quartzite is similar to the footwall of the

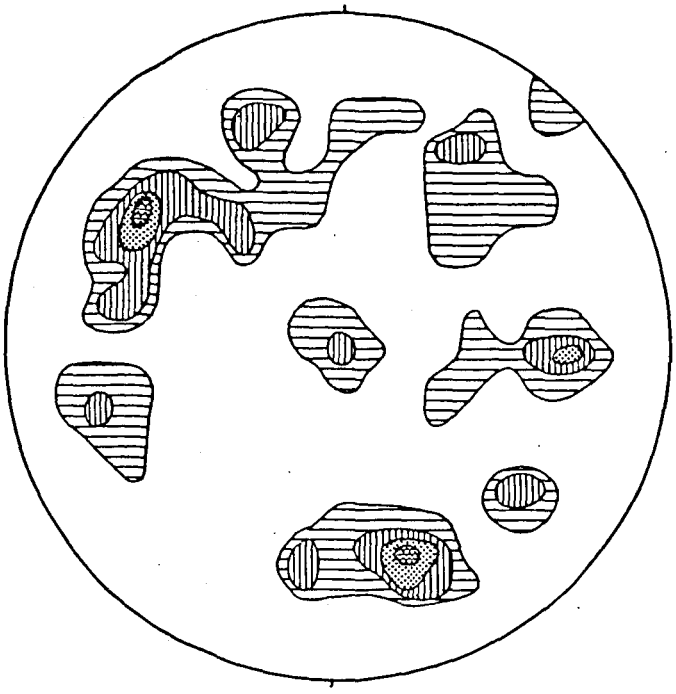

Figure 28 :
Fabric diagram prepared from specimen L 7. The c axes of 56 quartz grains were measured in thin section. Contours : 1-2-3-4 per cent per 1 per cent area, maximum 4 per cent.

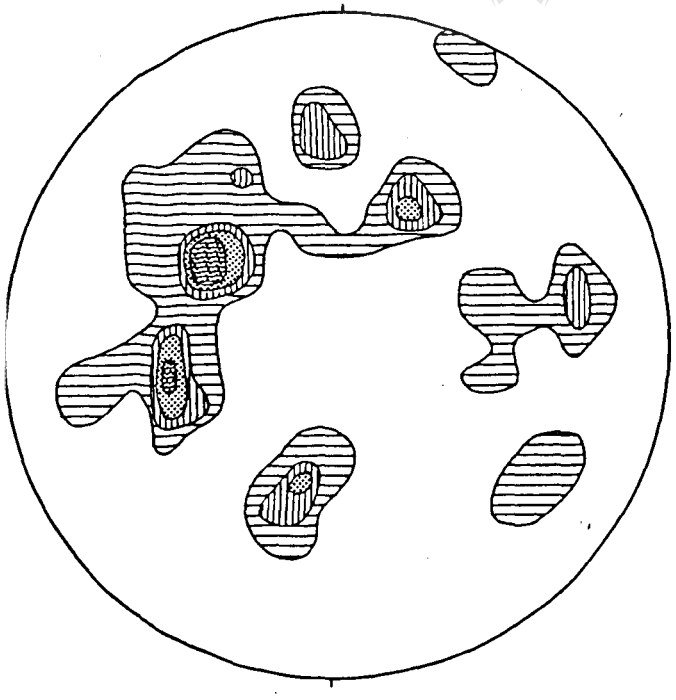

Figure 29 :
Fabric diagram prepared from specimen L 8. The c axes of 54 quartz grains were measured in thin section. Contours : 1-2-3-4 per cent per 1 per cemt area, maximum 4 per cent.

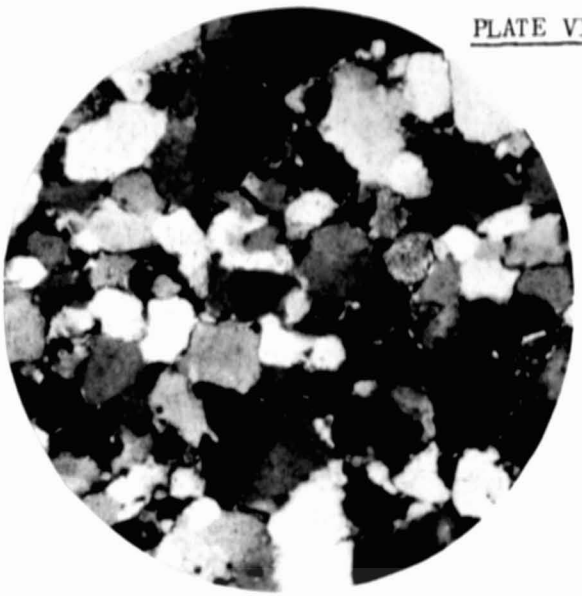

PLATE VIII Photomicrograph of Specimen L 7 from the Upper Main Bird Loraine Gold Mines, Limited. Crossed Nicols x 65 Diameters.

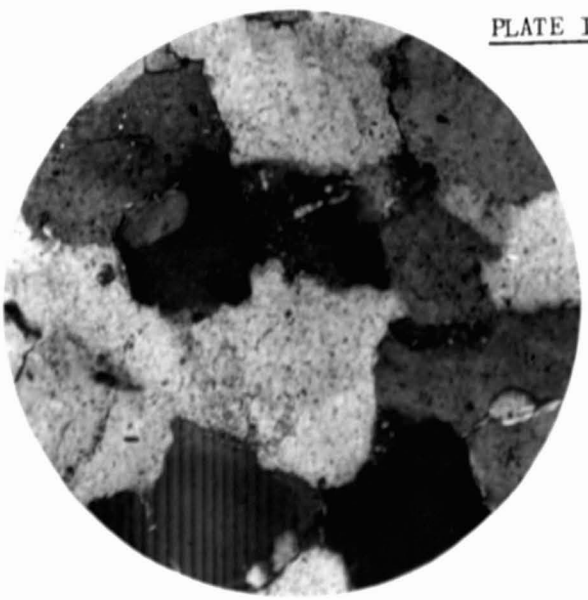

PLATE IX Photomicrograph of Specimen L 9 from the Upper Kimberley Zone Loraine Gold Mines, Limited. Crossed Nicols x 150 Diameters.

Basal Reef which makes it very difficult to distinguish between these two quartzites in a hand specimen. Like most of the quartzites in the Elsburg Formation, the rocks range from a medium-grained to a very coarse-grained light grey quartzwacke. Subangular shaped quartz grains, as large as 1,7 mm in diameter, have been observed in thin section under the microscope. The pyrite stringers and fragments of chert which are often found in this zone, accounts for the 5,6 per cent "other minerals" in table 6. The fabric diagram in figure 32 reveals some orientation of the optic axes of the quartz grains.

5.1.2.3. Elsburg Zone B.

The EB zone consists of a highly siliceous, light grey quartzite described as glassy, due to it having surface translucency when wet. The EB zone very closely resembles the Middling Quartzites of the Basal Reef in composition, texture and appearance. With an average content of 90 per cent quartz, this rock type can be termed quartz arenite. Thin pyrite stringers again mark the cross-bedding. Average grain size as determined under the microscope in thin section is in the vicinity of 0,8 mm with an occasional quartz grain reaching 1,2 mm in diameter. Specimens L 11, L 12 and L 13 were sampled in this zone.

The optic orientation of 115 quartz grains was measured in a thin section under the microscope for specimen L 13. The results shown in fabric diagram figure 35 clearly indicates a strong preferential orientation of the optic axes in the quartz grains, which is also evident in

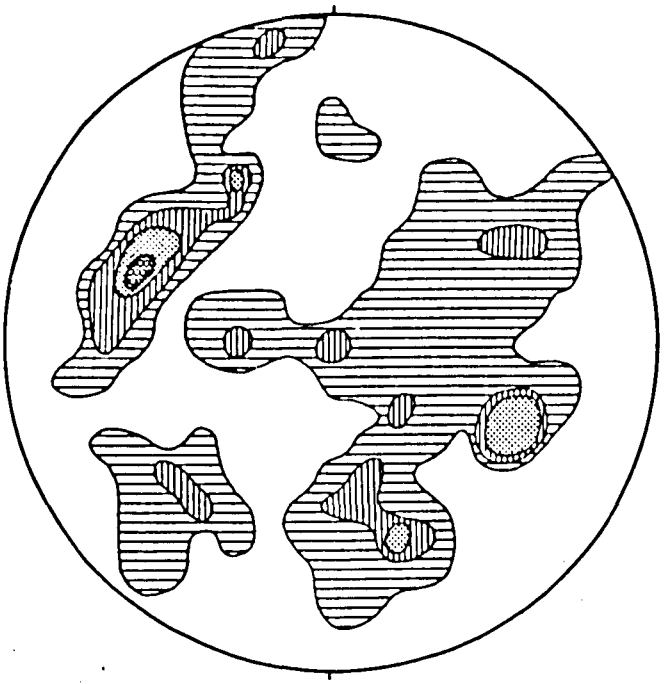

Figure 30 :
Fabric diagram prepared from specimen L 9. The c axes of 80 quartz grains were measured in thin sections. Contours : 1-2-3-4 per cent per 1 per cent area, maximum 4 per cent.

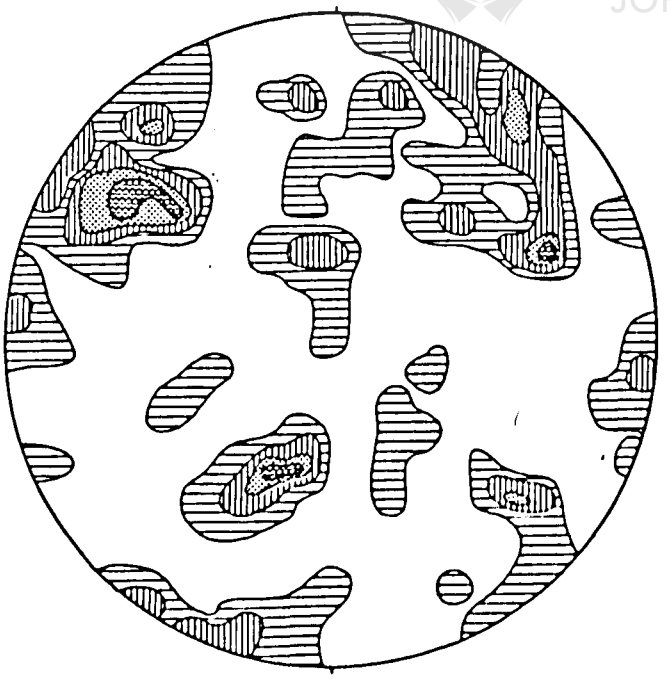

Figure 31 :
Fabric diagram prepared from specimen F 42. The c axes of 120 quartz grains were measured in thin section. Contours : 1-2-3-4 per cent per 1 per cent area, maximum 4 per cent. (Fuller, 1958, Plate V, Figure 2).

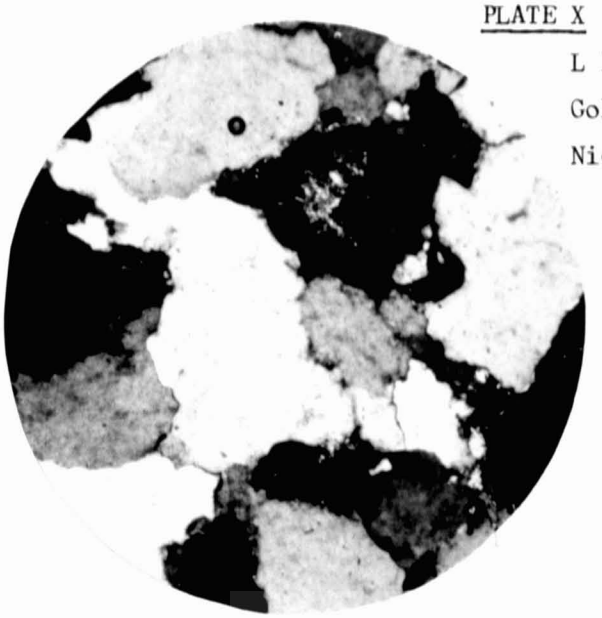

PLATE X Photomicrograph of Specimen L 10 from the ED Zone Loraine Gold Mines, Limited. Crossed Nicols x 65 Diameters.

PLATE XI Photomicrograph of Specimen L 12 from the EB Zone Loraine Gold Mines, Limited. Crossed Nicols x 65 Diameters.

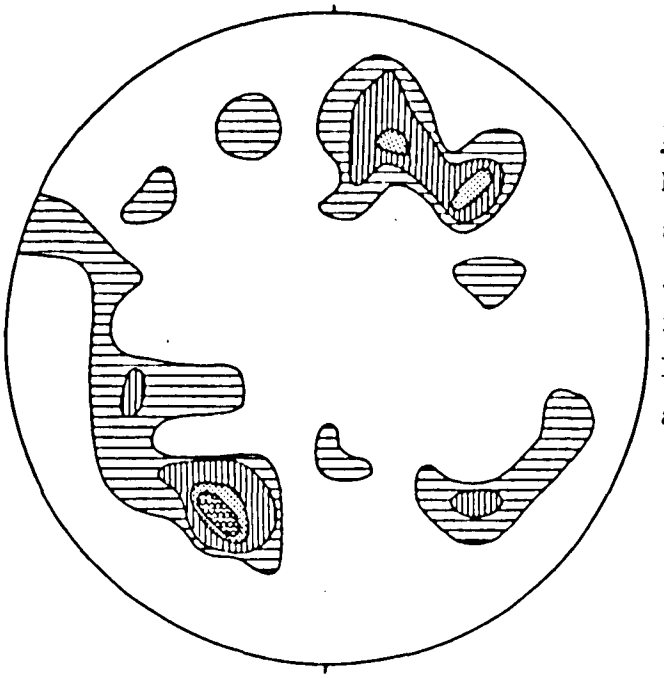

Figure 32 :
Fabric diagram prepared from specimen L 10. The c axes of 50 quartz grains were measured in thin section. Contours : 1-2-3-4 per cent per 1 per cent area, maximum 4 per cent.

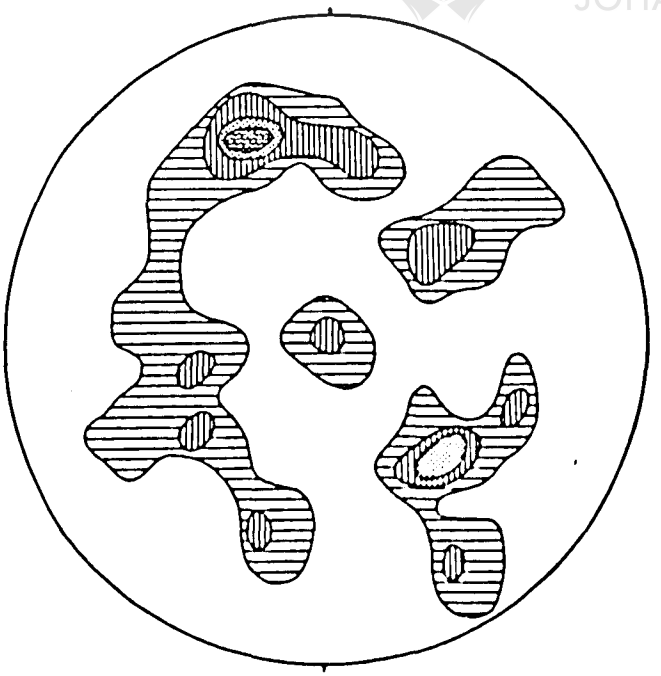

Figure 33 :
Fabric diagram prepared from specimen L 11. The c axes of 54 quartz grains were measured in thin section. Contours : 1-2-3-4 per cent per 1 per cent area, maximum 4 per cent.

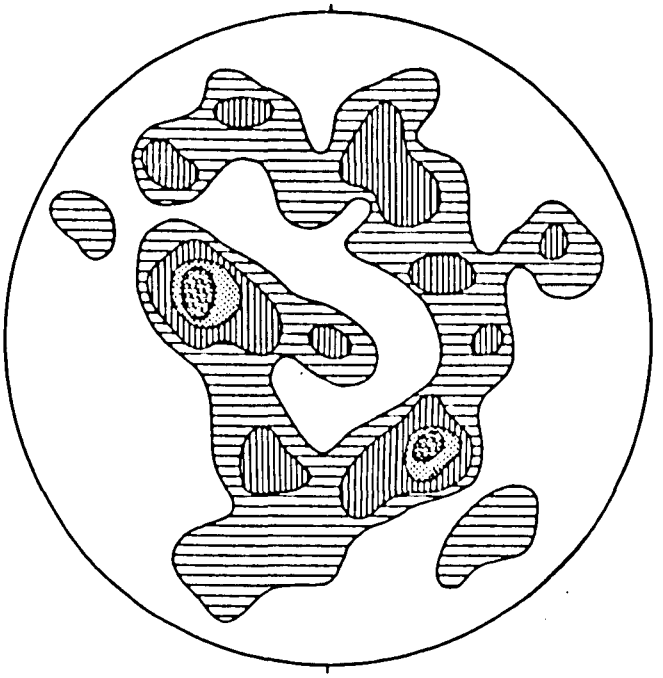

Figure 34 :
Fabric diagram prepared from specimen L 12. The c axes of 88 quartz grains were measured in thin section. Contours : 1-2-3-4 per cent per 1 per cent area, maximum 4 per cent.

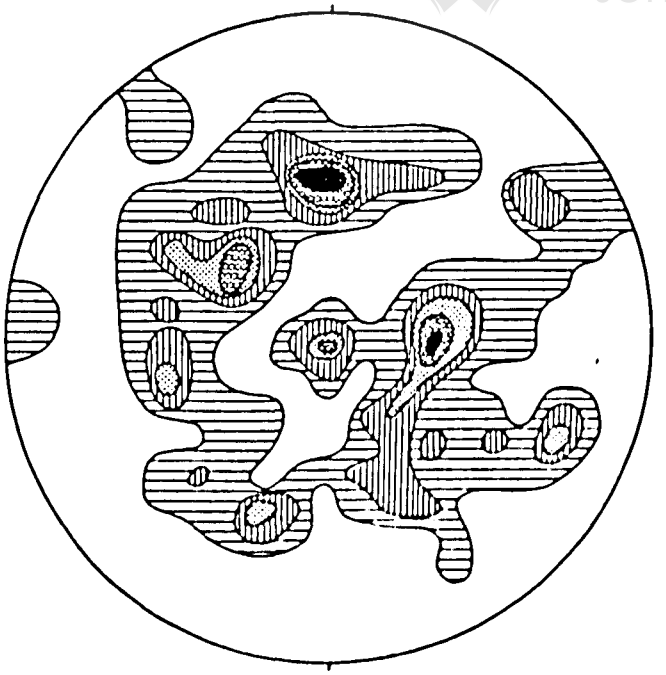

Figure 35 :
Fabric diagram prepared from specimen L 13. The c axes of 115 quartz grains were measured in thin section. Contours : 1-2-3-4-5 per cent per 1 per cent area, maximum 5 per cent.

figure 33 and figure 34 for specimens L 11 and L 12 respectively. This tendency is supported by work previously carried out by Fuller (1958, p34) on rocks of the Turffontein Subgroup, of which figure 31 is a reproduction.

5.1.3. Hospital Hill Subgroup.

Specimens HH 1 and HH 2 were collected from the outcrop of Brixton Formation quartzites in the road-cutting just North of the S.A.B.C. - T.V. tower in Brixton, Johannesburg. According to a description by Fuller (1958, p23), ninety-five per cent of this rock is composed of quartz grains with an average grain size of 0,9 mm. The subangular quartz grains show a complete contact between grains, whilst muscovite forms the matrix. These specimens were included in the study in order to test the validity of the theory of residual stress as a possible explanation for the occurrence of drift in some quartzites. Not having been subjected to any load stress for many thousands of years, this quartzite is expected to be totally destressed.

This validity test was even carried a step further when specimens of silcrete, that have never been stressed (load stress) before, have been included in the study.

5.1.4. Silcretes.

Specimens 7382 and 7420 are from an area near Ghanzi in Botswana, whereas 7392 comes from a locality North of Serowe in the same territory. Petrographic descriptions on the silcretes were made by Mr. R. Semple from the geology department on Loraine Gold Mines.

5.1.4.1. Silcrete 7382 is a fine-grained sediment where 80 per

cent of the grains are quartz and 20 per cent muscovite, with a silica rim of cement around grain boundaries. The well-rounded, well-sorted quartz grains vary in size between 0,1 mm and 0,3 mm with a long contact between grains. The very fine matrix is mostly quartz.

5.1.4.2. Silcrete 7392 as seen in thin section under the microscope, contains 50 per cent quartz and 50 per cent muscovite per total grain volume. The largest quartz grain observed under the microscope is 0,3 mm in diameter, with a long contact between the well-sorted grains. The matrix consists of very fine material composed of quartz.

5.1.4.3. Silcrete 7420 is a well sorted fine-grained sediment similar to the previous two silcretes. The floating contact between grains explains why the matrix of microcrystalline quartz forms about 60 per cent of the total area of the thin section under the microscope.

5.2. Procedure for Recording the Piezoelectric Effect in Quartzites.

Experimentation procedure for quartzite cylinders was the same as for quartz cylinders, except that, for an average piezoelectric effect, at least 100 times smaller than that observed in quartz, it became necessary to operate the electrometer at a very low and sensitive scale setting. This is shown on the load vs electric charge curves for quartz and quartzites plotted in figure 36. In this figure both quartzite L 1 (4) and STC 47 were recorded at an electrometer scale setting of 3×10^{-7} coulomb full range, whereas quartzite L 7 (3) was recorded at 10×10^{-9} coulomb full range.

Bearing in mind that a quartzite is composed of a large number of minute quartz crystals orientated in different directions, with a possibility of a preferential orientation of the optic

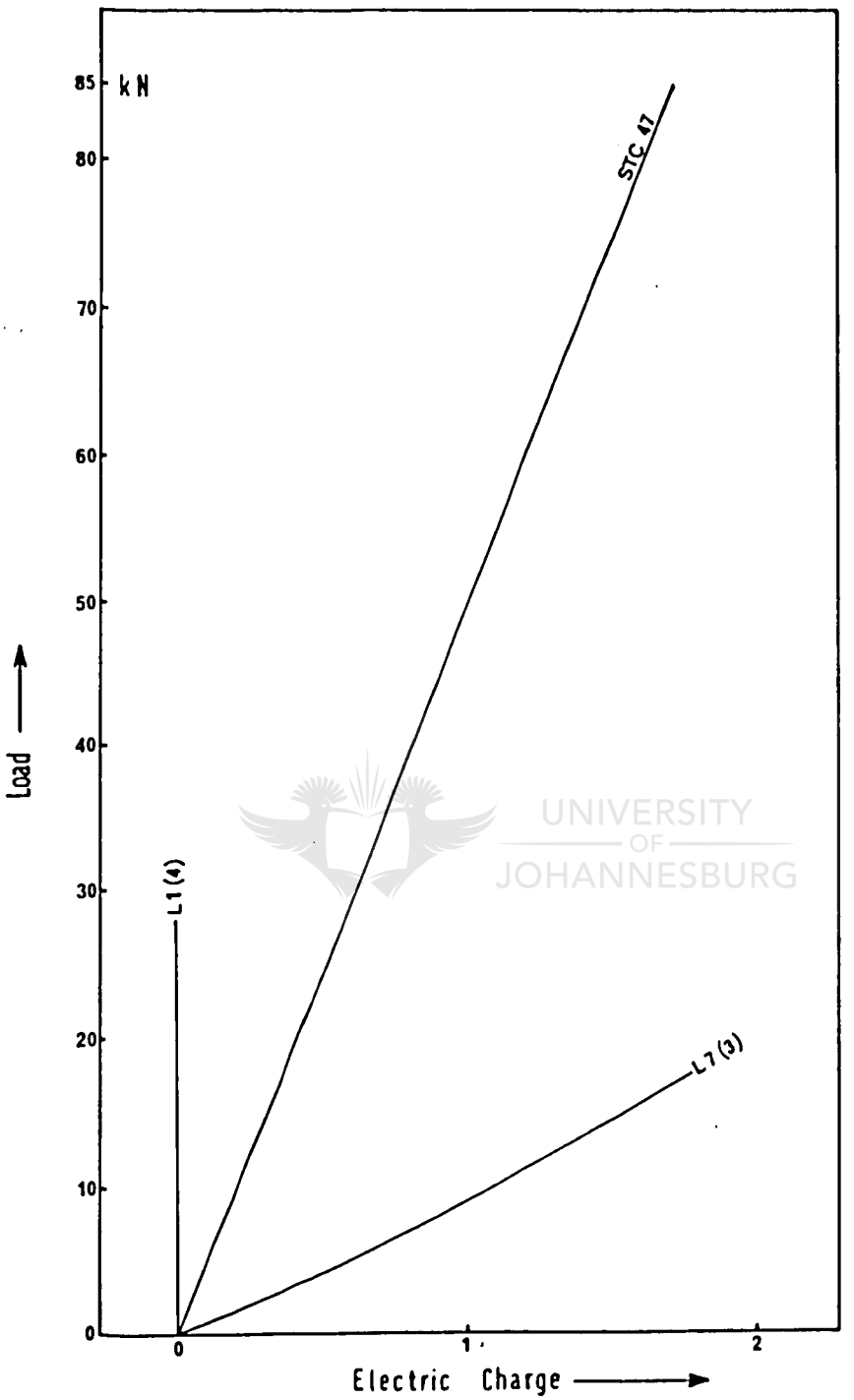

Figure 36 : Three load-electric charge curves to illustrate the sensitive electrometer scale setting required to record polarization values for quartzites; STC 47 and L 1 (4) were recorded at 3 X 10^{-7} coulomb full range, whereas L 7 (3) was recorded at 10 X 10^{-9} coulomb full range.

axes of the quartz grains, it was decided to record the longitudinal effect in some of the quartzite cylinders. The piezoelectric results from 61 quartzite cylinders are given in table 7. In column four, longitudinal polarization simply refers to readings taken with the electrodes coupled directly to the press, whereas transverse polarization was registered with the electrodes soldered onto the long sides of the cylinder. Each individual cylinder was subjected to a process of stressing to various stress levels more than once, before proceeding to a stress level where the applied mechanical stress exceeded the uniaxial compressive strength of the quartzite cylinder.

In columns 4 and 5 of table 7, the piezoelectric polarization value of each quartzite cylinder at a given stress level, is the mean value calculated from all the values obtained by repetitive stressing and destressing the same cylinder to that specific stress-level.

The percentage positive and negative deviation of an individual reading from the mean polarization value is given in columns 6 and 7.

5.3. Piezoelectric Behaviour of Individual Quartzites.

5.3.1. Drift in Electric Charge during Tests on Quartzites.

Due to very small piezoelectric charges generated by quartzites under stress, it became necessary to operate the electrometer at a scale value at least one hundred times more sensitive than when testing quartz. By doing this, a very strange phenomenon of drift was observed.

In this discussion that follows, only the drift effect in quartzites under zero load will be discussed. The effect

TABLE 7 PIEZOELECTRIC POLARIZATION VALUES AT DIFFERENT MECHANICAL STRESS LEVELS FOR DIFFERENT QUARTZITE SPECIMENS TESTED IN SMALL HYDRAULIC PRESS

QUARTZITE CYLINDER NUMBER	LOAD kN	UNIAXIAL COMPRESSIVE STRESS MPa	PIEZOELECTRIC POLARIZATION $C/m^2 \times 10^{-6}$		PER CENT DEVIATION FROM AVERAGE VALUE	
			LONGITUDINAL	TRANSVERSE	POSITIVE	NEGATIVE
L 1 (1)	5	63,5		2,10	56	30
	10	127,3		3,50	39	28
	15	192,0		4,30	11	11
	20	254,6		5,90	7	12
L 1 (2)	5	63,5		0,64	14	13
	10	127,3		1,33	6	8
	15	192,0		2,02	4	2
	20	254,6		2,67	1	2
	25	318,3		3,53	5	8
	28,5	362,8		3,96	10	7
L 1 (3)	5	63,5		0,40	26	41
	10	127,3		0,74	22	32
	15	192,0		0,87	27	23
	20	254,6		1,01	17	21
L 2 (1)	2,5	31,8		0,10 Neg.	0	0
	5	63,5		0,00	38	40
	10	127,3		0,20	21	15
	15	192,0		0,33	3	2
	20	254,6		0,60	5	5
L 2 (2)	5	63,5		0,20	13	15
	10	127,3		0.30	20	22
	12,5	159,0		0,34	4	1
	15	192,0		0,35	4	3
	17,5	222,8		0,37	0	0
L 2 (3)	5	63,5		0,97	15	8
	10	127,3		1,81	10	9
	15	192,0		2,77	4	18
	20	254,6		3,60	6	10
	25	318,5		4,67	1	2
L 3 (1)	5	63,5		0,68	3	2
	10	127,3		1,38	8	5
	15	192,0		2,02	7	6
	20	254,6		2,64	5	5
L 3 (2)	5	63,5		0,20	0	0
	10	127,3		0,50	13	13
	15	192,0		0,79	10	11
	18	229,2		0,92	9	6
	20	254,6		0,97	0	0
L 3 (3)	5	63,5		0,80	20	14
	10	127,3		1,20	16	14

TABLE 7 (CONTINUED) PIEZOELECTRIC POLARIZATION VALUES AT DIFFERENT MECHANICAL STRESS LEVELS FOR DIFFERENT QUARTZITE SPECIMENS TESTED IN STEEL HYDRAULIC PRESS

QUARTZITE CYLINDER NUMBER	LOAD kN	UNIAXIAL COMPRESSIVE STRESS MPa	PIEZOELECTRIC POLARIZATION $C/m^2 \times 10^{-6}$		PER CENT DEVIATION FROM AVERAGE VALUE	
			LONGITUDINAL	TRANSVERSE	POSITIVE	NEGATIVE
L 3 (4)	5	63,5		0,24	10	11
	10	127,3		0,53	9	6
	15	192,0		0,76	10	6
	18	229,2		0,83	0	0
L 3 (5)	5	63,5		0,21	6	12
	10	127,3		0,53	14	11
	15	192,0		0,91	10	8
	20	254,6		1,45	0	0
L 4 (1)	5	63,5		1,08	17	15
	10	127,3		1,91	16	14
	15	192,0		2,70	13	16
	20	254,6		3,62	13	3
	25	318,3		4,50	8	8
	30	381,9		6,00	0	0
L 4 (2)	5	63,5		1,26	18	21
	10	127,3		2,60	9	23
	12,5	159,0		3,77	15	12
L 4 (3)	5	63,5		0,92	9	20
	10	127,3		1,95	14	20
	15	192,0		2,82	14	16
	20	254,6		3,79	14	15
	25	318,3		5,60	5	4
L 4 (4)	2,5	31,8		0,34	30	27
	5	63,5		0,69	22	25
	7,5	95,5		1,02	27	30
	10	127,3		1,30	28	31
	12,5	159,0		1,56	22	29
	15	192,0		1,77	11	8
	17,5	222,8		1,95	0	0
	20	254,6		2,05	0	0
	22,5	286,4		2,10	0	0
	24,5	311,9		2,15	0	0
L 5A (1)	2,5	31,8	0,79		5	3
	5	63,5	1,80		2	8
	7,5	95,5	3,07		4	7
	10	127,3	4,33		1	1
	12,5	159,0	5,24		2	2
L 5A (2)	2,5	31,8	1,31		7	3
	5,0	63,5	2,66		1	2
	7,5	95,5	3,80		2	2
	10	127,3	4,65		3	1
L 5A (3)	2,5	31,8	0,50		15	10
	5	63,5	1,00		3	7
	6,5	83,0	1,60		2	2

TABLE 7 (CONTINUED) PIEZOELECTRIC POLARIZATION VALUES AT DIFFERENT MECHANICAL STRESS LEVELS FOR DIFFERENT QUARTZITE SPECIMENS TESTED IN SMALL HYDRAULIC PRESS

QUARTZITE CYLINDER NUMBER	LOAD kN	UNIAXIAL COMPRESSIVE STRESS MPa	PIEZOELECTRIC POLARIZATION $C/m^2 \times 10^{-6}$		PER CENT DEVIATION FROM AVERAGE VALUE	
			LONGITUDINAL	TRANSVERSE	POSITIVE	NEGATIVE
L 5B (1)	2,5	31,8	1,30		10	7
	5	63,5	2,00		4	5
	7,5	95,5	2,40		8	7
	10	127,3	2,70		7	2
	12	153,0	2,75		0	0
L 6A (1)	2,5	31,8		0,50	13	10
	5,0	63,5		0,80	8	18
	7,5	95,5		1,16	16	16
	10	127,3		1,48	14	11
	12,5	159,0		1,98	8	8
	14,5	184,6		2,37	6	6
L 6A (2)	2,5	31,8	1,32		6	2
	5	63,5	2,61		2	3
	7,5	95,5	3,65		5	5
	10	127,3	4,61		0	0
L 6B (1)	2,5	31,8	0,98		10	22
	5	63,5	2,08		7	1
	7,5	95,5	3,28		9	19
	10	127,3	4,70		8	19
	12,5	159,0	6,24		5	9
	15	192,0	7,70		6	7
	17,5	222,8	9,53		1	1
	20	254,6	11,33		0	0
L 6B (2)	2,5	31,8	1,11		3	9
	5	63,5	2,78		8	6
	7,5	95,5	4,19		8	9
	10	127,3	5,45		5	3
	15	192,0	6,37		0	0
L 6B (3)	2,5	31,8		0,15	22	22
	5,0	63,5		0,40	16	5
	7,5	95,5		0,69	16	8
	10	127,3		0,93	14	7
L 6B (4)	2,5	31,8	1,59		12	12
	5,0	63,5	3,06		8	2
	7,5	95,5	4,48		9	5
	10	127,3	5,84		7	6
L 6B (5)	2,5	31,8	0,40		8	8
	5	63,5	0,80		9	5
	7,5	95,5	1,10		2	4
	10	127,3	1,50		1	1
L 6C	2,5	31,8	1,04		10	15
	5	63,5	2,19		10	13
	7,5	95,5	3,37		8	9
	10	127,3	4,74		6	0
	12,5	159,0	6,49		0	0

TABLE 7 (CONTINUED) PIEZOELECTRIC POLARIZATION VALUES AT DIFFERENT MECHANICAL STRESS LEVELS FOR DIFFERENT QUARTZITE SPECIMENS TESTED IN SMALL HYDRAULIC PRESS

QUARTZITE CYLINDER NUMBER	LOAD kN	UNIAXIAL COMPRESSIVE STRESS MPa	PIEZOELECTRIC POLARIZATION $C/m^2 \times 10^{-6}$		PER CENT DEVIATION FROM AVERAGE VALUE	
			LONGITUDINAL	TRANSVERSE	POSITIVE	NEGATIVE
L 7 (1)	5	63,5		5,4	8	29
	10	127,3		8,5	6	6
	15	192,0		12,0	0	0
L 7 (2)	2,5	31,8		2,05	22	19
	5	63,5		4,60	20	22
	7,5	95,5		6,65	12	29
	10	127,3		8,05	21	17
	12,5	159,0		9,30	14	10
	15	192,0		10,30	3	3
	17,5	222,8		11,10	0	0
L 7 (3)	5	63,5		1,94	3	5
	10	127,3		3,59	2	2
	15	192,0		5,17	2	2
	17,5	222,8		5,83	0	0
L 8 (1)	2,5	31,8		1,37	32	27
	5	63,5		2,17	26	23
	7,5	95,5		2,40	3	4
	10	127,3		2,90	2	3
	12,5	159,0		3,30	0	0
	15	192,0		4,30	0	0
L 8 (2)	5	63,5		1,25	7	7
	10	127,3		2,88	8	7
	15	192,0		4,89	5	7
	20	254,6		6,89	0	0
L 8 (3)	2,5	31,8		3,80	12	18
	5	63,5		5,60	0	0
	7,5	95,5		8,30	0	0
	10	127,3		10,60	0	0
L 9 (1)	2,5	31,8		0,22	23	8
	5	63,5		0,49	20	12
	7,5	95,5		0,80	17	8
	10	127,3		1,00	0	0
	11,8	149,6		1,18	2	2
	12,5	159,0		1,27	0	0
	15	192,0		1,57	0	0
L 9 (2)	5	63,5		0,49	15	10
	10	127,3		1,13	4	1
L 9 (3)	5	63,5		0,15	12	14
	10	127,3		0,46	9	9

TABLE 7 (CONTINUED) PIEZOELECTRIC POLARIZATION VALUES AT DIFFERENT MECHANICAL STRESS LEVELS FOR DIFFERENT QUARTZITE SPECIMENS TESTED IN SMALL HYDRAULIC PRESS

QUARTZITE CYLINDER NUMBER	LOAD kN	UNIAXIAL COMPRESSIVE STRESS MPa	PIEZOELECTRIC POLARIZATION $C/m^2 \times 10^{-6}$		PER CENT DEVIATION FROM AVERAGE VALUE	
			LONGITUDINAL	TRANSVERSE	POSITIVE	NEGATIVE
L 9 (4)	2,5	31,8		0,15 Neg.	0	0
	5	63,5		0,20	23	10
	10	127,3		0,90	15	9
	15	192,0		1,75	14	11
	17,5	222,8		2,46	1	1
	19,5	248,2		2,90	0	0
L 9 (5)	5	63,5		0,60	0	0
	10	127,3		1,13	0	0
	15	102,0		1,73	0	0
	20	254,6		2,27	0	0
	20,7	263,5		2,33	0	0
L 10 (1)	2,5	31,8		0,25	5	1
	5	63,5		0,48	2	3
	7,5	95,5		0,71	6	4
	10,0	127,3		0,98	0	0
L 10 (2)	2,5	31,8		0,39	14	15
	5	63,5		0,75	13	16
	7,5	95,5		1,12	12	20
	10	127,3		1,46	9	18
	12,5	159,0		1,77	9	13
	15	192,0		2,06	8	12
	17,5	222,8		2,31	5	6
L 11 (1)	5	63,5		0,11	21	9
	10	127,3		0,30	18	23
	15	192,0		0,49	19	25
	20	254,6		0,68	7	7
L 11 (2)	5	63,5		0,32	3	18
	10	127,3		0,56	13	11
	15	192,0		0,85	8	10
	20	254,6		1,15	3	4
	22,5	286,4		1,35	0	0
L 11 (3)	5	63,5		0,21	19	21
	10	127,3		0,40	12	17
	15	192,0		0,73	0	0
	20	254,6		1,27	0	0
L 11 (4)	2,5	31,8		0,98	14	26
	5	63,5		2,00	14	14
	7,5	95,5		3,00	9	9
	10	127,3		4,00	6	6
	12,5	159,0		4,90	0	0
L 11 (5)	5	63,5		0,18	0	0
	10	127,3		0,36	0	0
	15	192,0		0,58	0	0
	20	254,6		0,78	0	0
	20,7	263,5		0,81	0	0

TABLE 7 (CONTINUED) PIEZOELECTRIC POLARIZATION VALUES AT DIFFERENT MECHANICAL STRESS LEVELS FOR DIFFERENT QUARTZITE SPECIMENS LOADED IN SMALL LOADING FRAME

QUARTZITE CYLINDER NUMBER	LOAD kN	UNIAXIAL COMPRESSIVE STRESS MPa	PIEZOELECTRIC POLARIZATION C/m² X 10^{-6}		PER CENT DEVIATION FROM AVERAGE VALUE	
			LONGITUDINAL	TRANSVERSE	POSITIVE	NEGATIVE
L 11 (6)	2,5	31,8		0,23 Neg.	60	60
	3,75	47,7		0,22 Neg.	25	25
	5	63,5		0,06	20	5
	7,5	95,5		0,40	5	5
	10	127,0		0,70	10	10
	12,5	159,0		1,00	10	10
	15	192,0		1,28	12	13
L 12A (1)	2,5	31,8	0,31		8	19
	5	63,5	0,66		9	13
	7,5	95,5	0,95		7	8
	10	127,3	1,27		10	5
	12,5	159,0	1,54		16	8
	15	192,0	1,78		0	0
L 12A (2)a	2,5	31,8	0,40		5	5
	5	63,5	0,77		13	9
	7,5	95,5	0,93		0	0
L 12A (2)b	2,5	31,8		0,30	11	8
	5	63,5		0,60	11	8
	7,5	95,5		0,85	9	6
	10	127,3		1,14	6	3
	12,5	159,0		1,43	5	2
	15	192,0		1,74	1	0
L 12A (2)c	2,5	31,8		0,33	0	0
	5	63,5		0,67	0	0
	7,5	95,5		1,00	0	0
	10	127,3		1,33	0	0
	12,5	159,0		1,70	0	0
	15	192,0		2,03	0	0
	17,5	222,8		2,37	0	0
	20	254,6		2,73	0	0
	22,5	286,0		3,07	0	0
	25	318,3		3,40	0	0
	27,5	350,0		3,73	0	0
L 12A (3)	2,5	31,8		0,26	5	5
	5	63,5		0,55	9	4
	7,5	95,5		0,84	7	9
	10	127,3		1,07	9	7
	12,5	159,0		1,38	8	6
	15	192,0		1,63	2	2
	17,5	222,8		1,94	0	0
	20	254,6		2,23	0	0
L 12A (4)	2,5	31,8	1,5		4	6
	5	63,5	2,8		4	4
	7,5	95,5	4,3		0	0

TABLE 7 (CONTINUED) PIEZOELECTRIC POLARIZATION VALUES AT DIFFERENT MECHANICAL STRESS LEVELS FOR DIFFERENT QUARTZITE SPECIMENS TESTED IN SMALL HYDRAULIC PRESS

QUARTZITE CYLINDER NUMBER	LOAD kN	UNIAXIAL COMPRESSIVE STRESS MPa	PIEZOELECTRIC POLARIZATION $C/m^2 \times 10^{-6}$		PER CENT DEVIATION FROM AVERAGE VALUE	
			LONGITUDINAL	TRANSVERSE	POSITIVE	NEGATIVE
L 13B (1)	2,5	31,8	1,50		44	41
	5	63,5	2,65		25	28
	7,5	95,5	3,77		21	21
	10	127,3	5,05		14	15
	12,5	159,0	6,71		8	16
	15	192,0	8,28		6	8
	17,5	222,8	9,91		4	6
	20	254,6	11,47		4	7
	22,5	286,4	12,48		3	3
L 13B (2)	2,5	31,8	0,89		14	4
	5	63,5	1,62		6	6
	7,5	95,5	2,40		8	7
	10	127,3	2,99		11	11
	12,5	159,0	3,44		6	2
	15	192,0	4,07		0	0
L 13B (3)	2,5	31,8	0,74		12	40
	5	63,5	1,60		19	25
	7,5	95,5	2,55		15	17
	10	127,3	3,36		12	13
	12,5	159,0	4,15		10	11
	15	192,0	4,72		4	6
	17,5	222,8	5,42		6	5
	20	254,6	6,36		4	4
	22,5	286,4	7,32		3	3
L 13B (4)	2,5	31,8	1,78		5	14
	5	63,5	3,35		10	7
	7,5	95,5	4,67		8	3
	10	127,3	5,87		8	12
	12,5	159,0	7,45		4	9
	15	192,0	8,31		6	10
	17,5	222,8	9,52		0	0
	20	254,6	9,92		6	3
	22,5	286,4	10,69		0	0
	25	318,3	11,97		0	0
L 13C (1)	2,5	31,8	1,32		0	18
	5	63,5	2,29		0	6
	7,5	95,5	3,06		6	6
	10	127,3	3,86		2	6
	12,5	159,0	4,74		3	5
	15	192,0	5,41		1	1
L 13C (2)	2,5	31,8	1,12		8	9
	5	63,5	2,18		5	6
	7,5	95,5	3,02		1	3
	10	127,3	3,98		0	0
	12,5	159,0	5,03		1	1
	15	192,0	6,04		0	0

TABLE 7 (CONTINUED) PIEZOELECTRIC POLARIZATION VALUES AT DIFFERENT MECHANICAL STRESS LEVELS FOR DIFFERENT QUARTZITE SPECIMENS TESTED IN SMALL HYDRAULIC PRESS

QUARTZITE CYLINDER NUMBER	LOAD kN	UNIAXIAL COMPRESSIVE STRESS MPa	PIEZOELECTRIC POLARIZATION $C/m^2 \times 10^{-6}$		PER CENT DEVIATION FROM AVERAGE VALUE	
			LONGITUDINAL	TRANSVERSE	POSITIVE	NEGATIVE
L 13C (3)	2,5	31,8	1,03		11	14
	5	63,5	2,20		10	13
	7,5	95,5	3,67		11	15
	10	127,3	5,21		11	12
	12,5	159,0	6,94		7	7
	15	192,0	8,34		5	5
L 13C (4)	1	12,7	0,40 Neg.		36	9
	2,5	31,8	0,10		0	0
	5	63,5	0,90		8	5
	7,5	95,5	1,90		5	5
	10	127,3	2,60		4	4
	11,5	146,0	2,90		0	0
	12,5	159,0	3,20		0	0
	14,25	181,4	3,70		0	0
HH 1	5	63,5		0,16	0	0
	10	127,3		0,34	0	0
	15	192,0		0,50	0	0
	20	254,6		0,67	0	0
	20,6	262,3		0,68	0	0
HH 2	5	63,5		0,10	0	0
	10	127,3		0,31	0	0
	15	192,0		0,38	0	0
	18	229,2		0,61	0	0

of drift in tests carried out on quartzites and silcretes under stress will be dealt with, where applicable, under results on individual quartzites.

It has been mentioned before that the Keithley electrometer model 610C is very sensitive when operated at scale values below 1 X 10^{-8} coulomb per full scale with the electrodes coupled to some quartzite cylinders under zero load. However, the electrometer was tested regularly with the electrodes open at scale values as low as 1 X10^{-10} coulomb per full scale in order to check for instrument drift. The minute drift thus observed could possibly have been the internal drift of 5 X 10^{-15} coulomb per second for the instrument claimed by the manufacturers.

These tests with the electrodes open, proved beyond all doubt that the drift recorded with the electrodes coupled to quartzite must have come from an external source.

At the beginning of the tests on quartzites when the problem was experienced for the first time, it was thought that it might have been caused by static or stray electricity in the surroundings. Various steps have been taken to try and eliminate these disturbances in case they might be the cause of the drift.

Special cables for the electrodes were designed and tried out together with a Faraday cage, but the improvement was so little, that it was decided to carry out the tests without the cage, and to replace the long cables with a short co-axial cable.

What makes this problem of drift such an interesting one, is the fact that very seldom did two quartzite cylinders cut from the same rock sample give, under exactly the same testing con-

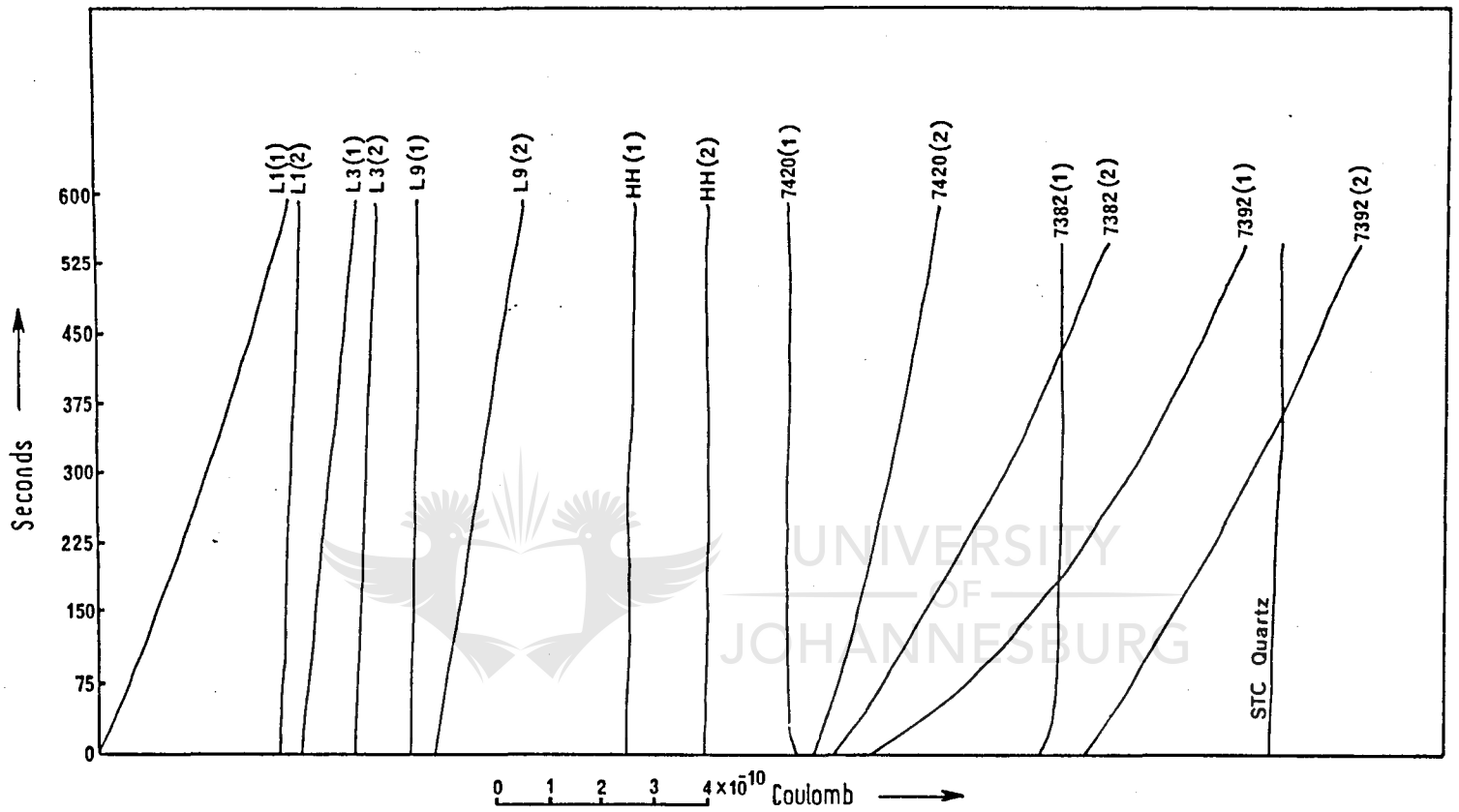

Figure 37 : A series of drift curves at zero load for quartzites, silcretes and STC quartz with electrometer scale setting at 1 X 10^{-9} coulomb full range.

ditions, the same drift curve. This is beautifully illustrated in a series of drift curves in figure 37, from tests carried out on various quartzites, silcretes and quartz at zero load. From the curves it can be seen that the drift for cylinder L 1 (1) is at least 13 times higher than that of L 1 (2), although they were both cut from the same hand specimen and both tested at an electrometer scale setting of 1 X 10^{-9} coulomb full range. This same quartzite cylinder L 1 (2) was later used to produce a perfect set of load-electric charge curves seen in figure 40. During the calculations of the piezo-electric polarization values for this particular cylinder, it was not even necessary to correct for drift.

Before putting forward any theories on the origin of this drift phenomenon, drift tests were carried out on quartz cylinders under exactly the same conditions. One of the results representative of many others, plotted in figure 37, proved that for quartz, quartzites and silcretes tested, drift only appears in quartzites, or rather most quartzites, and silcretes. In previous tests, quartz cylinders were tested for drift at a scale setting of 1 X 10^{-10} coulomb full range, but did not show any drift. However, on quite a few occasions some quartzite cylinders were tested at scale settings as high as 1 X 10^{-7} coulomb full range, and then the indication needle of the electrometer moved so fast that it was feared that it might be damaged.

5.4. Results on Individual Quartzites.

The piezoelectric behaviour of each individual rock specimen will now be discussed in the light of the results obtained. It will be noticed that in some quartzite cylinders only the

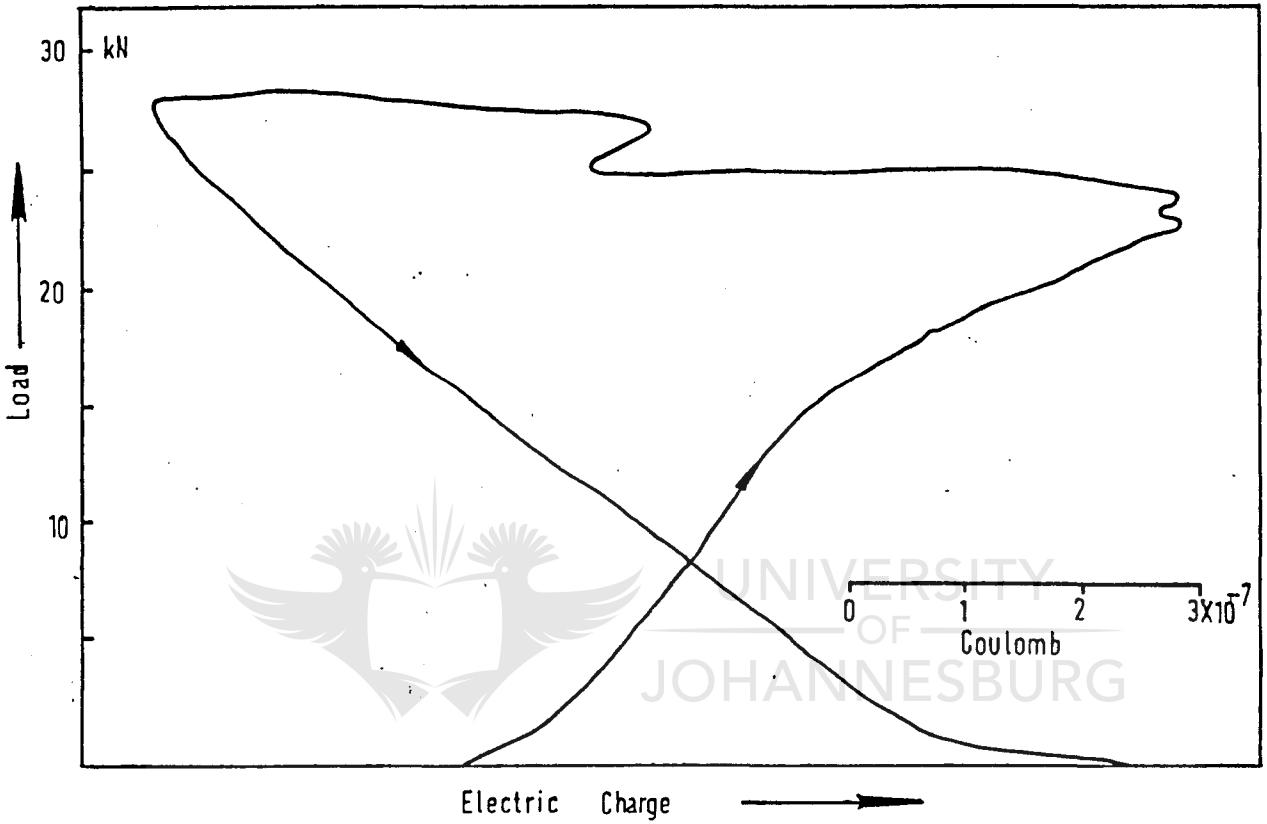

Figure 38 : Typical example of an irregular load-electric charge curve with a high drift recorded for quartzite L 13C (6). In this case the result was considered unreliable for calculating the piezoelectric effect.

results obtained on a few cylinders from the same rock specimen were considered reliable enough to be used for calculating the piezoelectric effect. This is either due to a very irregular load-electric charge curve, or to an exceptionally high drift rate of the cylinder with or without stress. The curve plotted for quartzite L 13(C) (6) in figure 38 is a good example of an irregular curve with high drift.

5.4.1. Results on Quartzite L 1.

Three out of five cylinders cut from the above quartzite produced readings reliable enough to be used for calculating the transverse polarization at various stress levels.

It can be seen in figure 39 that the polarization in cylinder L 1 (1) which started off rapidly at low stress-levels, gradually decreased with increase in stress up to approximately 190 MPa, whereafter it increased fast up to breaking point. This cylinder has a fairly high positive drift which had to be taken into account when polarization values were calculated. A total of 26 load vs electric charge curves were used to calculate the transverse polarization values for cylinder L 1 (2). From the load vs electric charge curves for this particular cylinder plotted in figure 40 as well as the low (maximum 14) percentage deviation from the average value in table 7, it can be seen that the readings recorded, fall on a straight line very similar to the results obtained for quartz. A gradual decrease in value with increase in stress was observed for cylinder L 1 (3). This cylinder produced a polarization value of $1{,}01 \times 10^{-6}$ C/m^2 which is almost six times lower

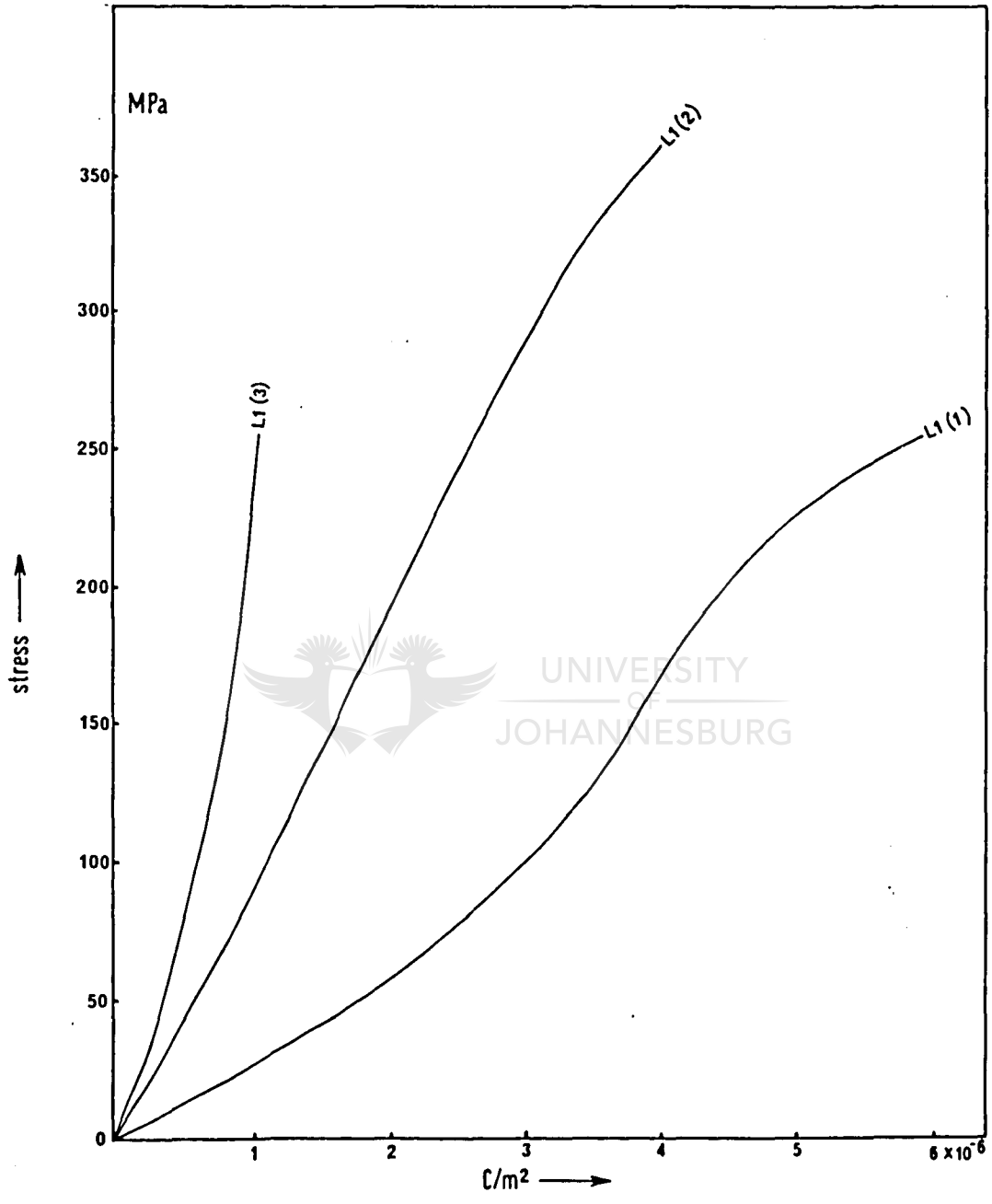

Figure 39 : Relationship between mechanical stress and piezoelectric polarization for cylinders cut from quartzite L 1, tested in small hydraulic press.

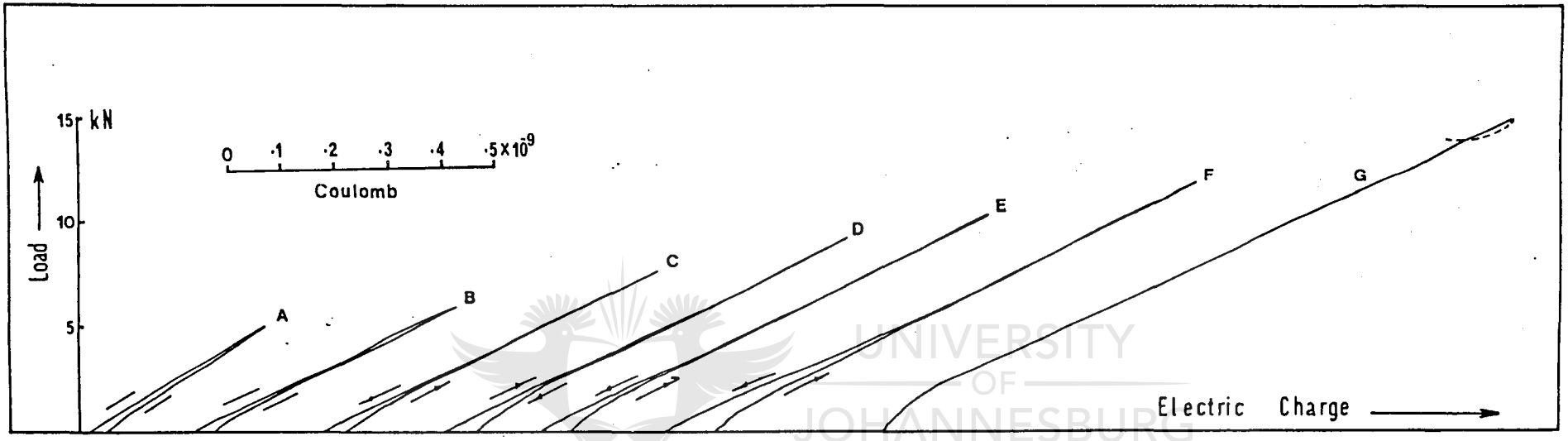

Figure 40 : Complete set of load-electric charge curves to determine the transverse piezoelectric effect for L 1 (2); curve G was recorded to breaking point. Tests carried out in small hydraulic press.

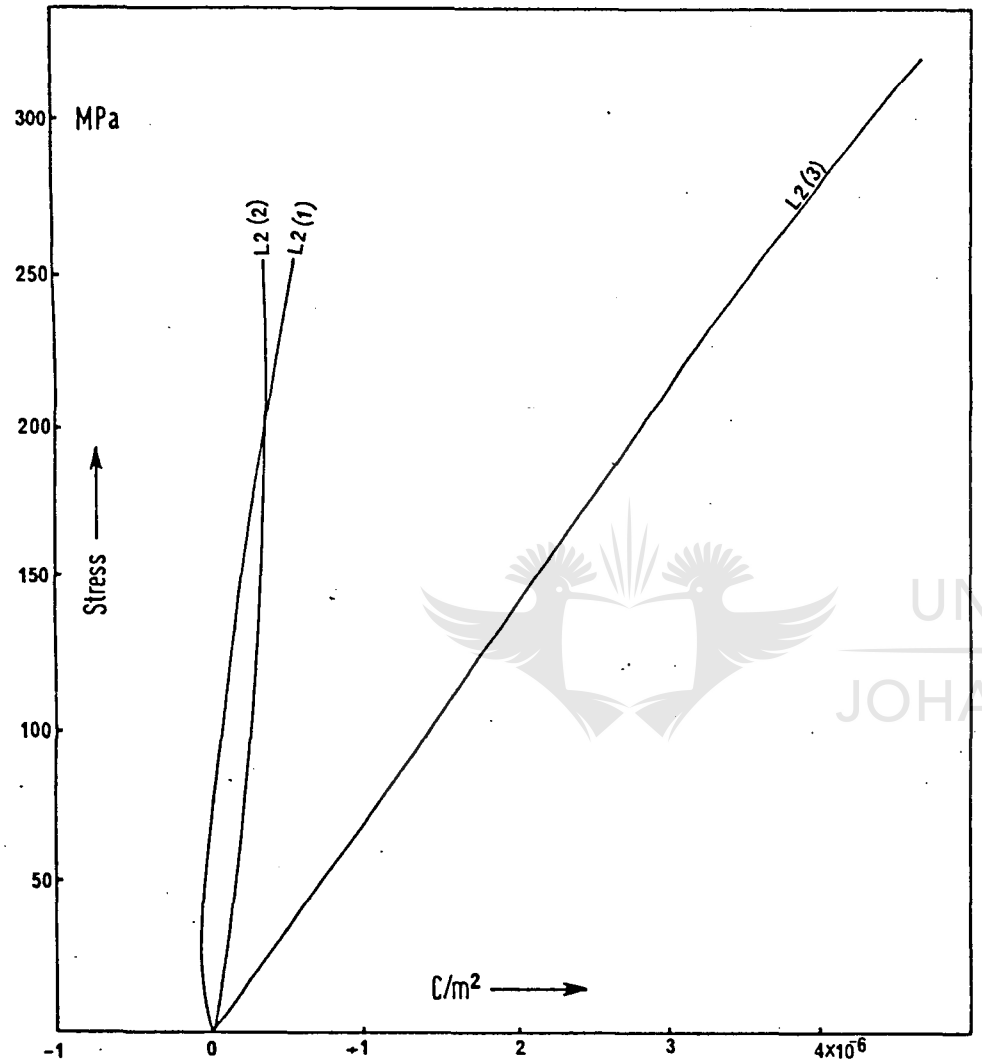

Figure 41 : Relationship between mechanical stress and piezo-electric polarization for cylinders cut from quartzite L 2, tested in small hydraulic press.

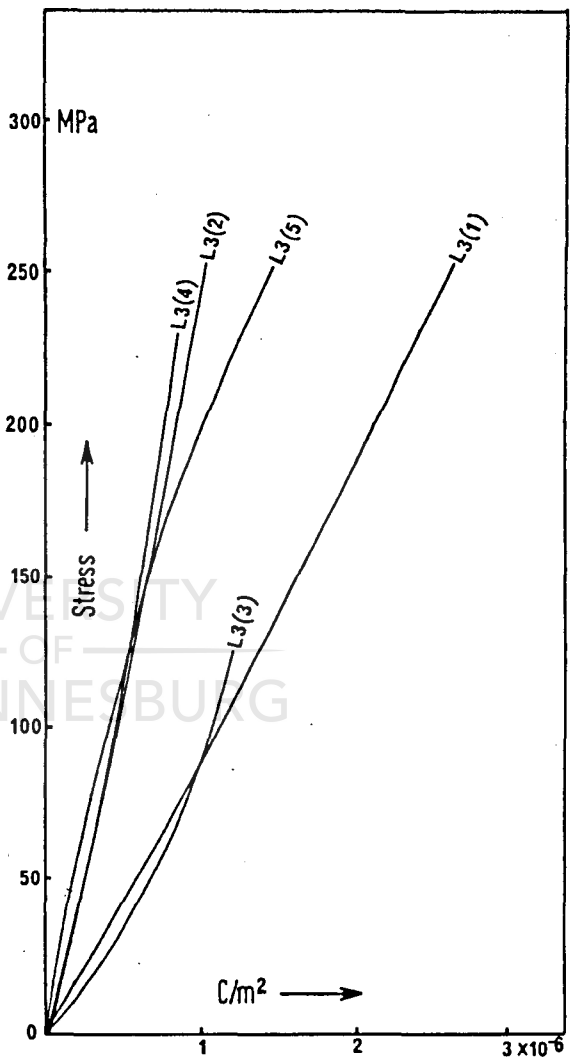

Figure 42 : Relationship between mechanical stress and piezoelectric polarization for cylinders cut from quartzite L 3, tested in small hydraulic press.

than the value for L 1 (1) at the same stress of 254,6 MPa.

5.4.2. Results on Quartzite L 2.

Very low electric charges were recorded on two of the three cylinders tested. Up to a stress-level of 31,8 MPa cylinder L 2 (1) generated a small negative charge, whereafter it reversed polarity and moved in a positive direction. A transverse piezoelectric charge of $1,17 \times 10^{-11}$ coulomb at a load of 17,5 kN was recorded for cylinder L 2 (2) which is a very low value. Thirteen load-electric charge curves were used to calculate the average polarization values for L 2 (3). The stress-polarization values for this particular cylinder plot virtually on a straight line with a slight increase in value above 260 MPa. This linearity in the plotted results in figure 41, is indicative of a constant increase in polarization with progressive stressing. For the above specimen it was necessary to apply drift corrections to two of the three cylinders.

5.4.3. Results on Quartzite L 3.

The transverse polarization values for cylinders L 3 (2), L 3 (4) and L 3 (5) plotted in figure 42 fall within a very close grouping on a linear curve up to 155 MPa, whereafter there is a slight increase in the value for L 3 (5). The values for the remaining two cylinders, L 3 (1) and L 3 (3) plot on a separate line with a gradual decrease in value for L 3 (3) with increase in stress.
Although there was a fair amount of drift experienced in the electric charge registered for all the above cylinders, the per cent deviation from the average value did not exceed 20 per cent in all five cylinders.

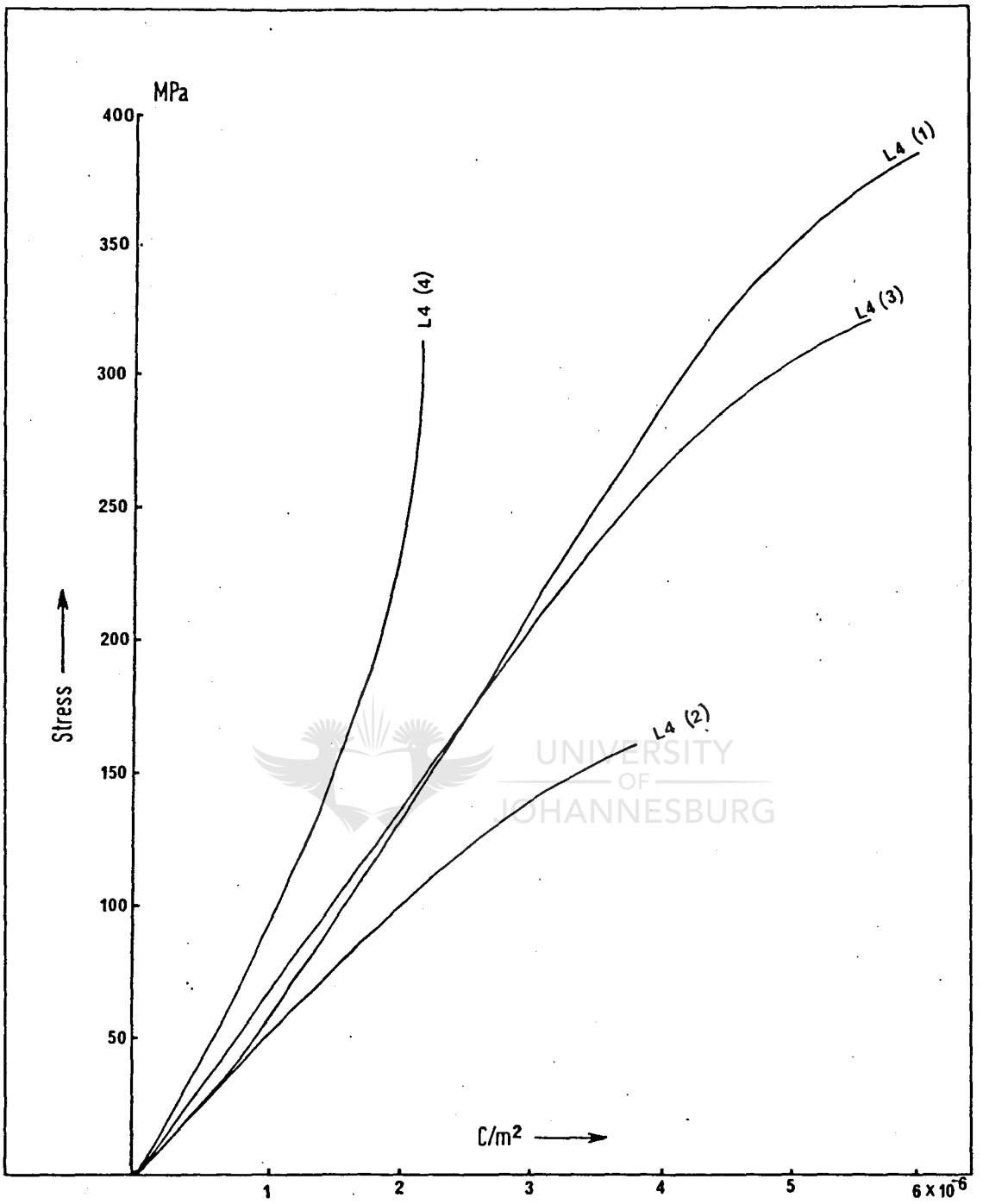

Figure 43 : Relationship between mechanical stress and piezoelectric polarization for cylinders cut from quartzite L 4, tested in small hydraulic press.

5.4.4. Results on Quartzite L 4.

The linear portion in each individual stress-polarization curve plotted in figure 43 for cylinders L 4 (1), L 4 (2) and L 4 (3) reflects a constant increase in transverse polarization with constant increments in stress. Curves L 4 (1), L 4 (2) and L 4 (3) show an increase in the rate of polarization at 320 MPa, 250 MPa and 120 MPa respectively, whereas L 4 (4) starts to decreased in value at approximately 120 MPa.

This decrease in polarization value is a result of lower readings registered for L 4 (4) in the last three load vs electric charge curves. It was thought that the cylinder might have been deformed due to repetitive stressing and destressing which could have had a possible influence on the piezoelectric values, but no sign of such deformation could be found in any of the six stress-strain curves recorded for this particular cylinder. An increase in drift rate was experienced in this cylinder after the fourth consecutive time of stressing. This increase in drift rate together with the decrease in polarization is responsible for the 31 per cent deviation from the average value in L 4 (4).

5.4.5. Results on Quartz L 5.

The longitudinal piezoelectric polarization values for cylinders L 5A (1) and L 5A (2) plotted in figure 44 show a rapid increase in value with progressive stressing compared to an almost linear stress-polarization relationship for L 5A (3). The original recorded load-electric charge readings for cylinder L 5A (2) is plotted in figure 45 to illustrate the effect of drift during recording. For cylinder L 5B (1) the values diminish very rapidly above 32 MPa and tends to

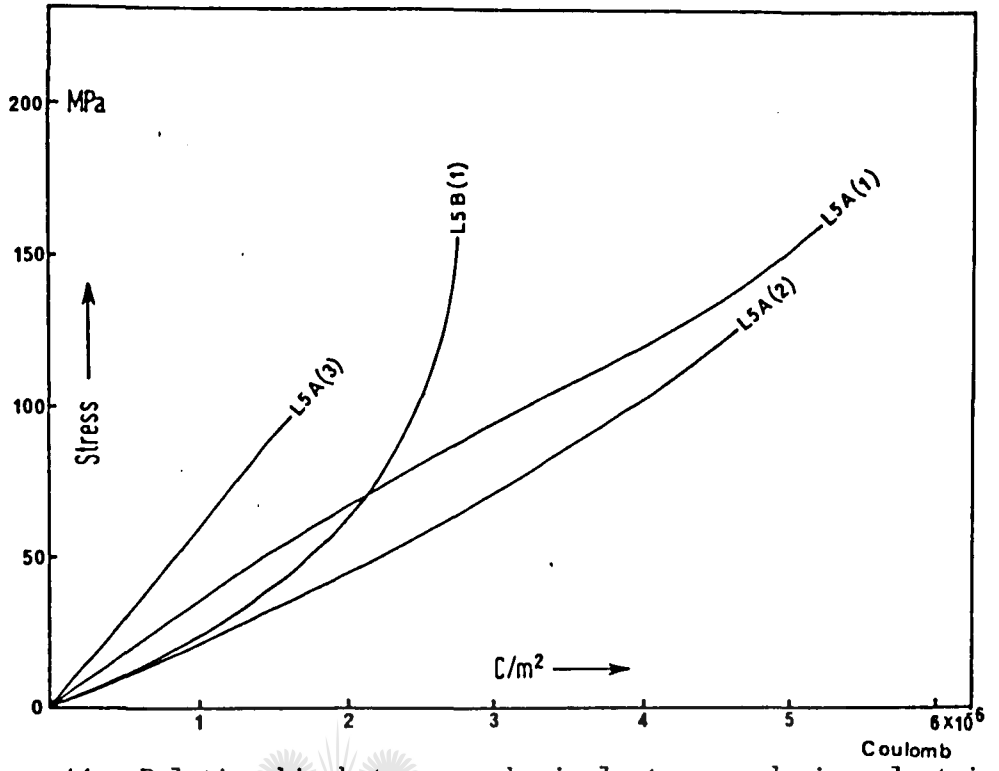

Figure 44 : Relationship between mechanical stress and piezoelectric polarization for cylinders cut in two different directions from quartzite L 5, tested in small hydraulic press.

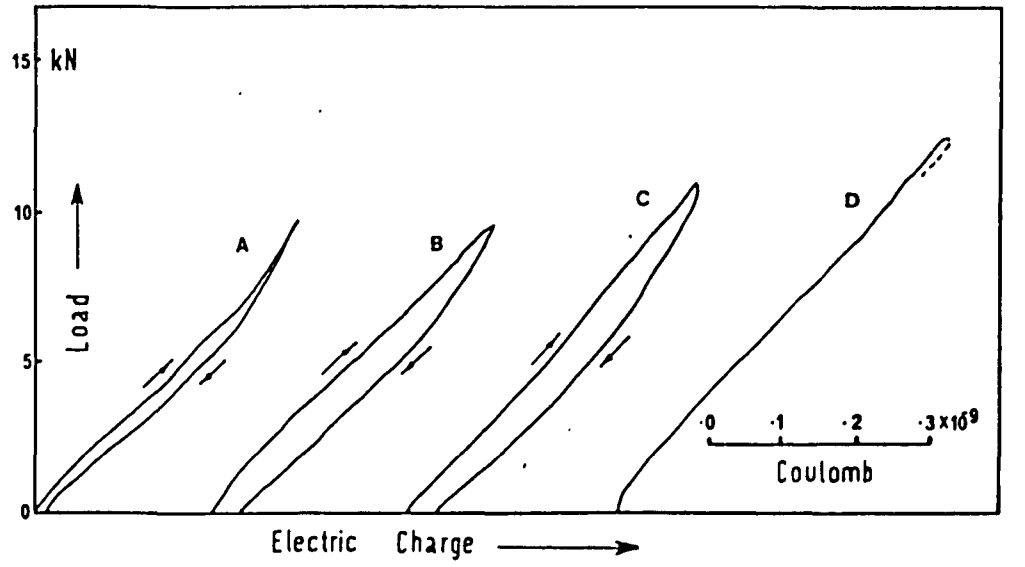

Figure 45 : Complete set of load-electric charge curves to determine the longitudinal piezoelectric effect for L 5A (2); Curve D was recorded to breaking point.

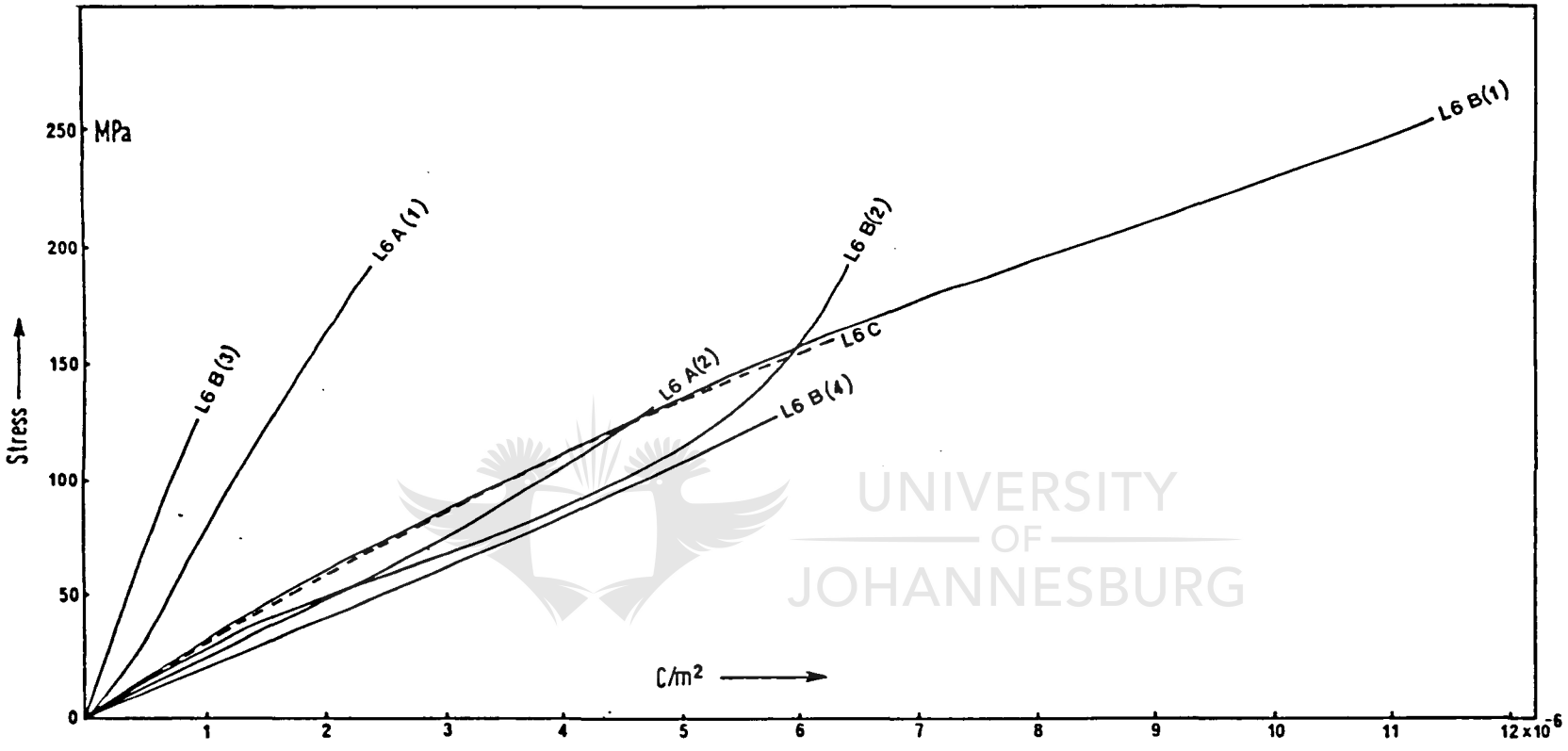

Figure 46 : Relationship between mechanical stress and piezoelectric polarization for cylinders cut in three different directions from quartzite L 6, tested in small hydraulic press.

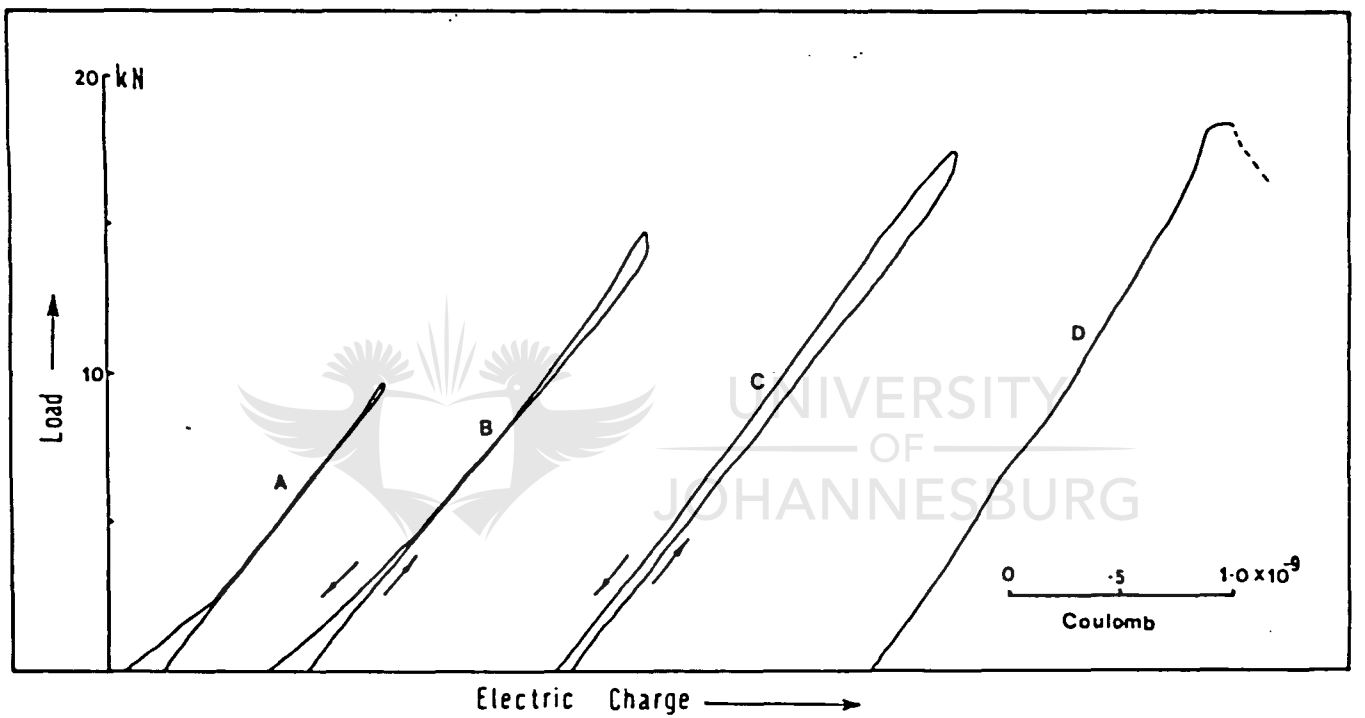

Figure 47 : Set of load–electric charge curves to determine the transverse piezoelectric effect for L 7 (3); curve D was recorded to breaking point. Tests carried out in small hydraulic press.

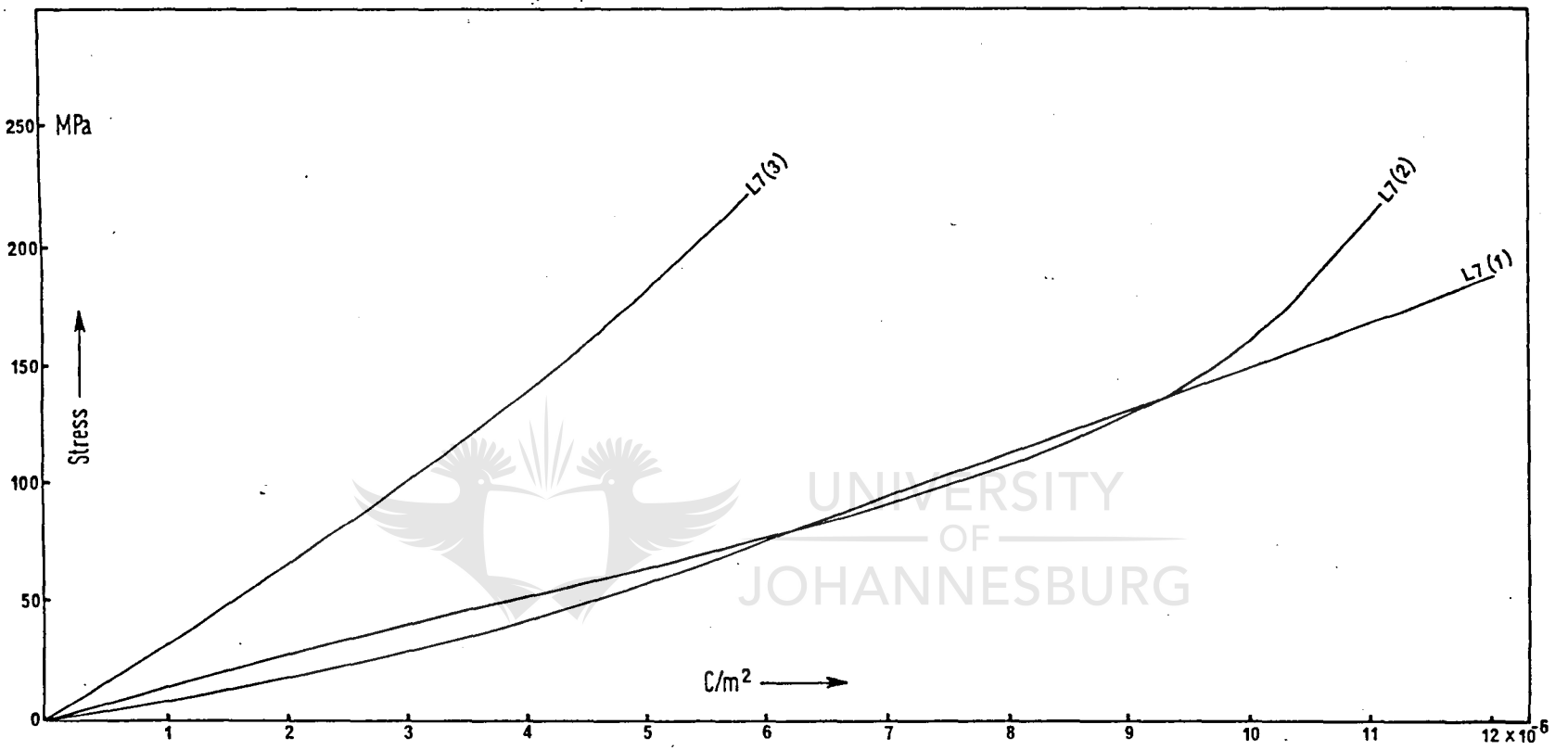

Figure 48 : Relationship between mechanical stress and piezoelectric polarization for cylinders cut from quartzite L 7, tested in small hydraulic press.

take on a constant value up to yielding point.

5.4.6. Results on Quartsite L 6.

There is a large difference to be observed in the transverse piezoelectric polarization for cylinders L 6A (1) and L 6B (3) on the one hand and the longitudinal effect for the remaining five cylinders plotted in figure 46 on the other. The plotted values for cylinders L 6A (2), L 6B (1), L 6B (2), L 6B (4) and L 6C fall within a fairly close grouping on almost a straight line. The only deviation from a straight line comes from curve L 6B (2) where a sharp decrease in values beyond 100 MPa is visible.

5.4.7. Results on Quartzite L 7.

Drift rates as high as $4,5 \times 10^{-11}$ coulomb per second was experienced in the recording of the transverse results for cylinders L 7 (1) and L 7 (2), even though an electrometer scale setting of 1×10^{-7} coulomb full range was used. Four of the six load-electric charge curves recorded for L 7 (3) are plotted in figure 47 where the linearity in the curves beautifully demonstrates the constant increase in electric charge with progressive loading. This result is similar to results obtained on quartz cylinders.
The sudden steep gradient in curve L 7 (2) beyond 120 MPa shown in figure 48, is due to a gradual drop in polarization as a result of repetitive stressing and destressing the cylinder.

5.4.8. Results on Quartzite L 8.

Curve L 8 (1) in figure 49 started off initially with a high transverse polarization but at approximately 30 MPa the rate of polarization declines slowly up to 130 MPa, whereafter there was a sharp increase again. In this case repetitive

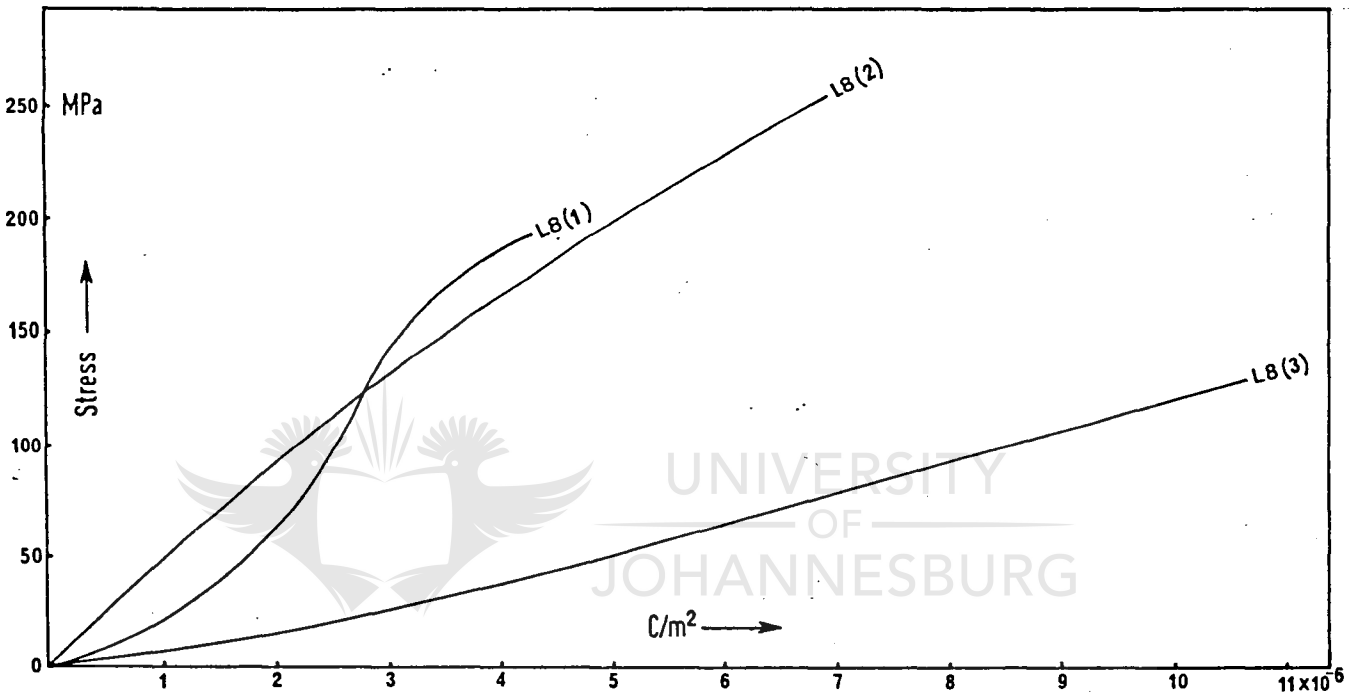

Figure 49 : Relationship between mechanical stress and piezoelectric polarization for cylinders cut from quartzite L 8, tested in small hydraulic press.

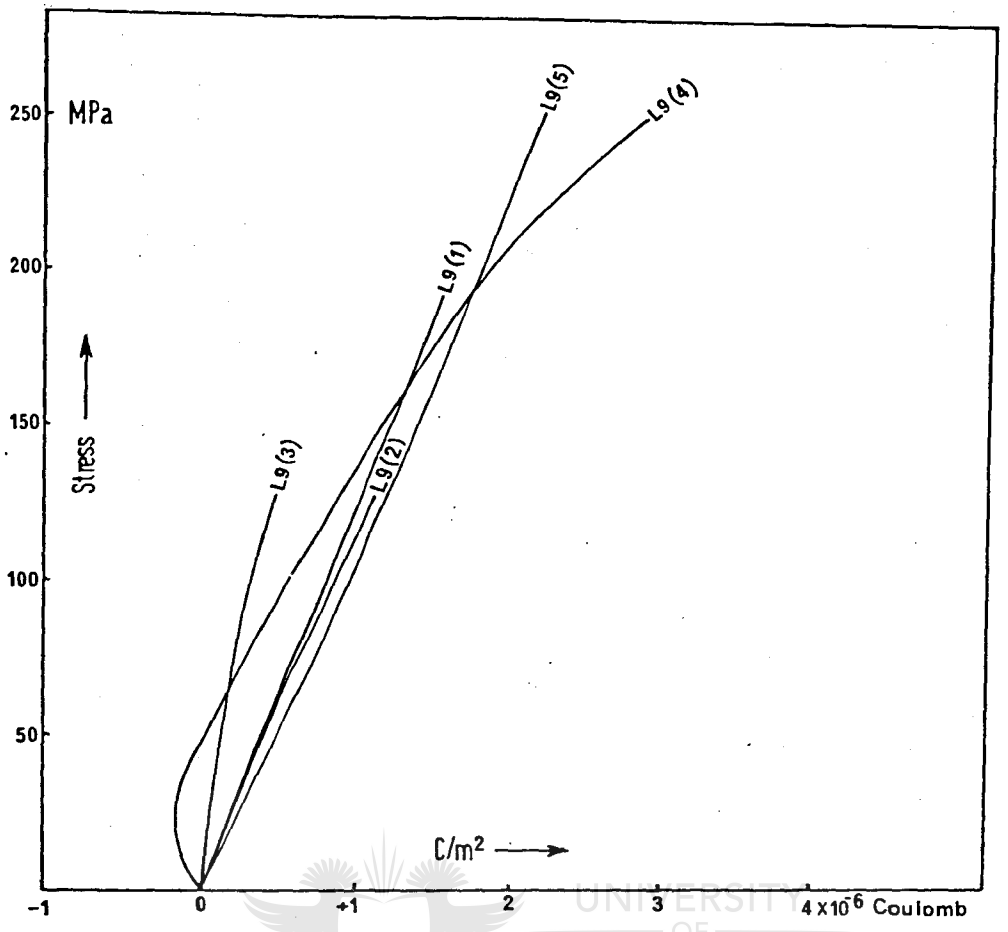

Figure 50 : Relationship between mechanical stress and piezoelectric polarization for cylinders cut from quartzite L 9, tested in small hydraulic press.

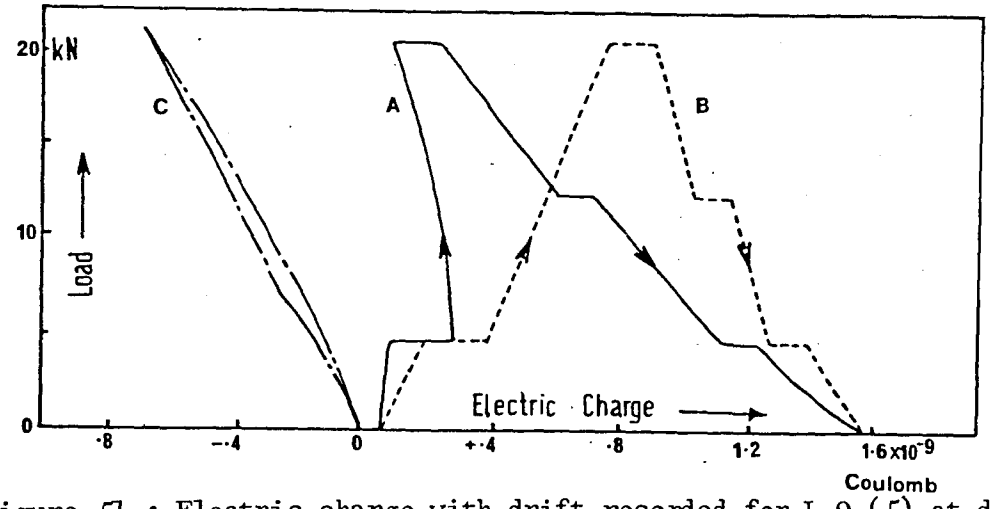

Figure 51 : Electric charge with drift recorded for L 9 (5) at different mechanical loads. In the original curve A loading, unloading and resting periods (plateaus) are 60 second intervals except for a 120 second interval in the second ascending limb of the curve; curve B is the drift curve calculated from curve A, and C the resultant curve with drift removed. Tests carried out in stiff testing machine.

stressing and destressing brought about a higher piezo-electric effect which is exactly opposite to what happened to so many other cylinders.

Cylinder L 8 (3) experienced a drift of 8,8 X 10^{-9} coulomb per second even though the electrometer was operated at a scale setting of 1 X 10^{-7} coulomb full range. Fortunately the magnitude of the drift was constant for stressing and de-stressing which made it still possible to apply drift corrections to all electric charge readings.

The accumulation in electric charge with progressive loading is reasonably constant for cylinders L 8 (2) and L 8 (3), with the latter reaching a very high transverse polarization value of 10,6 X 10^{-6} C/m^2 at 127,3 MPa.

5.4.9. Results on Quartzite L 9.

The transverse polarization values at various stress-levels for cylinders L 9 (1), L 9 (2) and L 9 (5) is closely grouped on a straight line in figure 50. This linearity in the individual stress-polarization curves once more indicates to a constant build-up of electric charge with augmentation in stress. The steep gradients displayed by all these curves are evidence of a fairly low piezoelectric effect for this rock specimen. Cylinder L 9 (4) started off with a negative electric charge up to 33 MPa, whereafter there was a sudden swing in the opposite direction. After climbing steadily to 190 MPa there was a gradual increase in polarization which persisted up to breaking point.

An experiment to determine drift under progressive loading was carried out on cylinder L 9 (5) in the stiff testing machine of the Chamber of Mines Research Laboratories in Johannesburg. The experiment was executed in a number of

loading and resting stages of 60 sec except for a 120 sec interval in the second ascending limb of the curve, as can be seen in figure 51, where the horizontal plateaus indicate 60 second periods of constant load (rest).
Curve A represents the actual load-electric charge curve with drift still included, B is the drift curve derived from curve A, and C is the final corrected load-electric charge curve.
The stress-polarization plot for this particular cylinder fits in well with the other cylinders from specimen L 9 in figure 50.

5.4.10. Results on Quartzite L 10.

Linearity in both curves plotted in figure 52 is very well defined. However, there is a very slight tendency in the gradient of L 10 (2) to steepen above 150 MPa. This steepening of the gradient is, in fact, again the result of repetitive stressing and destressing seen so often in this study.

5.4.11. Results on Quartzite L 11.

The set of stress-polarization curves presented in figure 52 is a very good example of a uniform build-up of polarization with progressive stressing. Only curves L 11 (5) and L 11 (6) tend to deviate from the linearity displayed by the set of curves.
There is a slight intensification in the transverse polarization rate of L 11 (3) starting just below 150 MPa. The phenomenon of reversing polarity in electric charge when under stress also occurred in cylinder L 11 (6).
Curve L 11 (5) was derived from figure 53 which is the result of an experiment carried out to determine the drift under progressive loading. In figure 53, A is the original load-

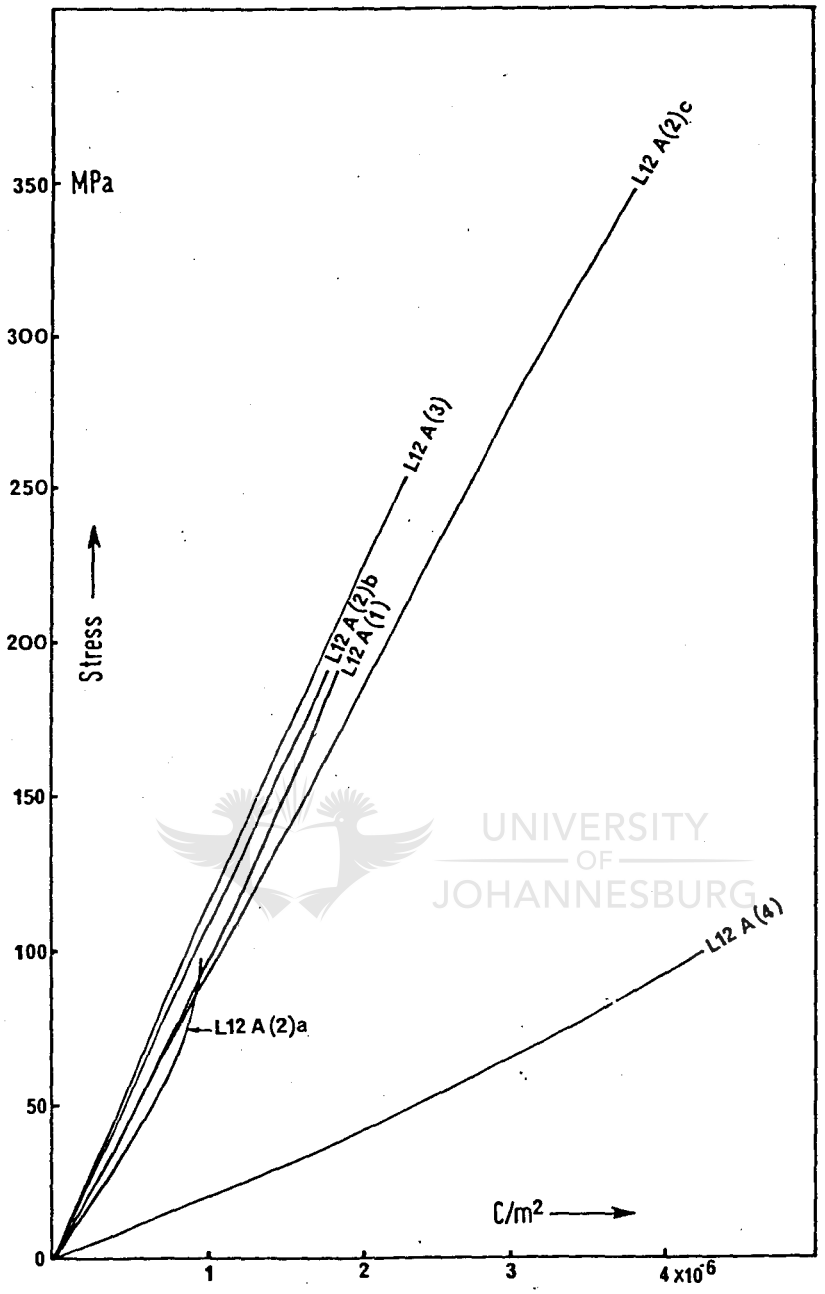

Figure 54 : Relationship between mechanical stress and piezo-electric polarization for cylinders cut parallel to dip from quartzite L 12, tested in small hydraulic press.

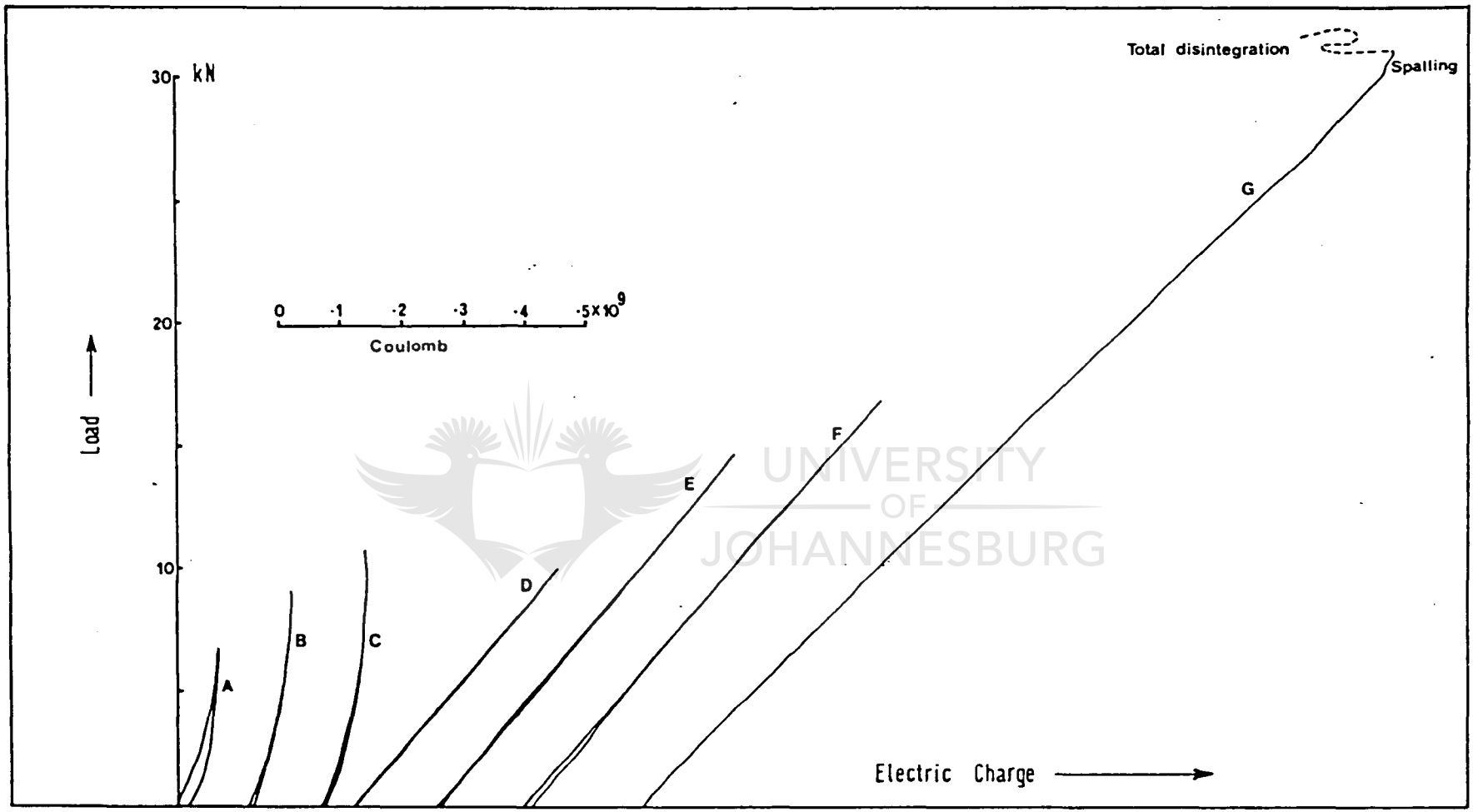

Figure 55 : Complete set of load–electric charge curves for quartzite L 12A (3). Curves A, B and C longitudinal piezoelectric effect; curves D, E, F and G transverse piezoelectric effect.

electric charge curve, B is the drift curve derived from curve A, whereas the corrected load-electric charge curve is given in curve C. Both loading and resting periods were taken at 60 second intervals. Except for L 11 (4) which has a final polarization value of 4,9 X 10^{-6} C/m^2 at a stress of 159 MPa, all the other curves indicate towards a very low piezoelectric effect for specimen L 11.

5.4.12. Results on Quartzite L 12.

Four out of a possible six cylinders cut from quartzite L 12, produced reliable enough results to be used for polarization calculations. Linearity, as well as good grouping, are two of the striking features observed in the stress-polarization curves plotted in figure 54. Cylinder L 12A (2) was tested for both the transverse and longitudinal piezoelectric effect. In the stress-polarization curves for this particular cylinder, the longitudinal effect is plotted in curve L 12A (2)a, the average values obtained from nine load-electric charge curves are plotted in L 12A (2)b, whilst L 12A (2)c was calculated from the load-electric charge curve G in figure 55 where the cylinder was stressed to breaking point.

The transverse effects for cylinders L 12A (2)b and L 12A (3) as well as the longitudinal effects for L 12A (2)a and L 12A (1) plot in a close grouping, except for L 12A (4) which falls far outside this grouping. The fairly high polarization value of 4,3 X 10^{-6} C/m^2 calculated for L 12A (4) is most probably due to a few large quartz grains, whereas the close grouping might be indicative of a fairly constant piezoelectric effect for specimen L 12.

5.4.13. Results on Quartzite L 13.

The outstanding feature in the curves plotted in figure 56

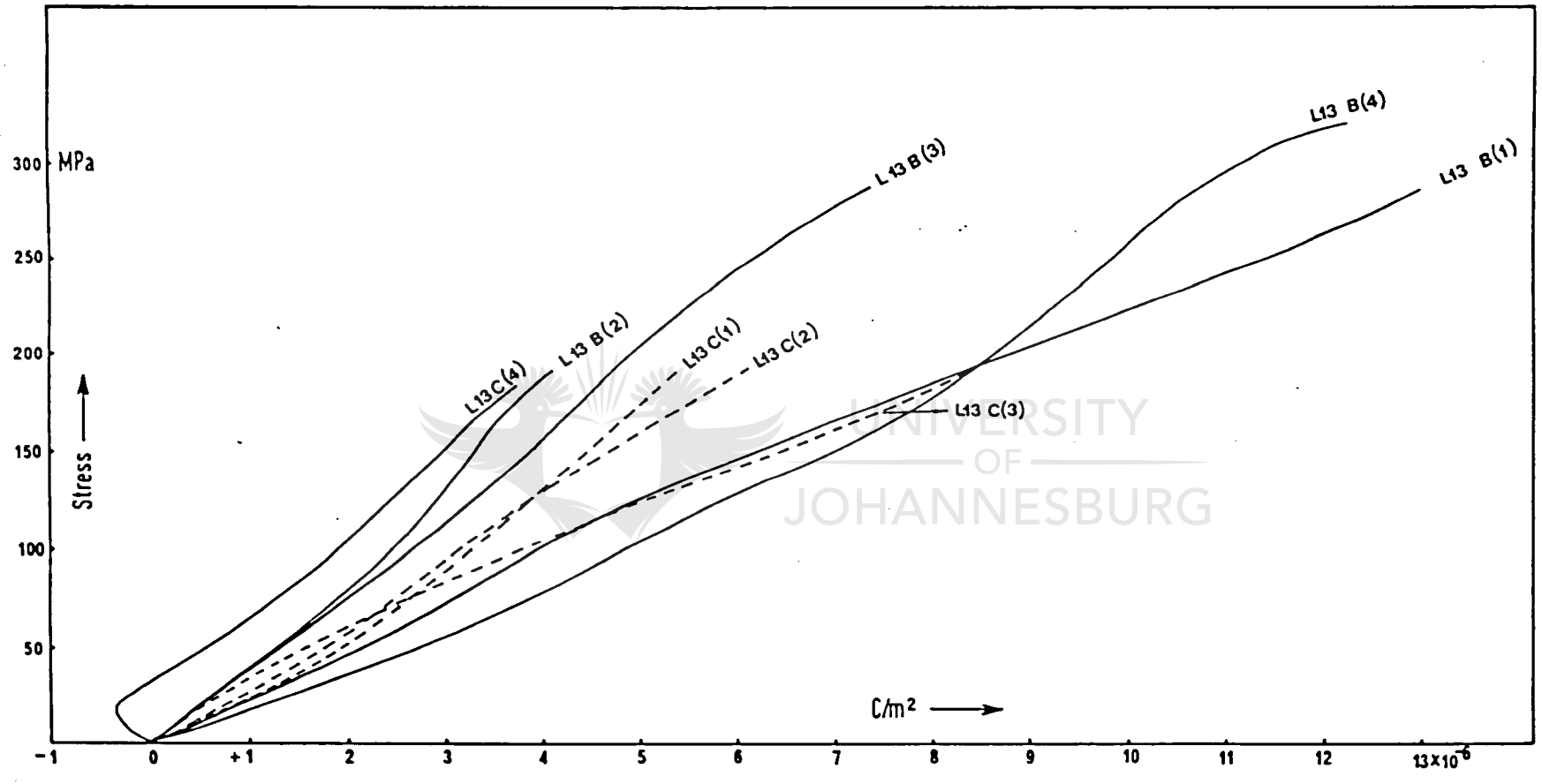

Figure 56 : Relationship between mechanical stress and piezoelectric polarization for cylinders cut in two different directions from quartzite L 13, tested in small hydraulic press.

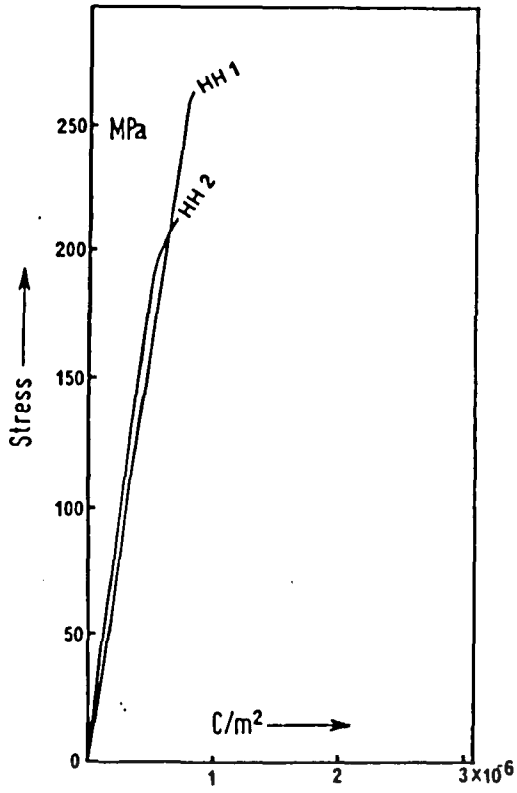

Figure 57 : Relationship between mechanical stress and piezoelectric polarization for Brixton Formation quartzite, tested in stiff testing machine.

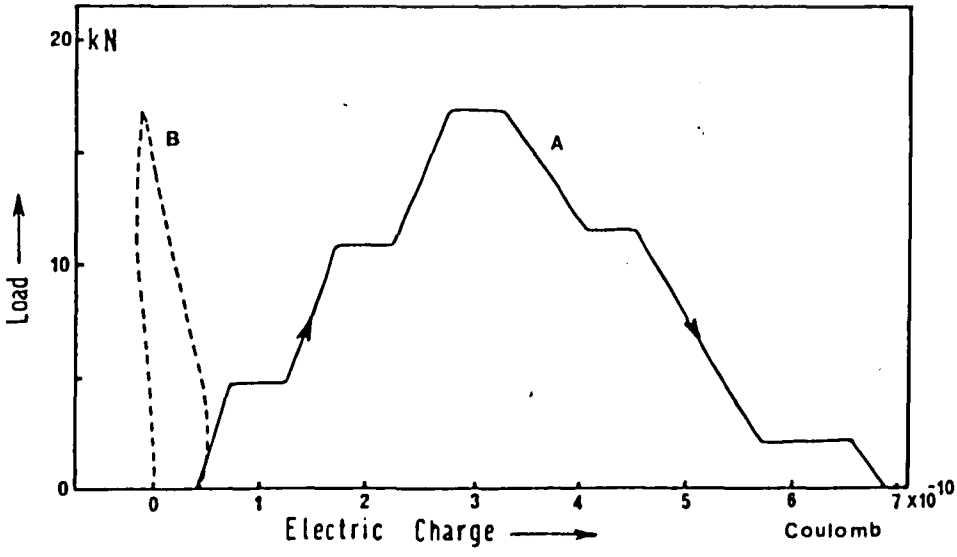

Figure 58 : Electric charge with drift recorded for silcrete 7382 at different mechanical loads. In the original curve A loading, unloading and resting periods (plateaus) are 60 second intervals except for a 90 second interval in the second descending limb of the curve; curve B is the resultant curve with drift removed. Tests carried out in stiff testing machine.

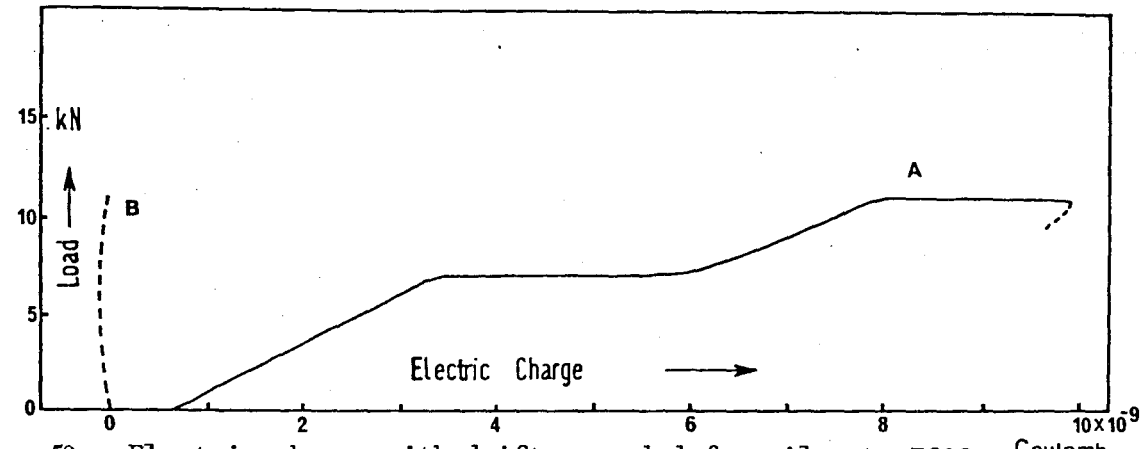

Figure 59 : Electric charge with drift recorded for silcrete 7392 at different mechanical loads. In the original curve A, loading, unloading and resting periods (plateaus) are 60 second intervals; curve B is the resultant curve with drift removed. Tests carried out in stiff testing machine.

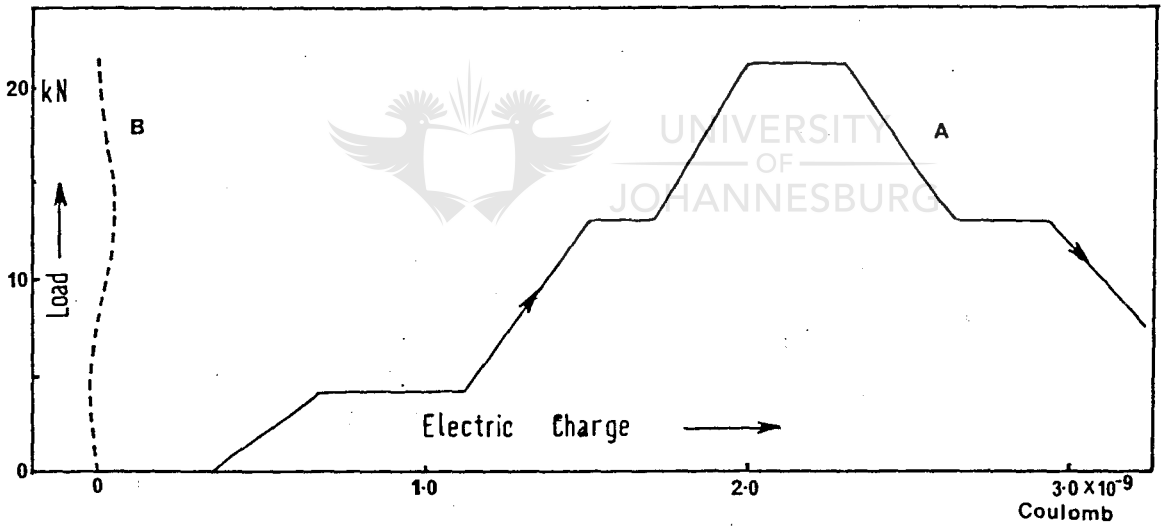

Figure 60 : Electric charge with drift recorded for silcrete 7420 at different mechanical loads. In the original curve A, loading, unloading and resting periods (plateaus) are 60 second intervals; curve B is the resultant curve with drift removed. Tests carried out in stiff testing machine.

is the high longitudinal polarization effect produced by each of the eight cylinders cut from quartzite L 13.
The close grouping of the piezoelectric polarization for cylinders L 13C (1), L 13C (2) and L 13C (3), all cut perpendicular to the dip and strike of the strata, is worthwhile mentioning. There is a tendency in more than sixty per cent of the curves to show a slight build-up in polarization with progressive stressing followed by a decline in value towards the end. When cylinder L 13C (4) was tested, a negative charge was liberated up to 48 MPa, whereafter the charge reverted to a positive charge.

5.4.14. Results on Brixton Formation Quartzite.

The steep gradients in the two curves plotted in figure 57 for cylinders HH 1 and HH 2 cut from the above quartzite, are indicative of a very low piezoelectric effect for this particular quartzite.

5.4.15. Results on Silcretes.

The results plotted in figures 58, 59 and 60 were derived from experiments carried out on silcretes 7382, 7392 and 7420 respectively in order to determine drift under progressive loading. In all three figures both loading, unloading and resting periods were taken at 60 second intervals, except for a 90 second interval in the second descending limb, with horizontal plateaus indicating periods of rest.
In each individual figure, the resultant curve B was obtained by removing drift from curve A. It is virtually impossible to try and interpret the three resultant curves for the silcretes, but there is a general trend in the curves to go up straight, which can only mean that these specimens do not possess any piezoelectric nature.

The purpose for including the silcretes in the studies was to establish whether the drift in electric charge readings was due to pre-stressing. The fact that silcretes, that have never been under any form of mechanical stress, do possess a strong drift is evident that there must be another explanation for the drift phenomenon.

6. DISCUSSION.

The linear relationship between load and electric charge or stress and polarization which was obtained in quartz and some quartzite cylinders, is in agreement with the theory for piezo-electric effects. However, there are two very important aspects of the values recorded for quartz that have an effect on the validity of the results which should be investigated, i.e. scatter in piezo-electric values between different quartz cylinders, and low piezo-electric values for STC quartz.

Although these aspects are inseparable, possible explanations for each will be given individually.

6.1. Scatter in Piezoelectric Values between different Quartz Cylinders.

6.1.1. Any cylinder not cut parallel to the Y axis of the mother crystal will lead to a lower reading, and any reading not taken exactly in the direction of the X axis will have lower values.

According to Parkhomenko (1971, p30) this could have a marked effect on the readings for, when applying a mechanical stress in a single direction, it could cause polarization components in two other components of direction which could interfere with the reading.

Vigoureux et al (1950, p47) mention in a publication two components of strain in the two other directions due to a force applied in any one direction.

Since stress and strain are related by the elastic constants or elastic moduli, strain could be responsible for the polarization components in the two other directions.

To cut down on the additional components of polarization, Parkhomenko made use of cubic shaped specimens with copper foil shielding on four sides of the specimen. With a small cylindrically shaped specimen, shielding was virtually an impossible task. This scatter in values was further reduced by Parkhomenko from 11,5 to 3 per cent in more than 100 samples by using electrodes which covered 95 per cent of the surface area of the sample.

In the laboratory tests on some quartz cylinders, the electrode areas were increased by putting two 3 mm wide silver epoxy resin strips or graphite lines parallel to the X axis on either side of the cylinder. This, however, did not bring about any noticeable decrease in the scatter between the piezoelectric readings for the various quartz cylinders put through the special test.

It must be admitted that Parkhomenko made use of the dynamic method to measure the longitudinal effect whereas, throughout this study, the static method was used to determine the transverse effect, except for 18 quartzite cylinders where the longitudinal effect was measured.

Although there is a difference in the two methods employed to measure the electric charges, the author is still of the opinion that if electrode area did have an influence on the scatter of the data on quartz cylinders, it should have come out in the 20 cylinders where epoxy resin or graphite were used.

6.1.2. The direction of the X axis marked on top of each individual

quartz cylinder by the suppliers could have been a few degrees out, which would have an effect on the readings. This has actually happened to a number of cylinders where it was virtually impossible to obtain an electric charge reading. Only after the direction of the X axis of each individual cylinder was checked by X-ray diffraction tests, was it possible to locate the error.

6.1.3. Cementing the electrodes onto the cylinder in line with the X axis marked on both flat ends is a very tricky operation. Any small deviation might cause differences in readings.

6.1.4. Although it is improbable, there might be a slight possibility of a small error in parallelism between the two flat faces of the quartz cylinder. Such an error will cause uneven application of load, thus resulting in an incorrect electric charge reading.

6.1.5. All precautions were taken to assure that each individual cylinder was dry and free from grease before inserting it between the two platens of the press, but a final touch of the fingers to move the cylinder into position on the bottom platen could have deposited some dirt that could lead to faulty readings.

6.2. Low Piezoelectric Values for STC Quartz.

It was shown previously that the piezoelectric effect for STC quartz is 38 per cent lower than the figure quoted for quartz, Vigoureux et al (1950, p53). An attempt has been made, below, to try and explain this lower piezoelectric value.

Parkhomenko (1971, p30) has recorded a difference of 34 per cent in the piezoelectric moduli for vein quartz when comparing the results obtained between the dynamic and the static method. In the light of Parkhomenko's finding, one of the possible

reasons for the low values recorded for STC quartz, as well as the quartzites, might lie in the method applied to bring about an electric charge. Reasons for this being :-

6.2.1. When applying the static method to study the piezoelectric effect it is, according to Parkhomenko (1971, p24-25), very important to insulate the specimen from all metal parts of the loading equipment. Complete insulation of the cylinder was very difficult, because any insulating material between the cylinder and the two platens would have affected the recording of strain measurements. However, in the tests carried out in the small hydraulic press, the top platen was insulated from the frame of the press by a nylon sleeve and a mica washer approximately 1 mm thick. Any dirt, dust or grease that might collect along the periphery of the mica washer will allow leakage of electric charge to the press, thus resulting in a lower value registered by the coulombmeter.

In a few cases 0,5 mm thick mica spacers have been placed between the quartz cylinder and the platens, but even at very low stress levels, this became so compressed that it served no purpose as insulator.

6.2.2. Another disadvantage of the static method is the possibility that one can get a flow of electrons from one side of the cylinder to the opposite via the platens at both ends, thus causing a short-circuit.

6.2.3. The time taken to collect the charge is dependent on the rate at which load is applied. This time has, according to Parkhomenko, a definite influence on the final reading. In tests carried out in the small hydraulic press on STC 25 and STC 26, there was an increase of more than 20 per cent in the

final reading in each case when the collecting time was decreased from 90 seconds to 22,5 seconds. Due to the fact that the intensifier crank of the small hydraulic press had to be turned by hand, it was impossible to reach loading rates exceeding 4 mm/min, because this would have required cranking by a synchronized motor at a very high speed.

The same tests repeated on STC 47 in the stiff testing machine, did not show any increase in electric charge with increase in loading rate. The most plausible explanation for this being that, even at the highest loading rate of 0,76 mm/min used during the test, the time taken to collect the charge was still relatively high.

6.3. General Observations.

It was found that the piezoelectric readings recorded on quartz, under stress in the small hydraulic press, are more than three times as high as those for quartz under stress in the stiff testing machine.

There is no doubt regarding the authenticity of the load obtained with the small press. Not only were the load cell and load cell amplifier calibrated on the stiff testing machine of the Chamber of Mines Research Laboratories in Johannesburg, but the calibration was also checked on two separate occasions on the same rigid press with satisfactory results.

When tested in the stiff testing machine, the quartz cylinders were never insulated from the top or bottom platen of the press, and with both platens at ground potential the charge nearest to the ends of the cylinders will leak straight to ground. This will result in a much lower reading recorded by the electrometer. The low piezoelectric readings might also be due to the massive

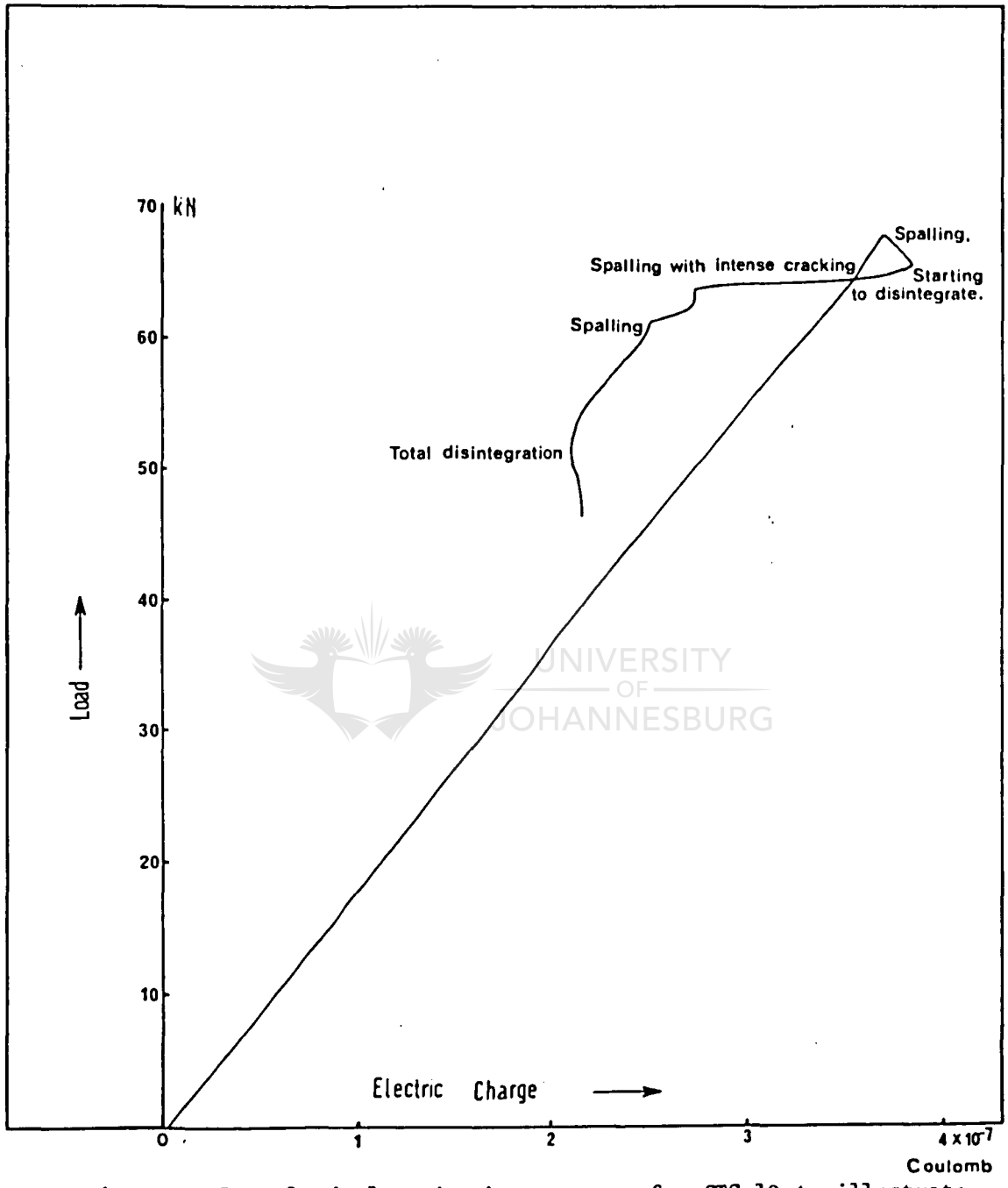

Figure 61 : Complete load-electric charge curve for STC 19 to illustrate the piezoelectric behaviour during the process of spalling with the electrodes still attached to the cylinder. Test was carried out in small hydraulic press.

steel frame of the press surrounding the quartz cylinder. As a result of the frame, a capacitance is created with the outside of the quartz cylinder forming one electrode, and the inside of the steel frame the other. Such a capacitance would absorb some of the electric charge generated in the quartz cylinder under stress. The electric charge readings on the 2 cm long quartz cylinders were expected to be two-thirds the value for 3 cm cylinders, but comparing the polarization values for 3 cm and 2 cm cylinders given in tables 4 and 5 respectively, one could see that they are almost the same. In actual fact, one of the smaller cylinders even produced a higher reading than some of the 3 cm cylinders.

It would be unfair to draw a conclusion on so few results, but if these results are reliable it is contradicting the statement made by Parkhomenko (1971, p31) that the ratio between the area under stress and the area over which the electric charge is measured has an effect on the size of the piezoelectric modulus.

An interesting result observed during the recording of the load-electric charge relationship in certain quartz cylinders, is the sudden small increases in polarization during slight spalling of the cylinder when stressed.

Only in a few cases was it possible to follow the act of intense spalling preceding total disintegration of the cylinder. The best example of this is given in final load-electric charge curve in figure 61 for STC 19.

At 67,5 kN on the curve, spalling started to take place accompanied by an increase of electric charge and a drop in load to 65 kN. After this point the electric charge decreased with each incident of spalling that followed. Only at a load level between 50 and 52 kN did the electrodes become dislodged, which coincides with

the zone of total disintegration on the curve. This sudden increase in electric charge might support the phenomenon of electric discharges associated with earthquakes reported in the olden days and mentioned in a report by Hoënig (1976, p1).

6.4. Discussion on Quartzites and Silcretes.

In quartzites, we are dealing with a polycrystalline rock where the individual quartz grains, during the recrystallization of the original sandstone, could become partly orientated in the existing stress field. The presence of a piezoelectric effect in a quartzite will only exist if a preferential orientation of the optical axis of the quartz grains does exist in the rock. Even with a minimal preferential orientation of the optical axis, we find an orientation of the electrical axis which makes the piezoelectric effect possible. This form of piezoelectric effect is referred to by Parkhomenko (1971, p117), as the piezoelectric texture of a rock.

The linear relationship observed between the applied mechanical stress and the piezoelectric polarization for quartzites is in agreement with the theory of piezoelectric effect, and proves that the piezoelectric constant is indeed constant over the pressure range.

The effect that the rate of strain has on the piezoelectric value has not been tested on the quartzites, but according to Parkhomenko (1971, p116-117), this could be a contributing factor to the low readings recorded.

Hoënig (personal correspondence) is of the opinion that, when a quartzite is stressed, one will induce ion migration from areas of compressive stress to areas of tensile stress. This will give a residual voltage or current that will add or

detract from the piezoelectric signal.

The intentions of the piezoelectric study was to investigate the magnitude instead of the polarity of the electric charge generated at various stress levels up to breaking point, this being the reason why all curves have been plotted in the same direction.

The presence of a piezoelectric effect in quartzites need not necessarily be the result of a piezoelectric texture of the rock, but could also be the consequence of a few large grains of quartz in the specimen with their electrical axes coinciding with the direction of applied load.

After having studied the magnitude of the piezoelectric effect on various sample dimensions, Parkhomenko (1971, p117-120), has found that in samples of medium - to coarse - grained rock with dimensions 2 cm X 2 cm X 2 cm the piezoelectric effect is considerably higher than for larger samples. This led to a conclusion that the observed piezoelectric effect in small samples may represent the effect from single quartz grains and not of the overall texture of the rock. Tuck (1977, pT7-T11) also expresses his doubts about the existence of a piezoelectric fabric, and believes that the effect might be due to a few large quartz grains.

The longitudinal readings are generally much higher than the transverse readings. One would expect the opposite to be the case because the area on which the charge appears in the transverse effect is almost four times as big as for the longitudinal effect. This is beautifully illustrated in figure 46 for quartzite L 6. There is the possibility of the development of an electrostatic charge due to friction between the cylinder and the plates which could have had an adding effect to the longitudinal values.

This electrostatic charge is described by Parkhomenko (1971, p239) as the triboelectric effect in rocks, and charges in the range of 10^{-11} C/m^2 have been registered.
It should be noted that no attempt has been made to calculate any piezoelectric modulus value for quartzite. The reason for this being that the cylinder has only been stressed in one direction with electric charge readings taken in another arbitrary direction, nor has any shielding been used to prevent interference from the other directions.
Nevertheless, if one calculates a coulomb-newton relationship value for any of the quartzites, a modulus value is obtained which is at least 10^3 times smaller than any of the values measured on quartzite by Parkhomenko.
These low values can be attributed to an appreciable electrical conductivity of the quartzites which can cause a rapid leakage of the charge, thus not permitting a true measurement of the piezoelectric effect. In a similar manner the existence of surface and volume conductivities can cause a redistribution of surface charges which can also have an effect on the magnitude of the piezoelectric reading.
The texture of all the quartzites tested from Loraine Gold Mines Limited, is medium- to coarse-grained with occasional large quartz grains in most of the rock samples. Although the quartzites do display some form of preferential orientation of the optical axes, Parkhomenko's results on grain sizes strongly support the possibility that the piezoelectric effects observed are really a consequence of a few large quartz grains rather than that of a piezoelectric texture of the rock. However, in quartzites L 7, L 8 and L 12 with fairly high preferential orientations of the optical axes and with a medium-grained texture, where a large

majority of the quartz grains are uniform in size, the piezoelectric effect could be attributed to a piezo-electric texture of the rocks.

The absence of preferred orientation and single large quartz grains in silcretes might explain why these specimens did not produce an electric charge when subjected to mechanical stress.

6.4.1. Possible Reasons for Drift in Readings on Quartzites.

It was first assumed that the drift might have been caused by the quartzite cylinder acting as an antenna picking up all electrical disturbances regardless of its nature.

This assumption was soon overruled when the Faraday cage failed to cancel this effect.

After having read the work of Vigoureux and Booth (1950, p10) where they make the statement that the longitudinal piezo-electric effect d_{11} in quartz disappears at temperatures above 573° C due to the change from α to β quartz, thus leaving only the shear effect d_{14}, further tests were carried out on some quartzites.

It was decided to heat a few quartzite cylinders in a kiln for 30 minutes at 1000°C and to allow it to cool slowly down to room temperature, whereafter it was tested for drift under zero load.

One quartzite cylinder had a drift eight times smaller after heating than before when recorded at the same electrometer scale setting. In another quartzite cylinder the drift recorded at a scale setting of 1×10^{-10} coulomb per full scale, was $1,40 \times 10^{-13}$ coulomb per second. After heating, this figure dropped to $3,30 \times 10^{-15}$ coulomb per second, which is a reduction of 43 times. With such a low drift rate

there is the possibility that these charge readings registered do not come from the cylinder, but that it is in actual fact the internal drift of the electrometer which is in the vicinity of 5×10^{-15} coulomb per second that was recorded.

6.4.2. Residual Stress in Quartzite.

The possibility that residual stress in the rock, after having been removed from underground, can produce an electric charge was considered as another possibility for the drift phenomenon. When a rock is still deep down a mine in the sidewall of a working place it experiences very high stresses, in the vicinity of 150 MPa or more. Once the rock has been removed from underground it becomes destressed. In the beginning this destressing process happens almost immediately, but does not stop abruptly, instead it gradually decays down to zero over a very long period, possibly years. The almost flat portion of such a destressing-time curve is referred to by the author as residual stress in the quartzites that is now being released.

Jaeger et al (1969, p362) defines residual stresses as 'locked-in' stresses associated with the previous history of rock, and can be retained indefinitely by materials possessing a yield stress.

After having studied the in-situ stress results at various localities in Southern Africa, as determined by several workers, Gay (1975, p447-459), came to the conclusion that the present-day state of stress includes components of early tectonic as well as gravitational forces. These residual components of stress in the rocks could be as old as 3000 million years. Making use of the fact that stress and strain is related

through the Young's modulus, Vigoureux et al (1950, p59), have shown that it should be possible to express the electric polarization of the direct piezoelectric effect in terms of strain instead of stress.

When any object, that has been strained, is destressed, it will, as a result of the theory of elastic rebound, return to its normal shape which is in actual fact straining in the opposite direction. Applying the argument of Vigoureux, to a quartzite where the multitude of quartz grains go through the same process of destressing or straining in an opposite direction, one could expect to observe a spontaneous electric charge liberated by the rock.

So far the argument that destressing the rock can liberate an electric charge sounds plausible, but in the case of the silcretes which were formed on surface and have never been subjected to any form of mechanical stress, the high drift rate cannot be explained by the theory of residual stress.

6.4.3. Thermal Stress.

Residual stress could also be related to thermal stress which might have originated as a result of a change in volume due to heat generated during metamorphism or solar heat in the case of silcretes.

On the contrary, if thermal stress is responsible for the drift in quartzites, it would be difficult to explain the substantial decrease in drift rates after the specimens have been subjected to high temperatures, whereby thermal stress is created in the rock.

It would have been interesting to see whether these rock specimens still display a drift or direct piezoelectric effect when under mechanical load. Unfortunately this was not possible

because the specimens became very brittle due to the high temperatures. This problem might have been overcome by initially heating a large piece of quartzite before cutting the cylinder.

6.4.4. Metallic Junctions.

In a personal letter from Hoenig, he mentions the possibility that the quartzite might contain metallic junctions that can act as diodes which could rectify any AC signal in the air. This rectified signal could also have been the drift observed. The metallic junction theory might still be applicable to some quartzites where galena or pyrite is present, but none of the silcretes tested, have revealed any such metallic junctions in thin section under the microscope.

With the above three possibilities failing to account for the drift rate in quartzites and silcretes, the spontaneous liberation of electrons recorded in so many rocks will remain open for discussion.

Whatever the explanation for the drift might be, it will have to explain why only some cylinders cut from the same piece of borehole core or small hand specimen display this drift phenomenon.

7. SUMMARY.

7.1. By carrying out tests on quartz cylinders it was established that various factors influence the results when using the static method of applying load, and recording the transverse piezoelectric effect:

7.1.1. Orientation.

When recording the transverse effect, orientation plays an important role. Maximum values are recorded when the

cylinder is cut with the long axis exactly parallel to the Y axis of the mother crystal, and the electrodes are coupled precisely in the X-direction. Any deviations from the above will lead to lower readings.

7.1.2. Static versus Dynamic Method.

Making use of the static method of applying mechanical load might be a possible reason for the lower piezoelectric readings recorded for STC quartz, compared to the figure quoted in the literature.

In tests carried out by Parkhomenko (1970, p30), both the dynamic and static methods were used on specimens of vein quartz. The results proved that the piezoelectric moduli obtained with the static method were on an average 34 per cent lower than that obtained with the dynamic method.

7.1.3. Insulation and Leakage.

Insulating the specimen from all metal parts of the loading equipment is very important when applying the static method. Lower readings can occur due to leakage of electric charge to the frame of the press along contact dirt. There is also the possibility of a short-circuit due to a flow of electrons from one side of the cylinder to the other at both ends via the platens.

7.1.4. The Effect of Various Loading Rates on the Piezoelectric Charge.

During the tests it was observed that there is a considerable increase in electric charge, with an increase in the rate at which the mechanical load is being applied to the cylinder.

7.2. It has also been established that:

7.2.1. Quartzites sometimes give a piezoelectric effect and sometimes not, whereas silcretes never produced any piezoelectric

effect at all. This could be the result of:

7.2.1.1. Preferred orientation of the optic axes of the quartz grains being present or not in the specimen.

7.2.1.2. Cylinder cut in the right direction relative to preferred orientation.

7.2.1.3. Large single quartz grains in the specimen which has the same effect as preferred orientation.

7.2.2. The electric charge values obtained with quartzites are much lower than those of quartz.

7.2.3. Quartzites and silcretes usually show a drift phenomenon in the electric readings, which is absent with quartz under the same conditions.

Possible reasons for drift could be:

7.2.3.1. Residual mechanical stress in quartzites. The validity of this assumption is supported by drift tests carried out on surface specimens of Hospital Hill quartzite in which case there was no drift at all. On the contrary, silcretes which had never been mechanically stressed, displayed a fairly large drift in electric charge readings.

7.2.3.2. Residual thermal stress in quartzites. Since quartz has expansion coefficients which are different in different directions, a polycrystalline rock will become stressed when the temperature is raised. This could be due to the geothermal gradient of the earth or by the sun, as in the case of silcretes. Drift could then be due to destressing of this thermal stress.

7.2.3.3. Presence of pyrite or galena crystals. Due to the presence of pyrite or galena crystals in the rock, the metallic junctions formed could act as rectifiers for any AC signal in the air, which could account for the drift phenomenon. However, silcretes are free of such metallic junctions but still show a high drift rate.

8. CONCLUSION

1. Quartzites do show a piezoelectric effect.

2. Measurements on the electric charge generated by quartzites under stress are more complex than that of quartz because:-

   (i) Piezoelectric values of quartzite are small compared to those of quartz. This requires a very low and sensitive recording range on the electrometer.

   (ii) Drift phenomenon in readings interfere with the actual piezoelectric effect generated under compressive stress.

   (iii) The orientation of the specimens to obtain the best results is very difficult to determine.

3. Piezoelectric effect of quartzite could possibly be used to measure stress in mines. Before a conclusion can be reached regarding the usefulness of this method, it is suggested that further investigation should be carried out in the laboratory particularly on :-

   (i) The drift phenomenon in quartzites with a possible means of controlling it.

   (ii) The possibility of cutting the cylinders relative to a preferred orientation of the quartz grains in the hand specimens, in order to obtain the highest readings.

   (iii) The possibility of measuring piezoelectric effect in quartzites by placing electrodes on the surface of the rock, or inside boreholes rather than on cylinders.

4. It is also suggested that the feasability of the dynamic, rather than the static method of applying load, be investigated in the laboratory.

8. ACKNOWLEDGEMENTS.

The author would like to thank the following persons and instances who were of great assistance in the preparation of this dissertation.

Prof W.J. van Biljon for his leadership, encouragement and new ideas at all times.

Prof A.G.K. Lutsch for his suggestions and assistance in the initial stages of experimentation.

The Chamber of Mines of South Africa for a bursary. In particular I would like to express my thanks to Messrs. C. Heins, J.P.M. Hojem and R.J. Maritz of the Chamber of Mines Research Laboratories in Johannesburg for constructing the hydraulic press.

Mr. H. Moire of Standard Telephones and Cables of South Africa (Pty.) Limited, Germiston, and his staff for cutting and supplying the quartz and quartzite cylinders. Also for his personal suggestions and advice.

Mr. A. Marèchel for designing and constructing the electronic equipment and also for his constructive ideas.

Anglo Transvaal Consolidated Investment Company, Limited, for allowing me to use material and information from Loraine Gold Mines, Limited.

Mr. J.P. Jonker for attending to the photomicrographs.

Mr. J.J. Bensch who was of great assistance in preparing some fabric diagrams.

Dr. J.P.R. de Villiers and Dr. C. Roering for their advice and the keen interest shown in this investigation.

Mr. C. Mason of Loraine Gold Mines, Limited, for computer processing of data, attending to the problems experienced with the small hydraulic press, as well as his words of advice.

Mr. D.R. Cloete of Hartebeestfontein Gold Mining Company, Limited, for reading and criticizing the section dealing with the purpose of the study.

Mr. J. van Aswegen of Loraine Gold Mines, Limited drawing office, for drawing the graphs and diagrams.

Mr. J. Abdo for his assistance with the printing of the photos.

Mrs. A.S. Davis for the typing of this dissertation.

The non-white staff of Loraine Gold Mines, Limited, for the printing process.

9. BIBLIOGRAPHY.

EMERY, C.L. (1950), The strain in rocks in relation to mine openings, The Mining Engineer, Paper No. 3834, p54-59.

FULLER, A.O. (1958), A contribution to the petrology of the Witwatersrand System, Trans. Geol. Soc. S.A. Vol. 61, p19-45.

GAY, N.C. (1975), In-situ stress measurements in Southern Africa, Tectonophysics, 29, p447-459.

GRIFFITHS, J.C. (1967), Scientific method in analysis of sediments, Mc Graw-Hill, NY, 508pp.

HOENIG, S.A. (1976), The application of electrostatic techniques to the analysis of pre-fracture phenomena in ceramic materials, Informal Report No. 2, The National Science Foundation, Washington, D.C. 20550, Contract No. ENG75-13639, p1-17.

INTERNATIONAL SOCIETY FOR ROCK MECHANICS COMMISSION ON STANDARDIZATION OF LABORATORY AND FIELD TESTS, (1972), Suggested methods for determining uniaxial compressive strength of rock materials and the point load strength index, p3-12.

ISAACSON, E. DE ST. Q. (1958), Rock pressure in mines, Mining Publications Limited, p185-186.

JAEGER, J.C. and COOK, N.G.W. (1963), Pinching-off and discing of rocks, J. Geophys. Res. Vol. 68, No. 6, p1759-1765.

JAEGER, J.C. and COOK, N.G.W. (1969), Fundamentals of rock mechanics, Methuen and Company, Limited, London EC4, 471pp.

KELVIN, Z. (1893), On the piezoelectric properties of quartz, Philosophical Magazine, Vol. 36, p331-340.

LEEMAN, E.R. (1964), The measurement of stress in rock, Journal of the South African Institute of Mining and Metallurgy, Vol. 65, p45-78.

MOHR, H.F. (1956), Measurements of rock pressure, Mine and Quarry Engng., p178-189.

NYE, J.F. (1972), Physical properties of crystals, Claredon Press, Oxford, 309pp.

PARKHOMENKO, E.L. (1971), Electrification phenomenon in rocks, (Translated from Russian by George, V. Keller), Plenum Press, NY. 285 pp.

PETTIJOHN, F.J. POTTER, P.E. and SIEVER, R. (1972), Sand and sandstone, Springer-Verlag, NY. 618pp.

TUCK, G.J., STACEY, F.D. and STARKEY, J. (1977), A search for the piezoelectric effect in Quartz-bearing rocks, Tectonophysics, No. 39, pT1-T11.

VIGOUREUX, P. and BOOTH, C.F. (1950), Quartz vibrators and their application, His Majesty's Stationery Office, London.